

GENETIC IDENTIFICATION OF PHAGE P22 ANTIGENS AND THEIR
STRUCTURAL LOCATION

by

Ruth Griffin Shea

B.A., Boston University (1971)

SUBMITTED IN PARTIAL FULFILLMENT
OF THE REQUIREMENTS FOR THE
DEGREE OF

DOCTOR OF PHILOSOPHY

at the

MASSACHUSETTS INSTITUTE OF TECHNOLOGY
(March 1977)

Signature of Author *Ruth Griffin Shea*

Certified by *[Signature]*

Accepted by *[Signature]*



Genetic Identification of Phage P22 Antigens and Their
Structural Location

by

Ruth Griffin Shea

Submitted to the Department of Biology on March 25, 1977
in partial fulfillment of the requirements for
the Degree of Doctor of Philosophy

ABSTRACT

The structure of bacteriophage P22 and its precursor particles has been studied by immunological methods. Rabbits injected with P22 proheads, tail-less phage, or mature phage produced hyperimmune sera that precipitated all P22 structures tested.

Characterization of the anti-prohead serum by immunoelectrophoresis showed that it contained antibodies against the scaffolding protein, gp8. Identification of this antibody class was facilitated by the characteristic immunoelectrophoretic patterns produced by several of the amber fragments of the gp8 polypeptide. They also showed reactions of partial identity with the full gp8 molecule.

In immunoelectrophoresis experiments, absorption of the anti-prohead serum with prohead structures resulted in the loss of the gp8 precipitin arc from the immunoelectrophoretic pattern. In experiments using electron microscopy, antibodies directed primarily against the scaffolding protein were generated by absorption of the anti-prohead serum with both phage and 8⁻ amber mutant lysates. These antibodies uniformly coated the prohead shell. The combined results suggested that scaffolding protein in proheads was available for reaction with antibodies in the external environment. Two interpretations are possible: either, scaffolding protein is normally accessible throughout the coat protein lattice, or, it becomes accessible after incubation of the prohead structure with the antiserum. In fact, incubation of the proheads with either anti-phage or anti-prohead serum apparently leads to a migration of the internal density, so that the prohead no longer excludes the negative stain.

Anti-phage, anti-prohead, and anti-head sera contained antibodies against the capsid protein, gp5, as assayed by immunoelectrophoresis of these three sera after absorption with a 5⁻ amber mutant lysate. Electron microscopy experiments using anti-phage and anti-prohead sera showed that these sera uniformly coated the capsids of phage and proheads. They also bound to P22 spirals, structures composed primarily of coat protein, that accumulate in the absence of scaffolding protein. A prohead-specific class of anti-capsid antibodies, generated by successive absorption of the anti-prohead serum, first with phage, and then, with a 5⁻ amber mutant lysate, continued to coat proheads. The existence of this antibody class indicated that there was a set of capsid determinants on proheads which had become altered or unavailable during virus maturation, so that phage were no longer able to interact with these anti-capsid antibodies. On the other hand, electron microscopy of anti-phage serum that had been absorbed with proheads showed that it no longer coated phage. Thus, all of the antigenic determinants present on phage also seemed to be present on prohead precursor structures, suggesting that no new antigenic sites were generated in the prohead-to-phage transition.

Anti-phage and anti-prohead sera inactivated phage; anti-head serum, produced in response to tail-less phage, did not. Results from serum blocking experiments indicated that most of the virus neutralizing antibodies in the anti-phage and anti-prohead sera were directed against the tail protein, gp9. As proheads do not contain tail protein, these antibodies were probably generated against contaminating phage ghosts in the prohead immunogen preparation. Anti-gp9 antibodies in the two phage-inactivating sera were also detected by immunoelectrophoresis. In the electron microscope, phage tails that had been incubated with anti-gp9 antibodies appeared coated.

TABLE OF CONTENTS

	<u>Page</u>
INTRODUCTION	1
MATERIALS AND METHODS	29
(a) Bacterial Strains	29
(b) Phage Strains	29
(c) Preparation of Phage Stocks	30
(d) Media and Chemicals	31
(e) Preparation of Rabbit Antiserum	32
(f) Preparation of Immunogens	34
i. Prohead preparation for first injection	34
ii. Phage and tail ⁻ head preparation for first injection	35
iii. Particles for second injection	38
(g) Neutralization Curves	38
(h) Serum Blocking Experiments	44
i. Protocol I	44
1. Lysate preparation	44
2. Serum blocking procedure	44
ii. Protocol II	44
1. Lysate preparation	44
2. Serum blocking procedure	45
iii. Preparation of purified particles	45
1. Preparation wild-type 13 ⁻ , 9 ⁻ 13 ⁻ , and 2 ⁻ 13 ⁻ lysates	45
2. Particle purification	45
(a) Purification of wild-type particles and tail ⁻ heads	46
(b) Purification of the proheads	46
(c) <u>In vitro</u> constitution of the phage particles and their purification	47
iv. Antiserum preparation	47
v. Tailing assay	48
vi. Theoretical serum blocking curves	49

	<u>Page</u>
(i) Immunoelectrophoresis Experiments	51
i. Preparation of antigens for immunoelectrophoresis	51
1. Preparation of concentrated lysates	51
2. Preparation of purified phage particles	51
(a) Phage and tail ⁻ heads	51
(b) Proheads	56
ii. Preparation of antisera for immunoelectrophoresis	58
1. Absorption with uninfected <u>Salmonella</u> cells	58
2. Preparation of partially purified anti-prohead serum	58
iii. Immunoelectrophoresis procedure	59
(j) Electron Microscopy Experiments	61
i. Particle purification	61
1. Wild-type phage and tail-less heads	61
2. Proheads	62
3. T4 phage	63
ii. Serum absorption	63
1. Prohead absorption of anti-phage serum	64
2. Phage absorption of anti-prohead serum	64
iii. Lysate preparation	65
iv. Lysate absorption of the serum	66
v. Antiserum clarification	67
vi. The antigen mixture	67
vii. Electron microscopy procedure	68

CHAPTER I: CHARACTERIZATION OF THE PHAGE-NEUTRALIZING ACTIVITY
OF SERA PREPARED AGAINST PHAGE P22 AND ITS PRECURSOR
PARTICLES.

	<u>Page</u>
A. Phage Neutralization Curves	70
B. Identification of the Targets of the Neutralizing Activity of Anti-phage Serum	73
1. Serum blocking experiments with lysates lacking specific gene products	76
2. Serum blocking activity of the amber fragments of gp9	93
3. Serum blocking experiments with purified particles and tail protein	94
C. The Neutralizing Activity of Anti-prohead Serum	103
1. The serum blocking activity of purified components	103
2. Blocking of anti-prohead serum by P22 amber mutant lysates	106
Discussion	110

CHAPTER II: INVESTIGATION OF THE TOTAL SPECIFIC ANTIBODY COMPOSITION
OF ANTI-P22 SERUM BY IMMUNOELECTROPHORESIS

	<u>Page</u>
A. Characterization of Precipitating Antibodies by the Technique of Immunoelectrophoresis	130
B. Immunoelectrophoresis of Structure-containing Lysates and Purified Structures	133
1. Anti-phage serum	133
2. Anti-prohead serum	139
3. Anti-head serum	142
C. Immunoelectrophoresis of Soluble P22 Antigens	143
1. Anti-phage serum	146
(a) Identification of the gp9 precipitin band	146
(b) Absence of a coat subunit precipitin band	150
2. Anti-prohead serum	151
(a) Presence of the gp9 precipitin band	152
(b) Identification of anti-scaffolding protein antibodies	155
i. gp8 and its amber fragemnts show different immunoelectrophoretic behavior	155
ii. gp8 and its amber fragments show reactions of partial identity	160
3. Anti-head serum	165
D. Cross Reactivity of P22 Structures	168
1. Common antigens	168
2. Unique antigens	168
(a) Capsid determinants unique to phage as shown by spur formation	168
(b) Capsid determinants specific to proheads as shown by spur formation	172

	<u>Page</u>
3. Investigation of prohead-specific antibodies by phage absorption of the anti-prohead serum	173
(a) Residual activity of phage-absorbed anti-prohead serum against proheads	173
(b) Absence of prohead-specific determinants on the necks of tail-less phage	180
(c) Absence of prohead-specific determinants on empty heads	183
4. Can proheads absorb anti-scaffolding protein antibody?	188
E. Sensitivity of the Immunoelectrophoretic Assay	200
1. Effects of antigen dilution	200
2. Effects of antiserum dilution	204
F. Discussion	206
Appendix	210

CHAPTER III: ELECTRON MICROSCOPY OF ANTIBODY COATED P22 STRUCTURES

	<u>Page</u>
A. Experimental Approach	227
B. Coating of Particles by Anti-phage Serum	233
1. Whole serum	233
2. Prohead-absorbed anti-phage serum	236
C. Coating of Particles by Anti-prohead Serum	241
1. Whole serum	241
2. Phage-absorbed serum	241
3. Lysate-absorbed serum	248
(a) Immunoelectrophoresis of absorbing lysates	250
(b) Rationale of the lysate absorption	254
(c) Technical difficulties	255
(d) Coating of particles by lysate-absorbed serum	256
1. Control sera	256
2. 3 ⁻ 5 ⁻ lysate-absorbed serum	260
3. 3 ⁻ 8 ⁻ lysate-absorbed serum	260
4. Discussion	261
GENERAL DISCUSSION	265

"My glory was, I had such friends." (Yeats)

Acknowledgements:

There were several people who contributed substantially to the technical aspects of this work: My thanks to Jon King, my advisor, whose experimental know-how, rapid-fire analysis of data, and powers of creative, scientific thought were a pleasure to behold. I also thank him for the enormous amount of work he put into the writing of this thesis. My thanks also to David Botstein, whose enthusiasm, generosity, and scientific advice were so important to me at several points throughout my graduate days. My thanks to Sherwood Casjens, from whom I learned a lot about the practical, as well as the technical, aspects of science. It was he who first discussed this line of investigation with me. My thanks to Chris Green who was most helpful in introducing me to several immunological techniques, and to Lisa Steiner, for her generosity in letting me use her equipment and materials in the early stages of this work. Many thanks also to Donna Smith, whose technical assistance in several of the serum blocking experiments was invaluable. This thesis could not have been finished in finite time without the expert typing done by Isabel Harrison, whose patience, diligence, and hard work beyond the call of sanity I shall never forget. And, but for Peter Berget, there would be no copies of this thesis. I also thank Roni McCall for helping me out of several tight spots along the way where my lack of secretarial skills, coupled with my unique sense of organization and tight scheduling, would have otherwise overwhelmed me. Finally, I thank the women in the kitchen, who not only provided clean glassware, sterile media, and endless pipettes, but also a real home for us on the fourth floor. I thank Betty Russell, Ellen Halverson, Eileen Twomey, Jean Peavey, Doris Stedman, Irene Bobricki, Kay Reddish, Thelma Watkins, Denise Viola, Helen Pelusi, and particularly, Josie Calareso and Annie Scali, two great ladies.

I have learned a great deal about many things through my associations with the people here at MIT. My friends know that, for me, there are not words enough to express my gratitude for all that they have taught me. To list their names is not enough, but to do them justice would put the heft of this thesis beyond the scope of many.

Finally, thanks to my folks who made all this possible, so to speak. Sincere thanks to my mother, who showed me what strength really is, and to my Dad, whose boundless faith in me stands by me to this day. And last, but not least, thanks to Ed.

INTRODUCTION

The study of viruses developed from their identification as agents of disease, originally in plants, and later in animals and humans. Since viruses utilize the synthetic apparatus of their host cell for their reproduction, antibiotics which act on the synthetic apparatus are not useful in therapy, since they tend to be toxic to the host. Immunoprophylaxis remains the most effective way to control virus diseases (Neurath and Rubin, 1971). The beneficial consequences of the development of vaccines for smallpox, yellow fever, poliomyelitis, and measles are well known. In the veterinary field, vaccines for canine distemper, canine hepatitis, Newcastle Disease virus, hog cholera, and foot-and-mouth disease virus (the most troublesome disease of farm livestock) have been used with success (Borek, 1972). With many other viruses, the prospects of effective vaccines seem less promising because of antigenic heterogeneity and other problems.

There have been close links between the fields of Virology and Immunology for a very long time. One might say they were born together in 1798, when Edward Jenner introduced vaccination with cowpox to protect against smallpox (Langer, 1976). Implicit in this discovery were the beginnings of the recognition of contagious viral disease, an appreciation of cross-reactivity between related viruses and the notion of active immunization. Almost a century later, Pasteur attenuated virulent rabies virus by serial passage through a novel host, the rabbit, thus introducing a method of preparing live virus vaccine which persists to the present day (Fenner, 1972).

There are two main approaches available in the treatment of viral infections. In the preventive approach, active immunization, as noted previously, makes use of the organism's own immune system. Vaccines can generally provide high-level immunity with long-lasting effects, but are of very limited spectrum; essentially, one vaccine, one virus. In addition, there are substantial problems in the manufacture of vaccines. Not only are there formidable difficulties in scaling up preparations, but the cell substrates used to grow viruses have a substantial probability of containing latent viruses. Thus, as far as immunization is concerned, it may be of considerable use to define which viral antigens produce antibodies that will protect the organism.

A second approach dealing with viral diseases involves chemotherapy. As noted earlier, the great success which attended anti-bacterial chemotherapy since World War II has not been paralleled for viruses, primarily because of the intimate dependence of viral replication on host metabolic processes. However, there are viral-specific processes which may be potential targets for the development of chemotherapy, for example, the reactions involved in virus assembly.

With respect to immunization, there was essentially no lapse between the general recognition that viruses were built from symmetrically arranged subunits (Crick and Watson, 1956; Caspar and Klug, 1962; Horne and Wildy, 1961) and the realization that isolated subunits might be used as immunogens (Appleyard, 1961; Wilcox and Ginsberg, 1963). Although most vaccines currently in use still consist of virus particles and soluble antigens, it has been demonstrated that not all antigens of a given virus are needed to induce antibody responses leading to protection (Kasel, et al., 1964; Davenport, et al., 1964). The useful proteins present in most vaccines, therefore, represent only a small proportion of the total macromolecular species. Therefore the use of vaccines made of purified components have a number of advantages. Superfluous proteins which may cause undesirable sensitization or toxic reactions will be eliminated; inoculation of viral nucleic acid will be avoided which even if lacking infectivity, might retain undesirable coding potential; hyper-immunizing doses can be used; and vaccine standardization may be based on chemical as well as biological criteria (Pereira, 1972). It is possible that such an approach may be taken one step further with the use of wholly synthetic molecules as immunogens. This depends on the detailed elucidation of the antigenic structure of the proteins. Such experiments have been done in model systems, for example with enzymes (Arnson, 1972).

The main focus of this thesis is the elucidation of the antigenic structure of a simple bacterial virus, Salmonella phage P22, by exploit-

ing the specificity of the immune response. In using antibodies to analyze phage structure, I also gathered information on the nature of the rabbit immune response to P22. As a result of the inherent complementarity of antigen:antibody studies, information about one of the reactants provided information on the other. Information derived from a simple system may not be directly transferable to more complicated organisms; however, because of the precision of the phage system, including the well-developed genetics, and detailed knowledge of protein composition and protein assembly, clear answers to well-defined questions can be obtained.

Viruses have been described as "vagabond genomes" (Rott, 1965). As such, viruses have evolved structures specifically designed to meet the demands characteristic of this life-style. As free agents in the environment, viruses must protect their genetic complement from degradation. However, the same structure which protects the nucleic acid must also serve as its vehicle of transfer. In this capacity, the virus particle must also function in recognition of, and adsorption to, the host cell, penetration of the cell envelope, and perhaps, transport of the nucleic acid to the proper site for its replication. Considering the complex series of progressive functional states which the relatively simple virus capsid must assume, I was intrigued as to how such structures are designed and assembled. This thesis presents the results of my investigation into the assembly and structure of bacteriophage P22. The genetics, protein composition, and morphogenesis of P22 have been defined in detail (Botstein, et al., 1973; King, et al., 1973). In these experiments, I attempted to discover, using antibodies as probes,

how the disposition of the proteins in precursor and mature virus particles are related to their biological functions.

Fraenkel-Conrat and Williams showed in 1955 that tobacco mosaic virus could be reconstituted from its protein and nucleic acid components. Thus, it seemed that virus parts contained within themselves blueprints for the construction of the virus. Around the same time, Crick and Watson (1956) postulated that the protein coats of viruses were made up of identical subunits. In this way, shells of considerable size could be coded for by a minimum of genetic material, and constructed in the most error-free manner. In 1962, Caspar and Klug were responsible for a major advance in the theory of construction of regular viruses. They provided a geometrical model for the packing of similar subunits into what they termed "quasi-equivalent" positions on the surface of an icosahedral shell. Such a shell has 20 faces and 12 vertices. Simply stated, quasi-equivalence allows for a certain bonding flexibility in identical subunits so that molecules can participate in arrangements having 6-fold local symmetry (on the faces) or 5-fold local symmetry (at the corners). Recent X-ray diffraction studies by Harrison and co-workers in tomato bushy stunt virus (Winkler, et al., 1977) have supported the icosahedral symmetry concept and showed that quasi-equivalent bonding may be accomplished by subunits containing rigid domains joined through flexible hinge regions.

As experiments dealing with virus structure became more sophisticated, however, it became clear that an accurate description of the mature virus shell was not a sufficient description of its for-

mation. Shortly after the introduction of Caspar and Klug's simple theory of icosahedral virus structure, Epstein and co-workers (1963) showed that the formation of the T4 phage head required the products of a very large number of genes. Subsequently, Laemmli showed that complex intermediate structures accumulated in cells infected with mutants in these genes (Laemmli, 1970).

As the genetic and structural complexity of the system unfolded, it became clear that the assembly of the large bacteriophages was not simply a self-assembly process involving the components of the mature virion. The functions of a number of accessory proteins seemed also to be involved. In fact, the study of the disposition of these auxiliary proteins during capsid assembly has been highly instructive in understanding how capsid shells are constructed (Casjens and King, 1975). It appears that all of the large bacteriophages augment the basic capsid-building capacity of the major head protein by the strictly ordered addition, processing, or release of auxiliary proteins.

Naively, one might think that there would be a number of ways to proceed to assemble the mature virion. Three general classes of packaging models are: 1. The capsid forms around a nucleic acid-containing core (Kellenberger, et al., 1968); 2. nucleic acid and the protein subunits combine cooperatively in a step-wise manner to form the capsid and 3. the nucleic acid is packaged into a pre-formed capsid, the "headful" encapsidation model (Streisinger, et al., 1967; Luftig, et al., 1971). In fact, the basic approach to capsid assembly

and DNA packaging is the same for all large viruses containing double-stranded DNA, ^{i.e.,} mechanism 3 above: the phages assemble a capsid shell first, then fill it with DNA. Condensing rigid double-stranded DNA molecules apparently requires very complex machinery. The precursor shell seems to be a major component of this machinery.

We therefore see that it is the precursor shell as a DNA packaging organelle, which must be constructed, and not just a passive protective shell. The assembly of such precursor shells has turned out to be quite an extraordinary process. In P22, the assembly of the major coat protein into a functional shell depends upon a scaffolding protein which polymerizes with it into a double-shelled structure containing both proteins (King and Casjens, 1974; Earnshaw et al., 1976). In concert with DNA packaging, all of the scaffolding molecules depart from the shell. These molecules complex again with newly synthesized coat protein to form more proheads.

Before describing the detailed pathway of P22 morphogenesis I'll briefly review the maturation of phages, T4, λ , and T7.

A major unsolved problem in phage assembly is the nucleation and polymerization of the capsid subunits to form a closed precursor capsid shell. Do you start at one pole and aggregate continuously to the other? Or, is it more efficient to build smaller assemblies first, perhaps the vertices, and then assemble these? Or, does an assembly core form and the major capsid subunits aggregate around that? Again there is a pattern common to all of the double-stranded DNA phages. Each initiates capsid formation with the help of an assembly core (Showe and Black, 1973) or scaffolding protein (King, et al., 1973) as with P22, made up of proteins which do not appear in the final

structure.

Simon showed, for example, that cores are actually visible inside early T4 capsid intermediates by using thin-section analysis of wild-type infected cells (1972). These core-containing particles had been described earlier as accumulating in mutant-infected cells (Laemmli, et al., 1970). Such particles were also found as kinetic intermediates in pulse-labelled wild-type T4 infected cells (Laemmli and Favre, 1973). Finally, Bijlenga, et al. (1973) showed that these core-containing particles, called tau-particles, made at high temperature in cells infected with a ts mutant in gene 24, were converted to phage when gp24 was activated by a temperature downshift. In an important control to this experiment, Bijlenga and co-workers (Bijlenga, et al., 1974) showed that this conversion was conservative, ruling out that the tau-particles were breaking down and reassembling during the post-shift period.

Biochemically, attempts to isolate tau-particles failed, apparently because of the tendency of these particles to adhere to each other or the membrane. Although it was not possible to analyze the protein composition of the tau-particles directly, examination of the behavior of several mutants suggested that the morphological internal core was composed of several proteins and served as an assembly core in shell assembly (Showe and Black, 1973). At least four phage proteins, gp22 and three internal proteins, IPI, IPII and IPIII, were part of the core. In the absence ^{of} these four proteins, no organized structures formed.

In phage λ , the development of an in vitro DNA packaging system (Kaiser and Masuda, 1973; Hohn, et al., 1974) allowed one to test directly whether a particular structure could serve as a precursor to

the mature virus. Morphogenesis of phage λ capsids involved precursor structures distinguishable from the mature phage. The term "petit λ " was used initially to describe the small, empty-looking particles seen in all negatively stained λ lysates except E^- lysates, which lack the major head protein gpE (Murialdo and Siminovitch, 1972; Casjens, et al., 1972). Several types of petit λ have been described, differing in their lysate source and protein composition (Ray and Murialdo, 1975; Hohn, et al., 1975). Originally it was thought that these small, head-like particles were aberrant by-products of the assembly pathway. However, experiments using purified petit λ particles as head donors in the in vitro DNA packaging system showed that one type of petit λ , called the prehead, was indeed a precursor of the mature phage (Hohn and Hohn, 1974; Kaiser, et al., 1975).

Although petit λ particles looked empty in negative stain, subsequent thin-section analysis of wild-type and mutant-infected cells showed a number of core-containing petit λ particles. These studies indicated that the core-containing prohead I petit λ was converted to an empty prohead II petit λ which had lost its core. The prohead II particle was subsequently filled with DNA to form the mature λ capsid (Zachary, et al., 1976). The authors observed core-containing structures in thin sections through every induced mutant lysogen analyzed with the exception of E^- lysates, which lack the major coat protein, and $Nu3^-$ lysates. $Nu3^-$ inductions produced misshapen, amorphous structures, which were variable and difficult to recognize. Furthermore, using analysis of double mutant inductions,

they showed that gpNu3 was required at a very early step in λ capsid morphogenesis. Therefore, these authors concluded that gpNu3 may be a scaffolding protein required for the formation of the λ prohead.

Protein analysis of various petit λ particles supported the conclusion that gpNu3 was part of an assembly core, as it was present in core-containing structures and absent in empty particles (Ray and Murialdo, 1975).

There is also an in vitro DNA packaging system for phage T7 (Kerr and Sadowski, 1974). Core-containing prohead structures have been purified and been shown to be capable of complementing in vitro a cell-free extract lacking heads (Roeder and Sadowski, 1977). Electron microscopic examination of negatively stained mutant cell lysates showed that no structures were produced in 10^{-7} lysates which lack the major head protein. However, 9^{-} lysates also contained no structures, suggesting that gp9 functioned as a scaffolding protein of prohead formation. The proheads produced after infection with mutants in genes 8, 14, 15 and 16, had aberrant protein compositions and lacked cores when examined in the electron microscope. Although some structure formation proceeds in the absence of these proteins large numbers of aberrant spiral-shaped or tubular structures are also observed. Thus, these proteins may also be involved in the formation of the assembly core.

The transition from prohead precursor to mature phage particle is a complicated process in which all the well-studied phages containing double-stranded DNA undergo a major change in their protein composition (King, et al., 1973). In phage T4, not only does the major

coat protein, gp23, get cleaved, but the internal assembly core proteins, IPI, IPII, IPIII, and gp22, are cleaved as well. While the gp23 cleavage step appears to occur prior to DNA packaging, the removal of the assembly core from the T4 precursor particle by proteolytic cleavage appears to be specifically linked to DNA packaging (Laemmli, et al., 1974). In phage λ , gpNu3, which is essential for prohead formation, is totally lost from the particle (Hendrix and Casjens, 1975) and may be degraded (Ray and Murialdo, 1975). Two core-related minor proteins, gpB and gpC, are retained in the finished head but in altered form: gpC fuses with the major head protein, gpE, and together they are cleaved; gpB is cleaved as well (Casjens and Hendrix, 1974). The final modification in λ head maturation involves the addition of the second major coat protein, gpD. Present in equal numbers with the gpE and present on the outside of the head, gpD does not seem to become part of the head until the head is filled with DNA (Hohn and Hohn, 1973).

In phage T7, the scaffolding protein, gp9, departs either before or during DNA packaging, and two other proteins leave the capsid once DNA packaging is complete (Roeder and Sadowski, 1977).

A consistent feature of these pathways is the mutual exclusion of the unaltered scaffolding protein and the DNA: there is no case in which both have been found to be present simultaneously within the capsid. There are several possible explanations for this: The core proteins may function exclusively in capsid initiation and coat protein aggregation. Once this function was complete, they would no longer be required and may simply be removed to make room for the

DNA. This hypothesis seems insufficient to explain the behavior of the core proteins in T4 and λ , because altered forms of at least some of the core proteins remain inside the mature head. The hypothesis gains somewhat more validity in the case of T7 (and in P22, as we shall see) where the scaffolding protein is completely removed. Alternatively, the virus may make efficient use of scaffolding proteins as active parts of the machinery involved in the condensation of the DNA. Laemmli (1975) has suggested such a role for a fragment of one of the core proteins, gp22, in T4 DNA packaging.

Bacteriophage P22 Assembly

P22 is a lysogenic phage of Salmonella typhimurium. It was discovered by Zinder and Lederberg (1952), who found that it transferred bacterial genes from one host to another. Morphologically, it is relatively simple. The mature phage head is isometric, about 60 nm in diameter (Lenk, et al., 1975) with a small tail at one vertex (Israel, et al., 1967). It contains one double-stranded DNA molecule (molecular weight, 27×10^6) which is circularly permuted and terminally repetitious (Rhoades, et al., 1968). The growth and DNA metabolism of infected cells has been studied in detail by Botstein and Levine (1968). The overall sequence of events in DNA packaging has been described by Tye and co-workers (1974). They have shown conclusively, by examining the distribution of mature chromosome ends, that Streisinger's headful packaging model is operating in P22 DNA packaging (Streisinger, et al., 1964, 1967).

Amber mutations defining 14 late cistrons have been isolated and mapped by Botstein, Chan and Waddell (1972) and Poteete and King

(1977). Twelve of these cistrons specify proteins involved in particle assembly, (the other two control lysis). The morphogenetic genes are clustered together on the chromosome, and they are further grouped according to their specific functions in particle assembly. This is shown in Figure 1. Genes 5 and 8 specify proteins directly involved in the construction of the capsid shell. The gene 5 product is the major coat protein while the gene 8 product is the scaffolding protein absent from mature phage. Genes 1, 2, and 3, code for proteins which are necessary for the packaging of the DNA into the precursor shell. Genes 4, 10 and 26 are responsible for the production of proteins which stabilize phage heads newly-filled with DNA. Genes 7, 16 and 20 specify proteins which are incorporated into the capsid at its inception, but which are not necessary for head formation; they appear to function later in the phage lifecycle, in the injection of DNA into the host cell (Hoffman and Levine, 1975; Poteete and King, 1977; R. Griffin Shea, unpublished experiments). Gene 9 is separated from the rest of the morphogenetic genes and codes for the baseplate protein (Israel, et al., 1967). The remaining two genes, 13 and 19, are involved in cell lysis.

I have summarized the defective phenotypes of the mutants in the morphogenetic genes in Table 1. I have paid particular attention to the state of the baseplate protein in the mutant-infected lysates, as this will be important in the discussion of the experimental results in Chapter I of this thesis.

The late mutants of P22 have been examined in detail by Botstein, King and their colleagues (Botstein, et al., 1973; King, et al., 1973;

Figure 1Map of the Morphogenetic Region of the P22 Chromosome

Gene sizes have been drawn proportional to the molecular weights of their polypeptide chains. The region to the left of gene 9 contains genes functioning in superinfection exclusion and control of lysogeny. The map is based on data from Botstein, et al. (1972) with additions from Poteete and King (1977).

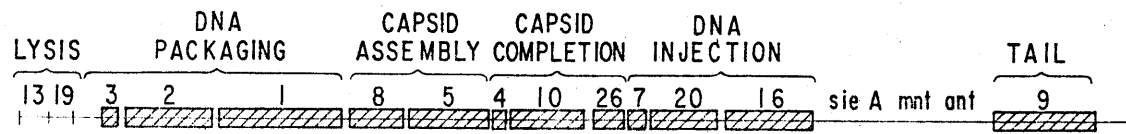


TABLE 1

Defective Phenotypes of Mutant Lysates

<u>Lysate</u>	<u>Function of Missing Gene Product</u>	<u>Major Capsid Structure</u>	<u>Form of Tail Spike Protein</u>
13 ⁻ , 19 ⁻	Cell lysis	Infectious phage particle	On particle, soluble
5 ⁻	Major coat protein	-	Soluble
8 ⁻	Scaffolding protein present only in proheads	Spirals, aberrant shells	Soluble
1 ⁻	Minor structural protein of proheads and phage, required for DNA packaging	Proheads (only)	Soluble
2 ⁻	Non-structural protein, required for DNA packaging	Proheads (only)	Soluble
3 ⁻	May be a minor phage structural protein, required for DNA packaging	Proheads (only)	Soluble
7 ⁻	DNA injection	Non-infectious, phage-like particles	On particle, probably also soluble
16 ⁻	DNA injection	"	"
20 ⁻	"	"	"
4 ⁻	Head completion (neck?)	Empty heads	Soluble
10 ⁻	"	"	"

TABLE 1 (Contd.)

Defective Phenotypes of Mutant Lysates

<u>Lysate</u>	<u>Function of Missing Gene Product</u>	<u>Major Capsid Structure</u>	<u>Form of Tail Spike Protein</u>
26 ⁻	Head completion	Empty heads	Soluble
9 ⁻	Tail spike	Heads	-

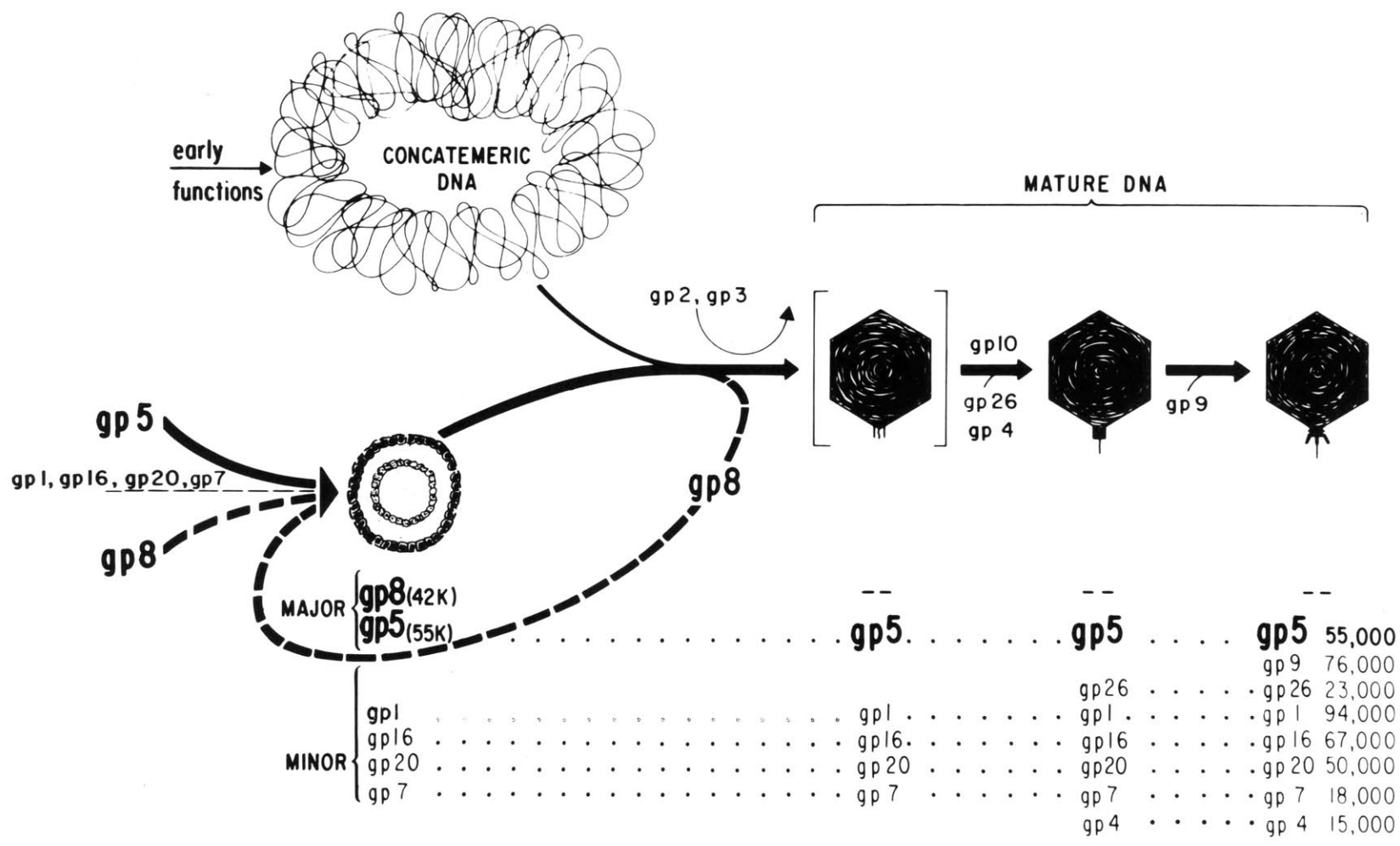
1 Defective phenotypes taken from Botstein, et al. (1973).

Poteete and King, 1977). The phenotypes of these mutants have been characterized in terms of the extent of DNA maturation, the production of head-related structures as seen in the electron microscope, and the protein compositions of infected cell lysates and the structural intermediates purified from them. The genes specifying all of the known P22 morphogenetic proteins have been identified. Conversely, the proteins corresponding to the known P22 morphogenetic genes have also been identified. Using the accumulated observations from these genetic, biochemical and electron microscopic analyses, the investigators have been able to define precisely, (though not yet understand completely) all of the steps in the assembly of the particle which are specified by phage genes. The pathway of P22 phage assembly is presented in Figure 2.

As illustrated in the figure, the products of genes 5 and 8 assemble to form the prohead precursor structure, the earliest structural intermediate which can be seen in infected cells (King, et al., 1973; Lenk, et al., 1975). Pulse-chase experiments using wild-type infected cells indicated that the proheads were precursor particles (King, et al., 1973). The prohead intermediates in the pulse-chase experiments were indistinguishable from proheads accumulating in 2⁻ and 3⁻ mutant infected cells. In fact, the proheads accumulating at high temperatures in an infection using a reversible 3^{-ts} mutant were shown to be precursors to phage. After activation of gp3 by temperature downshift, radioactive label was transferred from the prohead precursors into phage. Temperature shift experiments were also done

Figure 2
P22 Morphogenetic Pathway

This diagram shows the intermediate structures and gene controlled steps in the assembly of infectious bacteriophage P22 particles. Gene products are designated 'gp' followed by the number of the gene. The major coat protein gp5 polymerizes with the scaffolding protein gp8 and four minor protein species to form the precursor prohead. With the function of the gene 2 and 3 products, the prohead encapsidates a headful of DNA from the replicating concatemeric DNA (Tye, Huberman, and Botstein, 1974). All of the gene 8 product exits in this process and then recycles. Three gene products add to the unstable newly filled heads converting them to stable mature heads. In the absence of these steps the bracketed particle loses its DNA, yielding empty heads (not shown). Also not shown are the aberrant spiral and shell structures which form when the scaffolding protein is removed by mutation. The molecular weights shown are for the single polypeptide chains. The active form of some of the precursor proteins may be as multimers. This figure summarizes results from Botstein, Waddell and King (1973), King, Lenk, and Botstein (1973), King and Casjens (1974), and Poteete and King (1977).



using 2⁻ and 3⁻ ts mutants (Lenk, et al., 1975). In these experiments, the production of phage from proheads accumulated at high temperature was assayed by electron microscopic examination of ultra thin sections of infected cells at various times after temperature downshift. With time after the temperature shift, in concert with increasing viable phage titer, the proheads were converted to DNA-filled particles. With the recent development of an in vitro DNA packaging system in P22 (V. Jarvik, S. Gottesman, and D. Botstein; A. Poteete and D. Botstein, manuscript in preparation) it has been possible to test the precursor nature of the prohead particles directly. In agreement with the earlier in vivo results, wild-type, 2⁻ and 3⁻ proheads have been shown to be head donors in a cell-free DNA packaging system. Proheads from a 1⁻ infection, though morphologically normal, are inactive. The gene 1 protein is present in proheads from wild-type infected cells, and in the proheads accumulating in 2⁻13⁻ infected cells.

As indicated in Figure 1, three minor proteins are also present in proheads, gp7, gp16, and gp20. These proteins, though assembled early, are not required for the assembly of morphologically normal phage particles; however, these phage-like particles are non-infectious. The proteins probably function in DNA injection during the subsequent infection cycle (Hoffman and Levine, 1975; Poteete and King, 1977; R. Griffin Shea, unpublished experiments).

The P22 prohead precursor shell loses its scaffolding protein prior to, or during, the packaging of DNA. Unlike the other phages discussed, the scaffolding protein is released unclesaved from the particle (King and Casjens, 1974). In fact, the scaffolding protein is re-

cycled and used in multiple rounds of prohead assembly.

Thus it operates catalytically in prohead assembly within the cell even though the prohead can be isolated as a stable structure. The products of gene 1, 2, and 3, are required for DNA packaging, though their functions in this process are not well understood (Botstein, et al., 1973; King, et al., 1973). Given that proheads are precursors to DNA encapsulation and cutting, the products of genes 1, 2, and 3, must mediate this process because lysates defective in these genes accumulate proheads and uncut DNA. The product of gene 1 is a structural component of proheads, empty heads and phage, although, as noted above, inactive proheads, are formed in its absence. The product of gene 2 is not associated with any of the particles in phage-infected cells. Very little is known about its role in DNA packaging; however, DNA packaging in vitro is gp2-dependent and purification of the protein is underway using DNA packaging activity as an assay (A. Poteete, personal communication). The product of gene 3 is variably found associated with empty heads and phage (unpublished experiments). There is some indication that gp3 may be directly involved in DNA cleavage. There is slow solubilization of the concatemeric DNA which accumulates in 5⁻, 8⁻, 1⁻ and 2⁻ infections, but not in 3⁻ infections (Botstein, et al., 1973). In addition, Raj and co-workers (1975) have found that phage mutants giving high frequencies of generalized transducing particles map in gene 3, supporting this idea.

Continuing along the pathway, once DNA has been incorporated into the particle, it remains stably packaged only after the action of the products of genes 4, 10, and 26. Electron microscopic observation of

negatively stained preparations of particles from 4⁻, 10⁻, and 26⁻ mutant infections show that the heads are the size and shape of phage particles but they are empty (Botstein, et al., 1973); however, examination of ultrathin sections of cells infected with these mutants show that a substantial number of particles are filled with DNA inside the cell (Lenk, et al., 1975; Poteete and King, 1977). Thus, the empty heads derived from 4⁻, 10⁻, and 26⁻ infections were derived from particles initially full of DNA, but the DNA was substantially lost after cell lysis. The products of genes 4, 10, and 26 are not required for the cutting of the DNA (Botstein, et al., 1973; Poteete and King, 1977). The products of all three genes appear to be structural components of the phage, although gp10 is hard to detect because the gp10 band is obscured by the coat protein band in SDS-gels (King, et al., 1976). Empty heads lack scaffolding protein (King, et al., 1973). The unstably packaged heads that accumulate in 4⁻, 10⁻ and 26⁻ infections can be rescued to a limited extent by in vitro complementation with an extract containing these gene products (Botstein, et al., 1973; Poteete and King, 1977). The empty heads in a 26⁻ infection often show tails; 4⁻ and 10⁻ empty heads do not show tails.

Once DNA has been stably packaged, the particles show a distinct, short, cylindrical neck structure with a single fiber projecting from it (Yamamoto and Anderson, 1961; Botstein, et al., 1973). It is possible that the products of genes 4 or 10 and possibly 26, are situated in the neck region. Full heads showing this neck and fiber structure accumulate in cells infected with mutants of gene 9, the

tail protein cistron. They are stable and very similar to complete phage particles, except that they lack the gene 9 baseplate protein. The last step in P22 morphogenesis is the addition of this protein to the phage head (Israel et al., 1967). When tail parts are limiting, only about 3 tail parts/phage are required to form an infectious particle (Israel et al., 1967). In addition to its structural role in forming the P22 baseplate, the product of gene 9 also has enzymatic activity. It acts as a specific endoglycosidase (Israel et al., 1972) in cleaving the O-antigen, an important constituent of the outer membrane of gram-negative organisms (Wright and Kanegasaki, 1971; Iwashita and Kanegasaki, 1975; Takeda et al., 1975), and this process has been implicated in adsorption of the bacteriophage to the host cell (McConnell, 1976). Iwashita and Kanegasaki (1976) have purified P22 baseplate protein using its glycosidase activity as an assay. Recently, P. Berget and A. Poteete have purified the product of gene 9 of phage P22 using its tailing activity as an assay (unpublished experiments). Preparations of this material were used in the experiments of Chapters I and II.

As regards DNA maturation during head assembly, Botstein and co-workers (1973) showed that uncut, concatemeric DNA accumulated in cells infected with mutants blocked at or before the prohead assembly step. This includes 1⁻, 2⁻, 3⁻, 5⁻, and 8⁻ lysates. Therefore, the cutting of the DNA apparently requires that head assembly proceed to the point of encapsulation of the DNA. The actual entry of the DNA into the pre-

cursor shells is probably coupled to the exit of the scaffolding protein since all phage structures containing DNA, or which have contained DNA at some point in their history, lack the scaffolding protein (Casjens and King, 1974). P22 solves the problem of head assembly in a unique way. The scaffolding protein is released uncleaved from the precursor shell and is then re-used in several subsequent prohead assembly reactions. This was shown by pulse-chase experiments in which the radioactivity in labeled coat protein molecules chased out of the proheads, out of empty heads, and into phage. On the other hand the amount of radioactive scaffolding protein in proheads did not decrease during the chase (Casjens and King, 1974; King and Casjens, 1974).

The recycling of the scaffolding protein means that it must be released functionally unaltered from the prohead precursor shell. Thus, the disposition of the scaffolding protein is of a very different nature than that of the disposable assembly core proteins which are proteolytically processed in T4 and λ head morphogenesis. We might ask, then, how the coat protein and the scaffolding protein interact, both during assembly and in the prohead structure. I will discuss in some detail the states of these proteins in 5⁻ and 8⁻ lysates as these lysates have been used extensively in experiments throughout this thesis.

Proper shell formation by coat protein subunits is entirely dependent upon their association with the scaffolding protein (King, et al., 1973). Cells infected with amber mutants in gene 8 synthesize substantial amounts of gp5 coat protein but it cannot assemble efficiently into closed shells. Instead, three major types of coat

protein aggregates form slowly: spherical shells of the diameter of proheads; smaller spherical shells approximately 2/3 the prohead diameter; and spiral structures, which look as though one edge of the growing shell has missed the opposite edge and continued polymerizing (Lenk, et al., 1975). Tubular forms of P22 have never been observed suggesting that the coat protein itself has considerable form-determining specificity (King, et al., 1973). Low-speed centrifugation of radioactively labelled 8⁻ lysates indicates that about one-half of the coat protein present in an 8⁻ lysate associates with the membrane fraction.

What about the scaffolding protein? Does it show a tendency to form a shell in the absence of the coat protein? Apparently not. Electron microscopic studies examining either negatively stained 5⁻ infected cell lysates (King, et al., 1973) or ultra thin sections of 5⁻ infected cells (Lenk, et al., 1975) have failed to reveal any kind of particles in these cells. Sucrose gradient analysis of labelled 5⁻ infected cell extracts similarly fail to show any large aggregates of gp8 (Casjens and King, 1974). Therefore, it appears that the scaffolding protein must be activated for assembly by interaction with the coat protein. A mechanism for head assembly consistent with these observations is the formation of an initial complex between coat protein and scaffolding protein, and their subsequent co-polymerization.

It is not clear to what extent the scaffolding protein and the coat protein subunits continue to interact with one another in the prohead. Although the preceding data suggest that the scaffolding protein itself has little tendency to form a shell, several indepen-

dent experiments investigating the fine structure of proheads suggest that, in association with the coat protein, gp8 forms a shell within the outer gp5-containing shell. Negatively stained proheads appear as spherical structures with scalloped edges containing organized internal material (Botstein, et al., 1973). The images of proheads in thin sections also suggest the presence of an inner ball or shell (Lenk, et al., 1975). Conditions were found in which treatment of the proheads with detergent released the internal core material. The resultant empty shells were composed entirely of gp5, the coat protein. All of the gp8 was solubilized by this treatment, indicating that it might form the inner shell (Casjens and King, 1974). The structure of proheads was also studied using low angle X-ray diffraction of particles in solution (Earnshaw, et al., 1976). These studies show that proheads have a smaller radius than phage and contain considerable density at an inner radius. The simplest model to account for these observations is one in which the gp8 forms a thick shell within the outer coat protein shell. As expected, X-ray analysis also shows that treatment of the proheads with SDS detergent, which releases gp8, causes the loss of the inner material. In addition, the scattering experiments yielded information on the packing of the coat subunits in proheads and phage. Results indicate that there is no gross reorganization of the coat subunits; rather the whole lattice is expanded by about 10% during maturation.

Thus, the electron microscopic and X-ray evidence suggest that the bulk of the scaffolding protein is on the inside of the head. Analysis of the protein composition of proheads indicates that there are about 250 molecules of scaffolding protein for every 420 molecules of the

coat protein. Of course, this poses the problem of how 250 molecules of a protein of 42,000 daltons molecular weight get out of the pro-head during phage assembly. This question is specifically addressed in the experiments of Chapter III. ^{IP} The experiments presented in this thesis are based on the generation of antibodies directed against the genetically defined P22 antigens. Such a combination of immunology and genetics can be very powerful in the elucidation of fine structure. In 1965, Edgar and Lielausis developed a method to examine the role of various gene products in the synthesis of phage T4 antigens. Crude amber mutant lysates, which generally lack the product of a single gene, were tested for their ability to block the phage-neutralizing activity of anti-T4 phage serum. In the phage system, the titering of plaque-forming units is a very sensitive method for the detection of infectious particles. Thus, the methodology that they developed in the serum blocking experiments provided a very sensitive assay for the genetic identification of the phage target antigens of the neutralizing antibodies. The rationale of this approach and a set of theoretical serum blocking curves are presented in section of Materials and Methods. (This section should be read before considering the experimental results of serum blocking experiments using anti-P22 sera, which are presented in Chapter I).

In 1970, Yanagida and Ahmad-Zadeh extended the combined genetic and immunological approach to the localization of gene products on the phage structure. In these experiments, absorption of the serum with crude amber mutant lysates was used to generate monospecific sera. These sera were then incubated with phage or phage precursor structures, and the particles were examined for visible antibody binding in the

electron microscope. In this procedure, the binding of antibodies directed against known phage proteins to specific sites on the phage localize the gene product to that position on the structure. In later experiments, Yanagida (1972) fully characterized the anti-T4 sera he obtained by the technique of immunoelectrophoresis. In specifying the total phage-specific antibody composition of the serum, Yanagida was able to interpret the absence of binding by a component antibody class, as evidence that the target antigen was not exposed on the particle surface. I utilize similar experimental approaches in Chapters II and III to analyze the antigenic structure of bacteriophage P22.

MATERIALS AND METHODS

(a) Bacterial Strains

Bacterial host strains for P22 phage are from the collection of D. Botstein and are derivatives of Salmonella typhimurium LT2. Strain DB7004 is permissive for amber mutants and was used for plating and stock-making. Strain DB7000 was used as the restrictive host for amber mutants and was used to make non-permissive amber mutant lysates. These strains are described in Susskind, et al. (1974).

(b) Phage Strains

The P22 phage mutants are from the collection of D. Botstein and have been described previously (Botstein, et al., 1972, 1973; Poteete and King, 1977). Representative amber alleles for each gene were as follows: gene 1, amN10; gene 2, amH200; gene 3, amN6; gene 5, amN114; gene 8, amH202, amH1348, amN123; gene 9, amN108, amH1014, amE1017, amN110; gene 10, amN107; gene 13, amH101; gene 16, amN121; gene 20, amN20; gene 26, amH204; and gene 7, amH1375.

Each phage strain also contains the clear plaque mutation c_1^7 to ensure entry into the lytic growth cycle upon infection, except for amH104 (gene 9), which carries the clear plaque mutation c_2^5 . In general, the experiments were done with double amber mutants which contain, in addition to the allele of interest, an amber mutation in gene 13, amH101. Absence of the gene 13 product prevents natural cell lysis (though the cell contains lysozyme, the gene 19 product) and phage production continues past the normal lysis time. After shaking with chloroform (CHCl_3), 13^- infected cells lyse rapidly releasing a large burst of phage

or phage proteins.

When recombinant phage strains were constructed (Botstein, et al., 1973) each allele in a multiply marked recombinant was checked by recombination or spot complementation against strains carrying the parental allele.

(c) Preparation of Phage Stocks

Phage stocks were prepared by the following methods: plate stock method - 2×10^5 phage were mixed in soft top agar with approximately 2×10^7 DB7004 (su^+) bacteria and were spread on an LB agar plate. The plate was incubated at 30°C for 7-9 hours, and the soft top agar was then removed from the plate and suspended in several ml of DF. Agar and bacterial debris were removed by centrifugation at $6900 \times g$ for twenty minutes. Liquid stock method - A single plaque was suspended in 25 ml of LB broth to which 0.5 ml of an overnight bacterial culture of DB7004 was added. The infected culture was aerated vigorously at 25°C for 6-8 hours. Bacterial debris was removed by centrifugation at $6900 \times g$ for ten minutes, and the phage were pelleted by centrifugation at $35,000 \times g$ for 90 minutes and resuspended in 2 ml buffered saline. In experiments requiring large numbers of particles, secondary phage stocks were used to infect large volumes of cells. These stocks were prepared by growing 1 liter of DB7004 cells to about $2-4 \times 10^8$ cells/ml in LB. Phage stocks prepared by either of the above two methods were used to infect the cells at a multiplicity of about 7 phage/cell. The infected cells were aerated vigorously at 37°C until lysis (1-2 hours). Chloroform was added and the cells were incubated on ice for several minutes. Bacterial debris was removed by centrifuging the suspension

at 6900 x g for 20 minutes. The supernatant fraction was decanted for use as a secondary phage stock.

(d) Media and Chemicals

LB broth (Kikuchi and King, 1975) was used for growing bacteria and phage stocks. LB bottom and soft agar (Adams, 1959) were used for plating. Dilution fluid (DF) contains 1 g trypton (Difco) and 7 g NaCl per liter. Minimal medium for radioactive labeling experiments was made up from a filtered solution containing per liter: 5.8 g Na_2HPO_4 ; 3.0 g KH_2PO_4 ; 0.24 g MgSO_4 ; 1.0 g NH_4Cl ; and 0.5 g NaCl. The solution also contained 50 $\mu\text{g/ml}$ leucine which is required for growth of the auxotrophic strain, DB7000, used in these experiments. A freshly prepared 40% (w/v) glucose solution, also filtered, was diluted 1:100 into the minimal medium just prior to use. Buffered saline (BS) is described by Chan and Botstein (1972). Stock TM buffer is 1M Trizma base (reagent grade, Sigma Chemical Co.) and 10^{-1} M MgSO_4 brought to pH 7.5 with HCl acid. This is diluted 1:100 for use as TM buffer. Immuno buffer is made by a 1:50 dilution of stock TM into 0.85% NaCl. High resolution buffer (Gelman Instrument Co., No. 51104) at pH 8.8 was used as running buffer in immunoelectrophoresis experiments. Agarose (Electrophoresis grade) was obtained from Sigma Chemical Co. A 1% agarose solution, made up in 1:4 diluted high resolution buffer, was used as the gel matrix in immunoelectrophoresis.

Crystalline bovine pancreatic DNase I, DN-C1, was obtained from Sigma Chemical Co. CHCl_3 , A.C.S. grade was obtained from Fisher Scientific Co. Sodium azide was obtained from J.T. Baker Chemical Co.

Naphthol blue black (Amido Black 10B; Buffalo Black NBR), used for staining immunoprecipitates in immunoelectrophoresis, was obtained from Sigma Chemical Co. Antifoam A emulsion, from Sigma Chemical Co., was used to prevent foaming in lysate preparations involving 1 liter or more of cell cultures. ^{14}C -labeled amino acids mixture (0.1 mCi/ml) was obtained from New England Nuclear Corporation (NEC-445). Complete Freund's adjuvant was obtained from Difco Laboratories. Reagents for polyacrylamide gel electrophoresis were as described in Kikucki and King (1975).

(e) Preparation of Rabbit Antiserum

Hyperimmune sera, termed anti-phage, anti-prohead and anti-head serum, were obtained by injection of P22 phage, prohead and tail-head structures, respectively, into white, virgin female New Zealand rabbits. Immunogens at approximately 10^{13} particles/ml were emulsified with an equal volume of complete Freund's adjuvant. A volume of 0.5 ml of the emulsion was injected between the toes into each footpad and subcutaneously into the back, a total of 2.5 ml of each preparation per rabbit. In general, the rabbits were bled from the ear vein for three consecutive days, approximately every three weeks, as outlined in the accompanying table. The volume of blood withdrawn over a three day period was approximately 120 ml.

The rabbit which produced the anti-head serum was approximately six months old. The rabbits which produced anti-phage serum and anti-prohead serum had been injected previously at least once the year before with P22 phage and proheads, respectively, by S. Casjens. In this previous procedure, approximately 5×10^{11} particles in buffer were in-

TABLE 2INJECTION AND BLEEDING SCHEDULE

<u>Injection</u>	<u>Bleeding</u>	<u>Antiserum Pool Designation</u>
<u>1974</u>	<u>1975</u>	
12/30	1/13 - 1/15	1
	2/3 - 2/5	4
	2/24 - 2/26	7
	3/17 - 3/19	8
	6/9 - 6/11	9
	7/29 - 7/31	12
<u>1976</u>	<u>1976</u>	
3/9	3/30 - 4/1	14
	4/23 - 4/25	15
	5/17 - 5/19	16
	6/14 - 6/16	17

jected subcutaneously into the back 2-3 times a week for three weeks. After a period of three weeks or more, 5×10^{11} particles were again injected subcutaneously.

(f) Preparation of Immunogens (In collaboration with W. Earnshaw)

(i) Prohead Preparation for First Injection

An overnight culture of DB7000 (su^-) cells was diluted 100-fold into 12 liters of LB broth and grown with vigorous aeration at 37°C to approximately 2×10^8 cells/ml. Three hundred ml of 2^{-13} phage in LB at 10^{11} phage/ml were added to give a multiplicity of about 10 phage/cell. Cells infected with mutants defective in gene 2 are blocked in DNA packaging; proheads are the only class of particles accumulating in these cells. The infected cells were harvested three hours later by continuous centrifugation in a refrigerated Sharples centrifuge. The cell pellet was resuspended in approximately 15-30 ml TM buffer. Several drops of CHCl_3 were added and the solution vortexed vigorously. Cell lysis was evidenced by the extreme viscosity of the chloroformed mixture. A total of 1.5 mg DNase I was added and the solution was vortexed and kept on ice until the viscosity was significantly reduced. Cell debris was removed by centrifugation at $6900 \times g$ for 15 minutes.

The supernatant fractions were pooled and layered onto 15 ml of 15% sucrose over a CsCl shelf ($\rho = 1.6 \text{ gm/ml}$) of 1.5 ml and centrifuged in an SW 27.1 rotor at 25,000 rev/min for 4 hours at 20°C . An opaque band was collected from the shelf and dialysed overnight against TM buffer.

This material was centrifuged through a 15 ml 10-30% sucrose

gradient over a 15 ml CsCl shelf ($\rho = 1.6$ gm/ml) at 25,000 rev/min for 2.5 hours at 15°C in an SW 27.1 rotor. A clear blue diffuse band above the CsCl shelf was collected and dialysed overnight against TM buffer. This solution contained approximately 10^{13} proheads as roughly determined by electron microscopy. The prohead preparation is shown in Figure 3.

(ii) Phage and Tail⁻ Head Preparation for First Injection

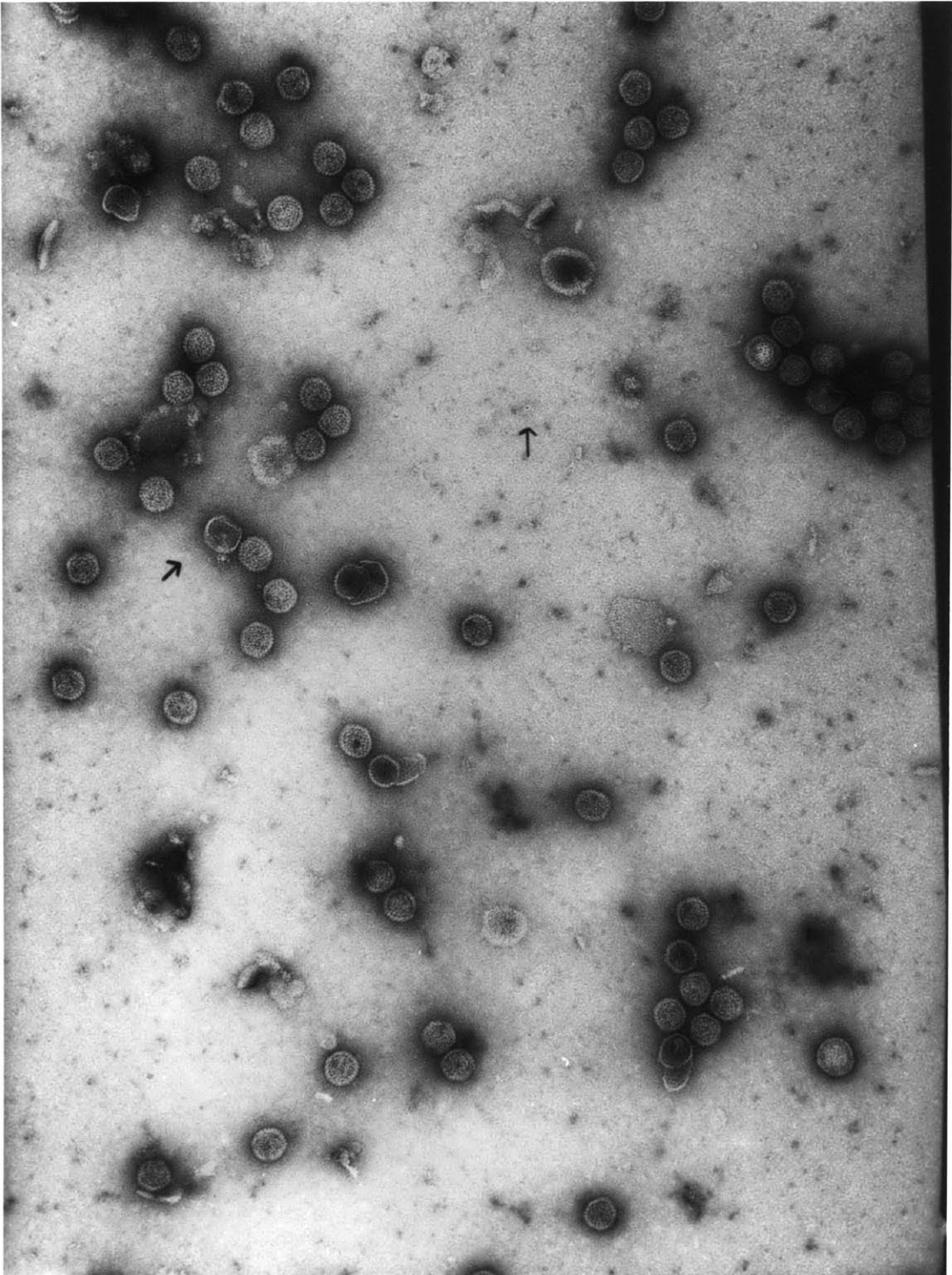
Two aliquots of an overnight culture of DB7000 (su⁻) cells were diluted 100-fold into each of two 12 liter batches of LB, and grown with vigorous aeration to 2×10^8 cells/ml at 37°C. To one culture, 300 ml of wild-type 13⁻ phage at 8×10^{10} phage/ml were added (moi = 10); to the other, 270 ml of 9⁻13⁻ phage at 10^{11} phage/ml (moi = 12). Cells infected with mutants of gene 9 accumulate complete phage heads, lacking only the gene 9 tail protein. The infections continued for 3 hours and 15 minutes.

The infected cells were pelleted by Sharples continuous centrifugation, first the 9⁻13⁻ preparation, and then the wild-type 13⁻ infected cells. The pellets were resuspended in 15-30 ml of TM buffer. The cells were lysed with several drops of CHCl₃ added with vigorous vortexing. A total of 0.75 mg of DNase I was added and the mixture stood on ice, with intermittent vortexing, for several minutes.

The preparations remained somewhat viscous and the material was centrifuged several times at 6900 x g for 20 minutes. The accumulated pellets were re-extracted 4 times. Several aliquots of 1.5 ml each of the pooled supernatant fractions were layered on top of 15 ml of 30% sucrose with a 1.5 ml CsCl shelf ($\rho = 1.6$ gm/ml).

Figure 3Proheads Purified from Cells Infected with an Amber
Mutant Defective in Gene 2

The proheads were purified as described in section f, i. Since these particles were isolated by sucrose gradient centrifugation, without a density fractionation, they are contaminated with higher levels of host material than were the DNA-containing particles. The arrow points to a phage ghost, presumably from the infecting phage used to prepare the infected cells from which the proheads were purified. These represented about 1% (3/283) of the particles seen in electron micrographs of this preparation. Another arrow points to what appears to be an isolated tail structure, probably the result of the breakdown of a phage ghost.



These were centrifuged at 25,000 rev/min for 2.5 hours at 15°C in an SW 27.1 rotor. A very sharp bluish-white band appeared in the area of the CsCl shelf from both the wild-type 13⁻ and 9⁻13⁻ supernatant materials. These bands were collected, and in the case of wild-type 13⁻ phage, titered. The concentration of wild-type 13⁻ phage in the pooled bands was 2×10^{14} phage/ml. The solutions from the bands were dialysed overnight against TM buffer. Electron microscopic examination showed both wild-type 13⁻ phage and 9⁻13⁻ head preparations to be free of large contaminating material as shown in Figures 4 and 5, respectively, and to be in the approximate concentration range of 10^{14} particles/ml. These solutions were diluted 1:10 in BS before emulsification with Freund's adjuvant for use as immunogens.

(iii) Particles for Second Injection

Sucrose gradient purified proheads at approximately 10^{13} particles/ml were provided by W. Earnshaw. The tail⁻ heads were from the original preparation described above. The solution had been stored at 4°C in azide for several months. The material was dialysed overnight against two changes of 3000 volumes of TM buffer. A 1:10 dilution of this material served as the immunogen. Wild-type 13⁻ phage, which had been purified through a CsCl gradient were provided by Dr. P. Berget. These were diluted in TM buffer to 10^{13} phage/ml.

(g) Neutralization Curves

Wild-type c₁⁷ phage were diluted in LB to 2×10^8 phage/ml. For the first neutralization experiment, anti-phage, anti-prohead, and anti-head serum were all diluted 500-fold in LB. In the second neutralization experiment, anti-phage and anti-prohead serum were diluted in LB

Figure 4

Phage Particles Used for Preparation of Anti-phage Serum

The particles were prepared as described in section
f, ii.

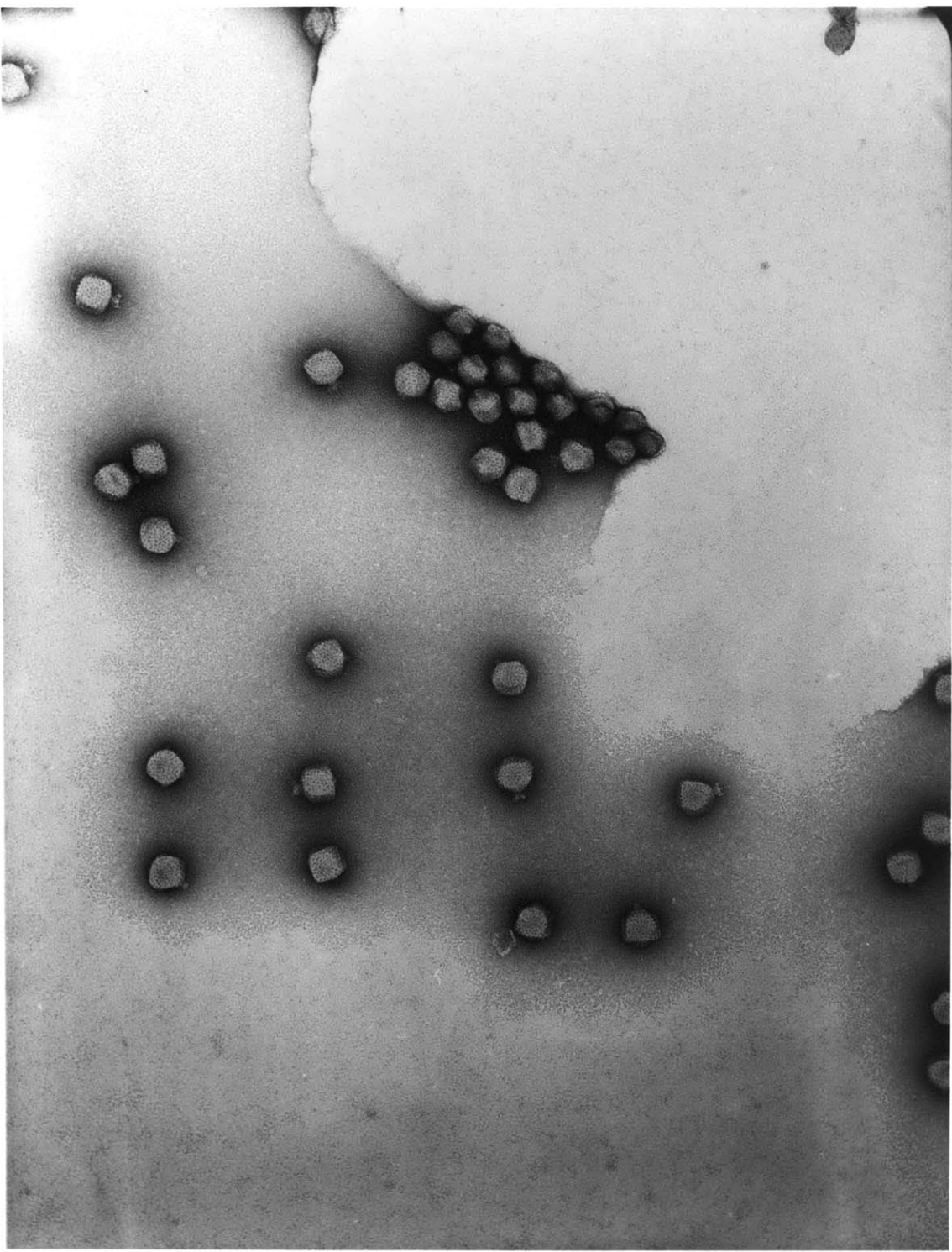


Figure 5Tail-less Heads Purified from Cells Infected with an
Amber Mutant of Gene 9

These particles were prepared as described in section f, ii. A small neck structure and protruding fiber can be seen on some of the particles. A contaminating prohead can be seen in the field. These represented about 6% (24/400) of the particles seen in the electron micrographs of this preparation.



to a k value of 0.1 min^{-1} . The phage and antiserum dilutions were warmed to 37°C prior to mixing. Incubations were started by mixing 2 ml of the phage solution with 2 ml of the appropriate antiserum. An LB broth control, containing no anti-serum was also mixed with phage to measure phage stability over the reaction period. The phage titer remaining after incubation with the antiserum was measured every 5-10 minutes. The initial rate of inactivation (k) was calculated according to the equation $\frac{P}{P_0} = e^{-kt}$. P_0 equals the initial phage titer, P represents the surviving phage, and t equals time. The reactions were stopped by 100-fold dilution into DF.

(h) Serum Blocking Experiments(i) Protocol I1. Lysate Preparation

The lysates were prepared by infecting DB7000 (su^-) cells at 2×10^8 cells/ml in LB broth with phage at multiplicities of 10 phage/cell. The infected cells were incubated with vigorous aeration for 2 1/2 hours at 37°C , lysed with chloroform, and diluted in broth for use as lysate samples.

2. Serum Blocking Procedure

Two-fold serial dilutions of the lysates were made in broth in volumes large enough for use in several experiments. The antisera were diluted so as to kill 95% of the tester phage in 2 hours if no blocking of the serum occurred. In the serum blocking assay, one ml of diluted lysate was mixed with one ml of antiserum at the appropriate dilution and the mixture was incubated overnight at 48°C . To assay the neutralizing antibody remaining after absorption, tester phage were added to a final concentration of about 10^7 phage/ml in the mixture. The samples were incubated for a further two hours at 48°C and titered to measure survival of the tester phage. In each experiment, controls were included to determine the amount of tester phage added, the k value of the unabsorbed serum, and the effect of lysate alone on the phage. The results of the serum blocking assay are presented as percentage serum blocked ($(1 - k_{\text{final}}/k_{\text{initial}})$) calculated as described by Edgar and Lielausis (1965).

(ii) Protocol II1. Lysate Preparation

DB7000 cells were grown to 2×10^8 cells/ml in LB broth at

30°C and infected with phage at a multiplicity of 5 phage/cell. The infected cells were incubated with vigorous aeration at 30°C for 1 hour. At that time they were concentrated 10-fold, and lysed by shaking with chloroform. The resulting lysate was centrifuged at 10,000 rev/min for 10 minutes in the cold to remove large debris and unlysed cells. The resulting supernatant fraction served as the lysate sample for serum blocking experiments.

2. Serum Blocking Procedure

The protocol was as described above except that the temperature of incubation was reduced to 47°C and the serum was used at a slightly higher k (0.04 min^{-1}) to yield a surviving phage fraction of about 1% after a 2 hour incubation.

(iii) Preparation of Purified Particles

1. Preparation of Wild-type 13^- , 9^-13^- and 2^-13^- Lysates

DB7000 (su^-) cells were grown to 6×10^8 cells/ml in one liter of LB broth at 37°C. The cells were infected with 500 ml of phage solution containing 4.5×10^{12} total phage to give a final multiplicity of about 10 phage/cell. The infected cells were incubated with vigorous aeration at 37°C for 2 1/2 hours. The cells were centrifuged at 7500 rev/min for 20 minutes and resuspended in approximately 15 ml of TM buffer plus 50 $\mu\text{g/ml}$ DNase. Chloroform was added to lyse the cells and the mixture was incubated at 4°C for 1/2 hour before being frozen at -80°C. The burst size of the wild-type lysate before concentration was 750 phage/input cell.

2. Particle Purification

The frozen lysate samples were passed through several cycles of

cooling and warming to promote cell lysis. A small aliquot of CHCl_3 was added during this procedure as well. The extract was centrifuged at 8000 rev/min in a Sorvall SS-34 rotor for 20 minutes. The supernatant fraction was decanted and clarified by centrifugation as above.

(a) Purification of Wild-type Particles and Tail⁻ Heads

The supernatant fractions from the wild-type and tail⁻ lysates were centrifuged at 15,000 rev/min in a Sorvall SS-34 rotor for 80 minutes to pellet phage and tail⁻ heads. The particles were resuspended in approximately 12 ml of TM buffer and applied in 2 ml aliquots to a CsCl step gradient containing 1 ml of CsCl at each of three densities, 1.3, 1.5, and 1.7 gm/ml. The gradient was centrifuged at 45,000 rev/min at 15°C for 30 minutes in a Beckman SW 50.1 rotor. The phage and head particles formed an opaque blue band at a position about 2/3 of the distance to the bottom of the centrifuge tube. These bands were collected by side puncture of the tube and dialyzed in the same flask against two changes of 400 volumes of TM buffer. The phage were titered and were found to be at a concentration of 9.2×10^{13} phage/ml. The optical density of the tail⁻ heads was measured at 260 nm. Using a conversion factor equating 1 O.D. unit to 5×10^{11} particles/ml, the concentration of the heads was 1.2×10^{14} heads/ml.

(b) Purification of the Proheads

Aliquots of 1.5-3.0 ml of the clarified 2⁻13⁻ lysate were layered onto 12 ml of a 15-30% sucrose gradient over a shelf of 3 ml of 60%

sucrose solution. All sucrose solutions were made in TM buffer. The proheads were centrifuged at 25,000 rev/min for 2 1/2 hours at 15°C. The proheads formed a light blue band approximately half-way down the centrifuge tube. The proheads were collected from the gradient by side puncture and dialyzed against 2 changes of 200 volumes of TM buffer. By SDS-gel analysis, the proheads were at a concentration of approximately 2.5×10^{13} proheads/ml).

(c) In Vitro Constitution of Phage Particles and Their Purification

In the in vitro constitution of phage, 1.5 ml of purified P22 heads in TM buffer at a concentration of 1.2×10^{14} heads/ml were added to 0.6 ml of a solution of purified gp9 containing 6×10^{14} phage equivalent units of tails. This mixture contains about a 3-fold excess of tails. The mixture was incubated for 1 hour at 37°C. The mixture was diluted with an equal volume of TM buffer and an aliquot of 0.1 ml was removed for titering. The remainder of the solution was layered onto two CsCl gradients and purified as were the phage and head particles in section a. The titer of the 1:2 dilution of the reaction mixture was 6.1×10^{13} phage/ml, one-half the concentration of the tail⁻ heads used in the reaction. The titer of the in vitro phage after dialysis was 1.1×10^{14} phage/ml.

(iv) Antiserum Preparation

All of the antisera used in the serum blocking experiments were from the earliest pool of bleedings (Series 1), and were not absorbed with Salmonella.

(v) Tailing Assay

The tailing activity of lysates used in serum blocking experiments was measured. The source of heads was gp9⁻ particles, prepared and purified as described in the preceding sections, h (iii) 1 and h (iii) 2a. The lysates were prepared as in Section h, Protocol II, and included wild-type 13⁻, 5⁻13⁻, and 2⁻13⁻ lysates. For the tailing assay, the lysates were centrifuged at 15,000 rev/min in a Sorvall SS-34 rotor for 90 minutes to remove endogenous phage which would contribute to the titer derived from phage produced specifically after tail addition; these lysates were not centrifuged prior to their use in the serum blocking experiments. Purified gp9 (P. Berget and A. Poteete, unpublished experiments) at a concentration of 1×10^{11} phage equivalents/ml in LB was included as a positive control. The samples to be assayed for tail donor activity were diluted through eight 3-fold serial dilutions. For the first point in each assay, an aliquot of 0.5 ml of the tail donor, undiluted, was mixed with 1.0 ml of the purified heads at a concentration of 3×10^{10} phage equivalents/ml in LB. For the remainder of the points, one ml of each serial 3-fold dilution of the tail donors was mixed with 2 ml purified head preparation. The reaction mixes were incubated for one hour at 37°C and then put on ice. The number of phage formed in vitro was titered.

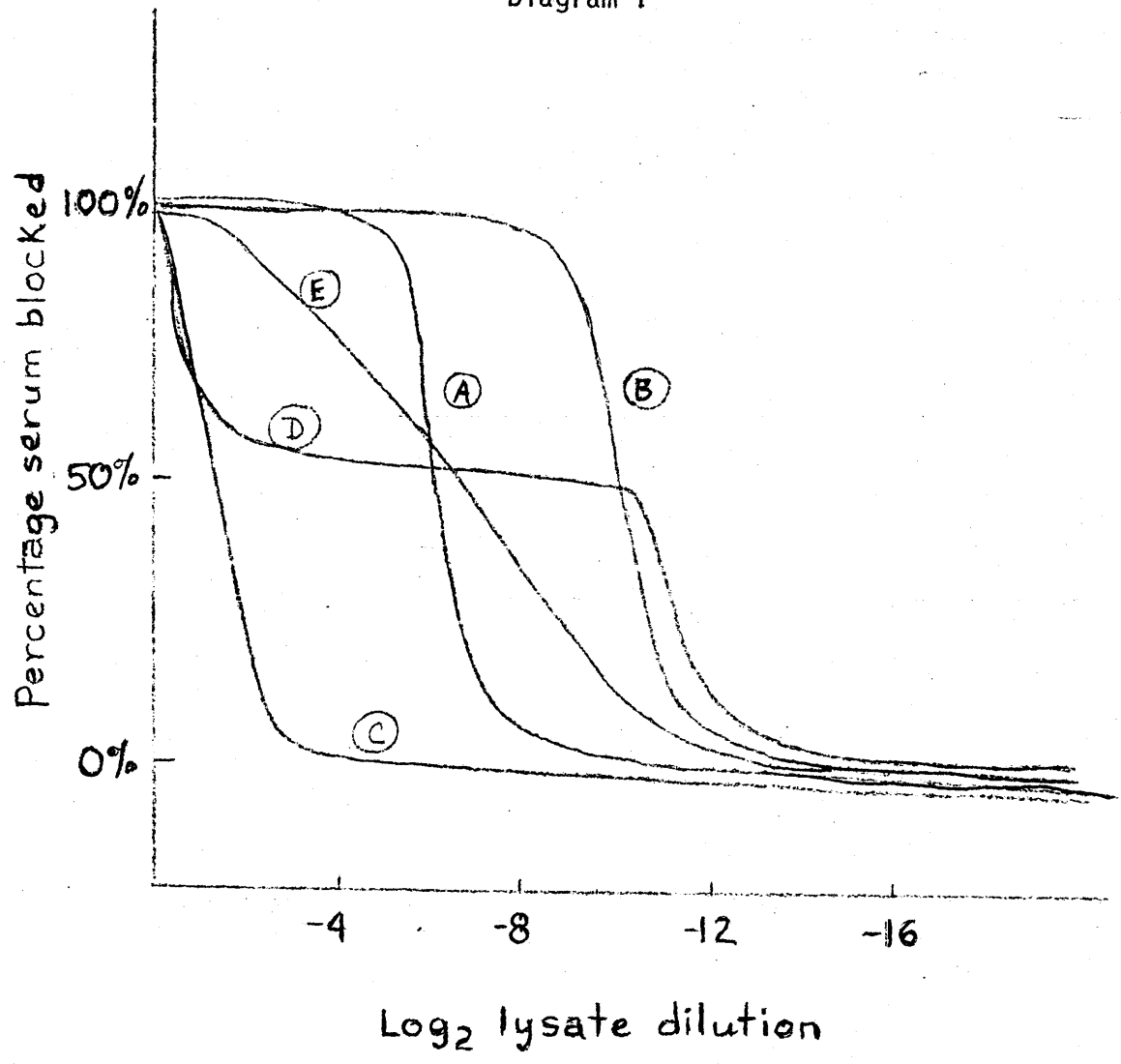
The number of phage equivalents of tails present in each tail donor was estimated according to the procedure of Israel, et al., (1967). The logarithm of the phage titer at each tail donor dilution was plotted against the logarithm of the corresponding dilution. As long as tails are in excess, the number of plaque-forming units/ml remains

constant, and the curve maintains a plateau level. Eventually, dilution reduces the number of tails to equivalence with the number of heads present in the reaction mix. With increasing donor dilutions, the log of the phage titer drops abruptly, with a slope of 3.3 according to Israel, et al.⁽¹⁹⁶⁷⁾. Therefore, a line having a slope of 3.3 was fitted to the data points. For each tail donor, the number of phage equivalents of tails added was equated to the number of heads at the equivalence points where the break in the curve occurred. The number of phage equivalents of tails present in the undiluted sample was calculated from this value.

(vi) Theoretical Serum Blocking Curves

Serum blocking curves provide a basis for determining whether a lysate contains, relative to a control lysate, smaller (or greater) quantities of an antigen, fewer (or more) species of an antigen, or "altered" antigens. Theoretical serum blocking curves illustrating these possibilities are presented in Diagram 1. Curve A is produced by control lysates. At low dilutions of lysate, all phage-neutralizing antibodies are removed by the targets present in the lysate. As the lysate is diluted, the number of target sites is reduced below that concentration necessary to saturate the antibodies, and the level of serum blocking falls. The percentage serum blocked decreases monotonically with increasing lysate dilution until finally, no serum blocking is detected. Curve B is produced when all antigens are present, but in concentrations greater than those present in control lysates. For example, lysates which block 50% of the serum at 2^{-12} lysate dilution (4,096-fold dilute) contain target antigens in 4-fold

Diagram 1



greater concentration than lysates which block 50% of the serum at 2^{-10} dilution (1,024-fold dilute). Therefore, differences in the concentrations of serum blocking antigens generate horizontal displacements of the curves. Curve C is produced by lysates which lack all target antigens, and therefore, cannot block any portion of the antiserum. Curve D is produced by lysates lacking a class of target antigens against which 50% of the phage-neutralizing antibodies are directed. Therefore, the vertical displacements of the curves reflect differences in the antigenic composition of the lysates; that is, the plateau levels of the curves define classes of target antigens which are absent from the lysates. Curve E is produced by lysates which contain "altered" antigens, but in which no classes of target antigens are missing. Because these antigens are in some way altered, their dilution results in a rate of decrease in serum blocking ability different from that of the antigens in the control lysate. No such class of lysates was found in these experiments; all serum blocking curves showed similar shapes.

Experimental error in the data does not contribute equally to the scatter in the points at both ends of the serum blocking curves. At low dilutions of the lysates, experimental error is less significant. For example, at 90% serum blocking levels, an error of 5% in the determination of the residual phage-neutralizing activity of the serum ($k_{\text{final}}/k_{\text{initial}}$) results in an uncertainty of $\pm 0.5\%$ in the percentage serum blocked. At 10% serum blocking, the same error leads to an uncertainty of $\pm 4.5\%$. Therefore, there is generally more scatter in the data points at low levels of serum blocking activity.

(i) Immunoelectrophoresis Experiments

(i) Preparation of Antigens for Immunoelectrophoresis

The source of the antigens used in the immunoelectrophoresis experiments are categorized in Table 3 according to batch numbers. The detailed description of their preparation is as follows:

1. Preparation of Concentrated Lysates

All lysate batches for immunoelectrophoresis were prepared in the same way. A 1/100 dilution of a DB7000 (su⁻) overnight was grown in LB at 37⁰C with aeration to 4×10^8 cells/ml and put on ice, with the aeration continuing. Samples of P22 amber mutants containing 2×10^{11} total phage were added to 100 ml LB medium and warmed to 37⁰C. A volume of 100 ml of the DB7000 cell suspension was poured into the warmed phage solution and the culture was aerated vigorously. The infection was stopped at 120' by chilling the cells on ice with aeration for approximately 15-30 minutes. The infected cells were centrifuged at 3,000 x g for 11 minutes. The cell pellet was resuspended in 0.5 ml immuno-buffer, containing 2.5 µg/ml DNase I solution, and frozen at -80⁰C.

Before immunoelectrophoresis, the suspensions were thawed at room temperature. Ten µl of DNase at 5 mg/ml was added to each extract before electrophoresis. These extracts, approximately 100-fold concentrated, were frozen and thawed several times for use as antigen preparations in immunoelectrophoresis.

2. Preparation of Purified Particles

(a) Phage and Tail⁻ heads

Batch 1: The phage and tail⁻ heads designated as Batch 1

Table 3
Particles and Lysates Used as Antigens in
Immunoelectrophoresis Experiments

<u>Figure</u>	<u>Purified Components</u> ¹	<u>Batch</u>	<u>Lysates</u> (13 ⁻²)	<u>Batch</u>
17a-20a	phage proheads	1 (8/2/75) 1	wild-type 5 ⁻ 5 ⁻ 9 ⁻ 2 ⁻	1 (6/12/75) 1 1 1
20b	gp9 6 x 10 ¹⁴ phage equivalents	8 (P. Berget and A. Poteete)	5 ⁻ 5 ⁻ 9 ⁻	2 (5/17/76) 2
20c			5 ⁻ 8 ⁻	1 1
21a	phage	1	5 ⁻	2
21b & c	gp9	8	5 ⁻ 9 ⁻	2
22a			8 ⁻ 5 ⁻	2 2
22b			3 ⁻ 8 ⁻ amH1348 3 ⁻ 8 ⁻ amN123 3 ⁻ 8 ⁻ amH202	2 2 2
23 a-c			5 ⁻ 3 ⁻ 8 ⁻ amH202 3 ⁻ 8 ⁻ amH1348 3 ⁻ 8 ⁻ amN123	4 (5/7/76) 4 4 4
24a			8 ⁻ 5 ⁻ 5 ⁻ 9 ⁻	1 1 1
24b			3 ⁻ 8 ⁻ amH202 3 ⁻ 8 ⁻ amH1348 3 ⁻ 8 ⁻ amN123	4 4 4
25a	phage	1	wild-type	1
25b			3 ⁻	2

Table 3 (Contd.)

Particles and Lysates Used as Antigens
in Immunoelectrophoresis Experiments

Figure	Purified Components ¹	Batch	Lysates (13 ⁻) ²	Batch
25c	phage (7.7×10^{12} ϕ /ml) proheads	2 (5/12/76) 3 (provided by W. Earn- shaw)	5 ⁻	2
26a	phage spirals	2 4 (provided by W. Earn- shaw)		
26b-c			3 ⁻ 5 ⁻ 8 ⁻ amN123 3 ⁻ 8 ⁻ amNT23 3 ⁻ 5 ⁻	5 (7/12/76 - lysates pre- pared for electron microscopy)
27a	phage tail ⁻ heads	1 1		
27b	phage empty heads	1 5 (from W. Earnshaw)		
28a	1 ⁻ 16 ⁻ 20 ⁻ proheads	6	wild-type	1
28b			8 ⁻ amH202 8 ⁻ amH1348 8 ⁻ amN123	2 2 2
29	proheads	7 (7/13/76)	wild-type	1
30			8 ⁻ 3 ⁻	1 1
31a-c	phage tail ⁻ heads proheads empty heads	1 1 1 5		

Table 3 (Contd.)

Particles and Lysates Used as Antigens
in Immunoelectrophoresis Experiments

<u>Figure</u>	<u>Purified Components</u> ¹	<u>Batch</u>	<u>Lysates(13⁻)</u> ²	<u>Batch</u>
32a-f			8 ⁻ wild-type	1 1

¹ Particle purification described in Materials and Methods, Section (i)
i. 2.

² Lysate preparation described in Materials and Methods, Section (i)
i. 1.

are from the immunogen preparation described in Materials and Methods, Section (f), (ii). These particles were diluted 10-fold in TM buffer and re-purified by centrifugation through a CsCl density step gradient. Twelve ml of sample were layered over a gradient containing 1.6 ml each of CsCl at densities of 1.7 gm/ml, and 1.5 gm/ml, and 2.8 ml of CsCl at a density of 1.3 gm/ml. The gradients were centrifuged in a Beckman SW27.1 rotor at 25,000 rev/min for 3 hours at 15⁰C. Bluish-colored bands appeared about 85% of the way down the tube. These were collected by side puncture. The pooled purified phage and pooled purified tail⁻ heads were dialyzed against two changes of 2,000 ml of TM buffer.

Batch 2: Wild-type lysate preparation: An overnight culture of DB7000 (su⁻) cells was diluted 100-fold into 1 liter of LB broth at 39⁰C and grown with vigorous aeration to 2×10^8 cells/ml. The temperature was shifted to 37⁰C prior to infection with a small volume (approximately 5 ml) of wild-type phage calculated to give a multiplicity of infection of 10 phage/cell. The infection continued for 2 hours with vigorous aeration. The infected cell culture was aerated on ice for an additional hour. The infected cells were pelleted by centrifugation in the cold at 5,250 rev/min for 10 minutes in a Sorvall GSA rotor. The pellets were resuspended in 5 ml cold TM buffer. DNase was added to a concentration of 2 μ g/ml. The resuspended cells were frozen at -80⁰C for several weeks.

The suspension was thawed at room temperature and then kept on ice. DNase was added again at same concentration as above. Shortly thereafter, 3 drops of CHCl₃ was added and the sample was vortexed

vigorously. This step was repeated. The lysate remained on ice for an additional 10 minutes. Then, the material was centrifuged at 10,000 rev/min for 10 minutes. The initial separation was not too good; some cellular material was decanted with the supernatant liquid. The pellet was extracted a second time in the same manner as above. The supernatant fractions were pooled and centrifuged again at 10,000 rev/min in a Sorvall SS-34 and the supernatant fraction was used as the starting material in the purification procedure.

Phage purification: The supernatant fraction was applied in 2 ml aliquots to a CsCl density step gradient containing 1 ml of CsCl at each of three densities, 1.3, 1.5 and 1.7 gm/ml. The gradient was centrifuged at 45,000 rev/min for 30 minutes at 15°C in a Beckman SW 50.1 rotor. Bluish-white bands, approximately 2/3 to 3/5 of the distance down the centrifuge tube, were collected by side puncture. The pooled bands were dialyzed against two changes of 200 volumes of TM buffer. The final, purified phage titer was 7.7×10^{12} phage/ml.

(b) Proheads

Batch 1: The proheads designated as Batch 1 are from the immunogen preparation described in Materials and Methods, Section (f), (i). Aliquots of 4 ml of these proheads were re-purified through a sucrose gradient containing steps of 7 ml each, ranging from 5% to 40% sucrose in 5% increments. The gradients were centrifuged in a Beckman SW25 rotor at 22,000 rev/min for 4 hours at 15°C. Bluish-colored bands, approximately 3/4 of the distance down the centrifuge tube, were collected by side puncture. The pooled material was dialyzed against two changes of 200 volumes of TM buffer.

Batch 6: The 1⁻¹⁶-20⁻ proheads used in these experiments were prepared in collaboration with Dr. S. Casjens. Their preparation is described in W. Earnshaw, et al., 1976.

Batch 7: 2⁻¹³ lysate preparation: An overnight culture of DB7000 (su⁻) cells was diluted 100-fold into 1 liter of LB broth at 37°C and grown with vigorous aeration to 3×10^8 cells/ml. A volume of 280 ml of 2⁻¹³ phage at 10^{12} phage/ml in pre-warmed LB were added to give a multiplicity of 4 phage/input cell. The infection proceeded for 2 hours at which time the infected cells were chilled on ice with aeration for 10 minutes. The infected cells were pelleted by centrifugation at 7,000 rev/min for 10 minutes in a Sorvall GSA rotor. The pellets were resuspended in TM buffer. DNase was added to a concentration of 25 µg/ml. The final volume of the cell suspension was 10.7 ml, so that the cells were about 100-fold concentrated. The concentrate was frozen at -80°C.

Prohead Purification: The frozen cell suspension was thawed at room temperature and then kept on ice. Six drops of CHCl₃ were added with vortexing. The lysate was incubated on ice for 10 minutes before centrifugation at 10,000 rev/min for 10 minutes in a Sorvall SS-34 rotor. The supernatant fraction was decanted and centrifuged again as above. This material was layered in 1 ml aliquots on top of 17 ml of a 15-30% sucrose gradient and centrifuged at 25,000 rev/min for 2 1/2 hours in an SW 27.1 rotor. Bluish bands, approximately half-way down the tube were collected by side puncture. The pooled bands were dialyzed against two changes of 200 volumes of TM buffer.

(ii) Preparation of Antisera for Immuno-electrophoresis

1. Absorption with Uninfected Salmonella Cells

The antisera used in the immuno-electrophoresis experiments were absorbed with whole, uninfected Salmonella typhimurium to remove anti-Salmonella antibodies. The cells were concentrated 200-fold prior to mixing with the sera; then, the mixtures were incubated overnight in the cold, followed by centrifugation at speeds of 8,000 - 10,000 rev/min for 10-15 minutes. This centrifugation removes not only immune precipitate which has formed, but also any unreacted bacterial cells which pellet at these speeds. The clarified supernatant fractions were used as antiserum samples and are referred to as "whole" antisera. The dilutions of the sera during absorption were negligible.

In general, Salmonella absorption removed 3-4 precipitin arcs from the immuno-electrophoretic patterns of P22 lysates.

2. Preparation of Partially Purified Anti-prohead Serum

Anti-prohead serum from series 15 was partially purified and concentrated two-fold by ammonium sulfate precipitation (0-40% saturation at 0°C). Portions of the solid ammonium sulfate (from Schwartz/Mann Co.) were added to 65 ml of the serum at intervals with constant stirring over a 15-20 minute time period. After addition of the ammonium sulfate was complete, the mixture was stirred in the cold (0°C) for 1 hour. The mixture which contained a substantial amount of precipitate, was centrifuged at 10,000 rev/min for 10 minutes in a Sorvall SS-34 rotor. The supernatant fraction was discarded. The pellet resuspended poorly in 4 ml of immuno buffer (probably because it was too

concentrated) and the suspension was stored overnight in the cold (4°C). It was then dialyzed overnight in the cold against two changes of 600 volumes of immuno buffer containing 0.002 M sodium azide. Virtually complete solubilization occurred during the first dialysis procedure. The dialysate was centrifuged at 10,000 rev/min for 10 minutes in a Sorvall SS-34 rotor. The final volume of the supernatant fraction was 30 ml. This 2-fold concentrated, partially purified serum served as the starting material in all experiments using anti-prohead serum from series 15. These included the immunoelectrophoresis experiments of Chapter II, and the electron microscopy experiments of Chapter III.

(iii) Immunoelectrophoresis Procedure

Six glass microscope slides were placed in a polystyrene frame (Gelman Instruments, Immunoelectrophoresis Frame, No. 51447) which holds 6 slides, 3 slides in each of 2 sides. Approximately 13 ml of melted 1% agarose was added to each side, covering the three slides and the exposed part of each frame. Troughs and holes were cut into the agarose by an apparatus from Gelman Instrument Co. (No. 51449). Concentrated lysates or purified particles, prepared for use in immunoelectrophoresis as described above, were placed in the antigen wells using volumes between 1 and 2 μ l. Electrophoresis was carried out in high resolution buffer, pH 8.8 (Gelman Instrument Co., No. 51104) at 10-15 milliamperes, until marker hemoglobin reached a distance of approximately 1 cm from the antigen well. Electrophoresis times ranged from 1-2 1/2 hours. After electrophoresis, the agarose gel in the trough was removed and 100 μ l of anti-P22 serum was added. After over-

night incubation at room temperature in a humidity chamber, agarose gels with developed precipitin bands were washed three times, 4-8 hours each, in immuno buffer plus 0.2% sodium azide. The final wash was in double-distilled water for at least four hours. The gels were covered with lint-free paper (Gelman Instrument Co.) and dried by evaporation overnight. After drying, the paper was removed, and the slides were stained in 1.5% amido black in 10% HAc. The destaining solution is a methanol: water: acetic acid mix in the ratio of 4.5:4.5:1. After 5 minutes of staining, rinsing solution was added, the slides gently shaken, and the destaining solution poured off. This procedure was repeated until the obvious blue color was gone. For the final destaining, the slides were immersed in destaining solution for one hour. The slides were dried by evaporation, standing several hours at room temperature.

(j) Electron Microscopy Experiments

i. Particle purification

1. Wild-type phage and tail-less heads

The wild-type λ phage used in the absorption experiments included three different preparations of CsCl purified phage. One preparation, containing 7.7×10^{12} phage/ml is described in Materials and Methods, Section i,2,a. Another preparation was provided by Dr. P. Berget and contained 1.9×10^{13} phage/ml. The third preparation and a preparation of tail-less heads were prepared in parallel as follows: for each infection, 1 liter of DB7000 cells was grown with aeration to 2×10^8 cells/ml at 37°C in LB. One ml of either wild-type λ phage or λ -tailless phage at 1.6×10^{12} phage/ml was added to each culture to give a multiplicity of infection of about 8 phage/cell. The infection continued for 2 1/2 hours and was then aerated while cooling on ice for 20 minutes. The infected cells from each culture were centrifuged at 7000 rev/min in a Sorvall GSA rotor for 10 minutes. The supernatant fractions were discarded and the cell pellets resuspended in 6 ml of TM buffer. The final volume of each suspension was 14 ml to which DNase was added to a final concentration of $7 \mu\text{g/ml}$. The lysate suspensions were frozen at -80°C .

The lysates were thawed at room temperature and put on ice. Three drops of CHCl_3 were added as well as two additional $10 \mu\text{l}$ aliquots of a DNase solution at a concentration of 1 mg/ml DNase. The suspensions were vortexed vigorously and incubated on ice for 10-20 minutes. Cell debris was removed by centrifugation at 10,000 rev/min for 20 minutes in a Sorvall SS-34 rotor at 4°C . There was poor separa-

tion of pellet and supernatant fractions so the supernatant fractions were centrifuged twice again as above. Aliquots of 2 ml each of the supernatant fractions were layered onto CsCl step gradients containing 1 ml steps of CsCl at densities of 1.3, 1.5 and 1.7 g/cc. The gradients were centrifuged at 45,000 rev/min in a Beckman SW50.1 rotor for 30 minutes at 15°C. The phage and heads formed bluish-white bands about 60% of the way down the centrifuge tubes. The bands were collected by side puncture. The wild-type 13⁻ phage bands were pooled, as were the 9⁻13⁻ head bands, and these were dialyzed overnight against two changes of 1,000 volumes of immuno buffer. The titer of the dialyzed wild-type 13⁻ phage was 6×10^{13} phage/ml.

2. Proheads

One liter of DB7000 cells were grown with aeration to 3×10^8 cells/ml at 39°C in LB, and then cooled on ice with aeration for 10 minutes. The cells were warmed to 37°C and a 2⁻13⁻ phage stock, containing 1×10^{12} total phage in 280 ml of LB, was added to give a multiplicity of infection of about 4 phage/cell. The infection continued for 2 hours. The infected cells were then cooled on ice with aeration for 10 minutes and centrifuged at 7,000 rev/min for 10 minutes. The supernatant fraction was decanted and the pellets resuspended in TM buffer containing 25 µg/ml DNase to a final volume of 10.7 ml. The suspension was frozen at -80°C.

The lysates were thawed at room temperature and then kept on ice. Six drops of CHCl₃ were added and the suspension was vortexed. The lysates were incubated for 10 minutes on ice and then centrifuged at 10,000 rev/min in a Sorvall GSA rotor for 10 minutes. The super-

natant fraction was removed and centrifuged again as above. Two ml aliquots of the supernatant fraction were added to 17 ml of a 15-30% sucrose gradient. The gradients were centrifuged at 25,000 rev/min for 2 1/2 hours at 15°C in an SW27.1 Beckman rotor. The prohead bands, running about half-way down the centrifuge tube, were collected by side puncture and pooled. The proheads were not dialyzed.

3. T4 phage

T4 phage ($rII\Delta/t^-$) which had been purified through two CsCl gradients and dialyzed were provided by Dr. P. Berget. These were purified through a third CsCl gradient in a procedure similar to that described for the wild-type P22 phage and tail-less heads in Section i,1.

ii. Serum absorption

In general, the sera were absorbed by the addition of small aliquots of antigen, between 0.1 and 0.2 ml. every 10 minutes or so at 48°C. Control sera were absorbed in parallel using TM buffer. After 1-2 ml of antigen were added in this way, the serum was incubated at 4°C for at least one hour, and often overnight. The resultant immune precipitates, and in the case of Salmonella absorption, the unreacted whole cells, were pelleted by centrifugation at 10,000 rev/min in a Sorvall SS-34 rotor for 10 minutes at 4°C. This procedure was repeated using the supernatant fraction until antigen addition no longer resulted in visible immune precipitate formation. At this point, one more addition of a small volume of antigen, usually 0.5 ml or so, was added to ensure complete serum absorption. This final absorption mixture was treated as above. The extent of serum

absorption was checked in each final supernatant fraction by immunoelectrophoresis of the absorbed serum with the absorbing antigen.

1. Prohead absorption of anti-phage serum

Anti-phage serum was from series 1, the earliest pool of bleedings, which was also used in the serum blocking experiments. The serum was absorbed, as described above, first with a 200-fold concentrated preparation of uninfected Salmonella cells. Complete absorption of the serum required approximately 6×10^{10} cells/ml serum. Then, a 1/5 dilution of the Salmonella-absorbed anti-phage serum in TM buffer was absorbed, as above, with the purified proheads described in section 2. In all, the serum was diluted 18-fold to give a final k value of 280 min^{-1} at 37°C . As a very rough estimate, full absorption of the anti-phage serum at a k of about $5,000 \text{ min}^{-1}$ required about 7×10^{14} proheads/ml of serum.

2. Phage absorption of anti-prohead serum

The anti-prohead serum was from series 15 and had been partially purified and concentrated (2-fold) by ammonium sulfate precipitation as described in section i, ii, 2. The anti-prohead serum was first absorbed with uninfected Salmonella cells as described above. As in the case of anti-phage serum, complete absorption of the serum required about 6×10^{10} cells/ml serum.

The Salmonella-absorbed anti-prohead serum was then absorbed with the CsCl purified phage from each of the three preparations described in section j, i, 1. Absorption of the serum to the point where antigen addition no longer resulted in immune precipitation was accomplished through six separate cycles of phage addition in the manner described

above. At the conclusion of this absorption series, the serum was 22-fold diluted and used in some of the immunoelectrophoresis experiments as phage-absorbed anti-prohead serum ($\emptyset 6$). A final small aliquot of purified phage was added to the serum, and this was processed to yield the final phage-absorbed serum ($\emptyset 7$) used in the electron microscopy and several immunoelectrophoresis experiments.

iii. Lysate preparation

The following lysates were prepared for use in absorbing the phage-absorbed anti-prohead serum described above: 3⁻¹³⁻, 3⁻⁵⁻¹³⁻, 3⁻⁸⁻¹³⁻ and 3⁻⁵⁻⁸⁻¹³⁻. A wild-type lysate was also prepared in parallel to monitor the infection.

DB7000 cells were grown with aeration to about 5×10^8 cells/ml in 1,500 ml LB at 34°C. The culture was chilled on ice with aeration for 2 hours prior to infection. A total of 6×10^{11} phage of the appropriate genotype were added to 160 ml LB and incubated at 30°C. The infection was initiated by adding 160 ml of the bacterial culture to the phage solution. The infected cells were aerated vigorously for 3 hours and 10 minutes, and then chilled for 10 minutes on ice. The infected cells were centrifuged at 7,000 rev.min in a Sorvall GSA rotor for 10 minutes at 4°C. The supernatant liquid was decanted and the cells were resuspended in 1.5 ml TM buffer containing 20 $\mu\text{g/ml}$ DNase. The lysates, approximately 100-fold concentrated were frozen at -80°C. The burst of phage from the wild-type lysate was 1,700 phage/cell.

The lysates were thawed for 2 hours on ice. Four drops of CHCl_3 was added to each lysate with vortexing. The lysate was incubated on ice for 45 minutes with intermittent vortexing. Cellular debris was

removed by centrifugation of the lysates at 10,000 rev/min in a Sorvall SS-34 rotor for 30 minutes. The supernatant fractions were decanted and their antigenic composition was determined by immunoelectrophoresis.

iv. Lysate absorption of the serum

A 0.7 ml aliquot of each lysate described in the preceding section was diluted in TM buffer to 4.5 ml total volume. Four aliquots of 0.6 ml of the phage-absorbed serum described in section ii, 2 were each diluted to 1.5 ml with TM buffer. The four pools of diluted serum were warmed to 48°C and one ml aliquots of the appropriate diluted lysate was added to each pool every 10 minutes. Immuno-precipitates formed immediately. At the completion of the additions, the mixtures were incubated for an additional hour at 48°C and then stored overnight at 4°C. The precipitates were pelleted by centrifugation of the lysate-absorbed sera at 10,000 rev/min for 30 minutes at 4°C. The supernatant fractions were clarified as in the following section, and used in the electron microscopy experiments.

Initially, there was not enough residual antibody activity in these lysate-absorbed sera to produce a sufficient level of coating even in the case of the positive control. Therefore, the sera were concentrated 10-fold by ammonium sulfate precipitation as described in section i, ii, 2. In this procedure, the ammonium sulfate pellet from 4.5 ml of each absorbed serum was resuspended in 0.3 ml TM buffer and dialyzed. The dialysate, which was centrifuged at 10,000 rev/min for 10 minutes at 4°C in a Sorvall SS-34 rotor, was diluted to a final volume of 0.45 ml in TM buffer. These 10-fold concentrated supernatant fractions were used as the lysate-

absorbed sera in the electron microscopy experiments.

v. Antiserum clarification

In the electron microscopy procedure to be described, antigen samples are absorbed to electron microscope grids prior to their incubation with the antiserum. This means that antiserum components are also absorbing to the grid during the incubation period. In an effort to reduce the background material in all of the sera, though particularly in antisera which had been incubated with concentrated lysates, I centrifuged the absorbed sera and their controls at speeds sufficient to remove ribosome-sized particles. The sera were centrifuged at 45,000 rev/min for 4 hours at 15°C in a Beckman SW50.1 rotor. Even in the control sera, some material was pelleted. The supernatant fractions were carefully decanted and used as clarified sera in the electron microscopy experiments.

vi. The antigen mixture

The antigen sample in the electron microscopy experiments consisted of a mixture of purified structures including P22 phage, tail-less heads, proheads, spirals and T4 phage. The P22 phage from one of the three preparations described in section j, i, 1. The tail-less heads are described in the same section. The proheads are described in section i, 2. T4 phage were provided by Dr. P. Berget and are described in section i, 3. Spirals were provided by W. Earnshaw and are described in Earnshaw, et al., 1976.

The structures were diluted in TM buffer to about 5×10^{11} particles/ml and were mixed together in equal volumes. The initial concentrations of the particles and the amounts added were adjusted empirically as the experiments progressed to provide the proper distri-

bution of particles on the grids.

Vii. Electron microscopy procedure

A drop of sample was applied to a carbon-coated copper electron microscope grid (200 μ ^{mesh}). The sample was absorbed to the grid for 30-45 seconds and washed off with two drops of double distilled water. If the sample was to be reacted with antiserum, the grid was inverted onto a drop of antiserum placed on a para-film sheet. The samples were incubated with the antiserum for 30 minutes except in the case of whole and phage-absorbed anti-prohead serum which were incubated for 15 minutes. At the end of the incubation period, the grid was removed from the antiserum drop, washed with two drops of double-distilled water, and stained according to the standard negative staining procedures used for samples not reacted with antiserum. The grid with absorbed sample was washed with one drop of 2% uranyl acetate and incubated for 30 seconds with a second drop. This was washed off with a single drop of 0.1% uranyl acetate. The excess moisture was removed by touching a piece of torn filter paper to the edge of the drop. The samples were examined in a JELCO-100B electron microscope. Micrographs were taken on Kodak Electron Image Plates at an instrumental magnification of about 45,000 x, or 80,000 x at 80 kV.

The particles had a tendency to desorb from the grids during antiserum incubation which was counteracted if the antiserum contained antibodies specifically against the structures. In one experiment, I compared the amount of desorption which occurred during 10 and 15 minute incubation times. Although desorption was approximately the same for the two samples, antibody binding was not. It seems that antibody binding is

not linear with time. In the sample incubated for 10 minutes, there was no detectable antibody binding; at 15 minutes, antibody binding was clearly present. In a separate experiment, the level of antibody binding did not detectably increase between 15 and 30 minutes.

Chapter I: Characterization of the Phage-neutralizing Activity of Sera Prepared against Phage P22 and its Precursor Particles

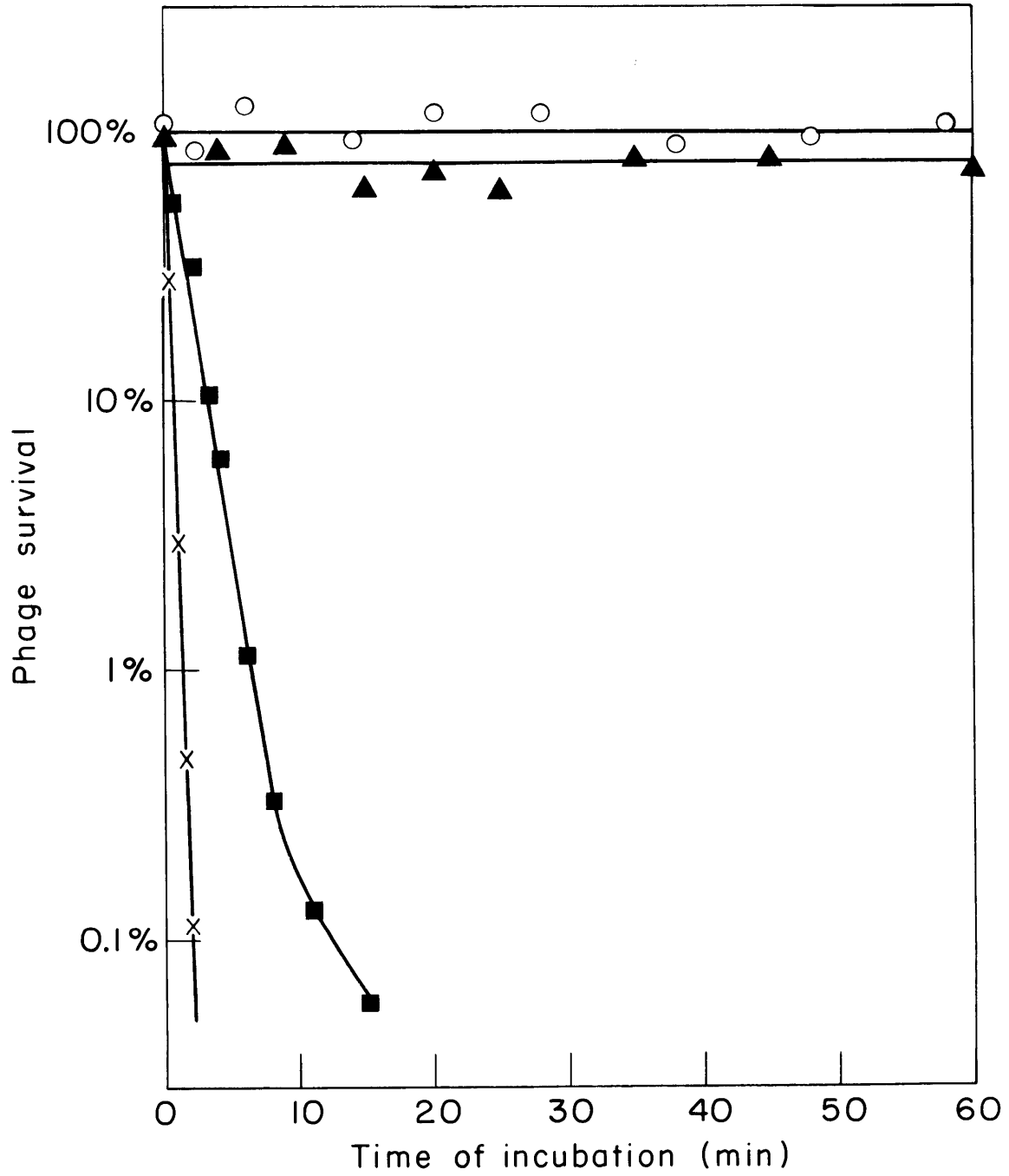
A. Phage Neutralization Curves

Antibodies specific to P22 structures were generated by injecting rabbits with preparations of P22 phage, proheads and tail-heads. The sera produced were collected at various intervals in order to obtain samples of antibody classes which might be present only transiently. Also, the rabbits were injected more than once so that the response of antibody species that may have been only weakly present initially might be enhanced. Characterization of the antisera, as described below, showed these precautions to be unnecessary: though the antibody titer rose and fell in intensity over time, no transient antibody classes were detected; booster injection served solely to increase the response of antibody classes that were detectable in the earliest bleedings.

Several pools of antisera were characterized by their ability to kill phage. In these experiments, phage and antisera are incubated together at high dilution so that phage killing by the antisera represents direct inactivation rather than a reduction in titer due to phage agglutination. Representative killing curves for anti-phage, anti-prohead, and anti-head sera are shown in Figure 6. In this experiment, all three sera have been diluted by the same factor to directly compare their relative killing power. Anti-phage and anti-prohead serum kill phage rapidly, with anti-phage serum being about five times more potent a killing agent than the anti-prohead serum.

Figure 6Inactivation of Phage P22 by Anti-phage, Anti-prohead
and Anti-head Serum

Aliquots of P22 $13^{-} c_1^7$ tester phage at 2×10^8 phage/ml were mixed with equal volumes of 500-fold dilutions of anti-phage serum (-x-x-), anti-prohead serum (-■-■-), and anti-head serum (-▲-▲-), in broth at 37°C. A control sample (-o-o-) was incubated with broth only. All samples were pre-warmed at 37°C before mixing. Aliquots were withdrawn and diluted 100-fold immediately to stop the reaction, prior to plating for surviving phage. The surviving phage produce a range of plaque sizes, ranging from minute to normal-sized plaques. At times of incubation longer than those shown (90 minutes to 2 hours), the phage titer of the mixture containing anti-head serum decreased with multi-hit kinetics.



Anti-head serum, which was generated against phage which lacked the tail protein, gp9, did not kill phage at a rate detectable in the first hour of incubation. At later times, the phage titer decreased reflecting aggregation by the serum as will be described in Chapter II.

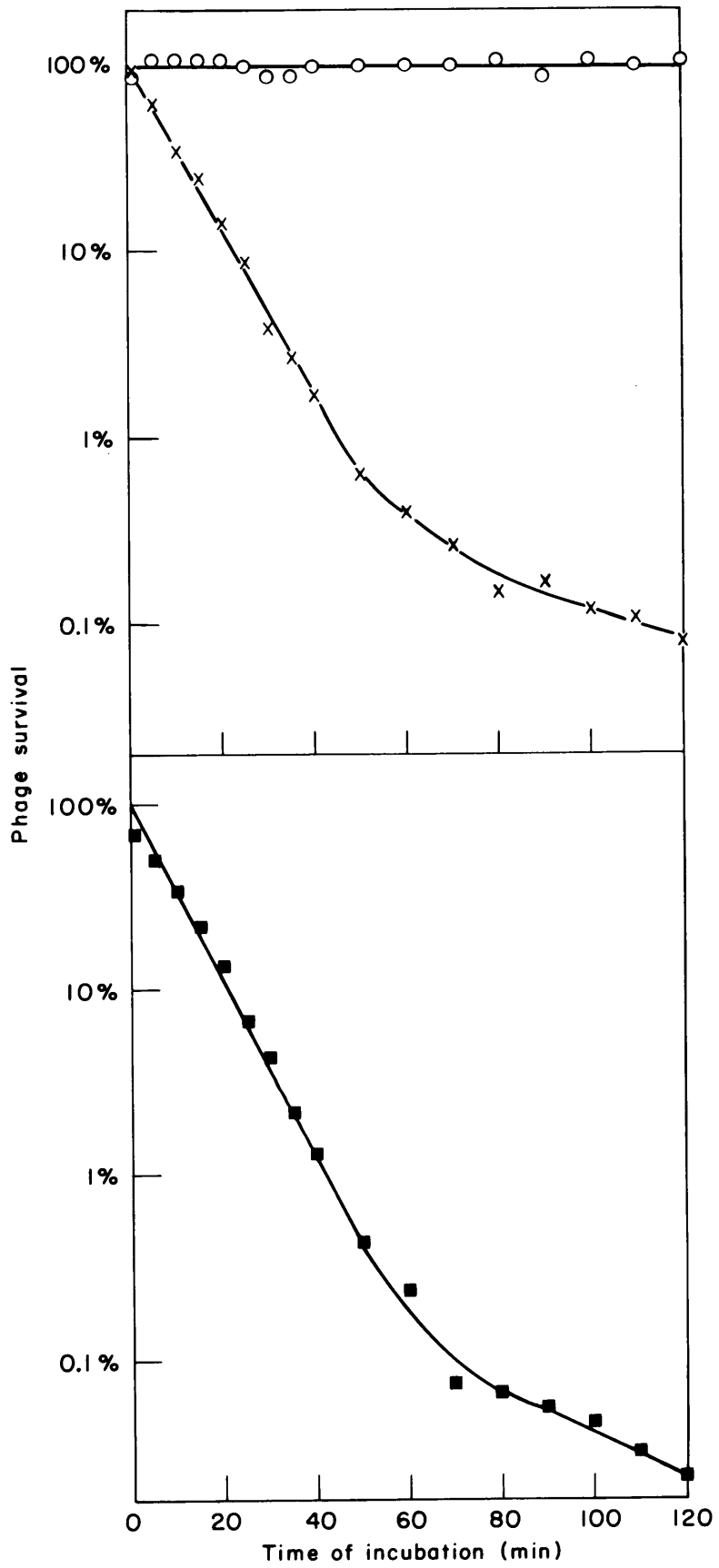
The kinetics of the phage-killing activity of anti-phage and anti-prohead serum were examined in more detail in the experiment shown in Figure 7. The two antisera have been further diluted so as to kill phage at a slower rate. The dilutions were chosen so as to yield the same final k value for the two sera. Under these conditions, the curves are exponential from zero time indicating that one hit is sufficient to inactivate the phage. The kinetics of phage inactivation are exponential down to 10^{-2} phage survival; between 10^{-2} and 10^{-3} phage survival, the rate begins to decrease for both sera. The initial first order rate constants for phage inactivation of the undiluted antisera (K) at 37°C calculated from these data are $2,150 \text{ min}^{-1}$ for anti-phage serum and 450 min^{-1} for the anti-prohead serum.

B. Identification of the Targets of the Neutralizing Activity of Anti-phage Serum

Phage structural proteins may be deleted systematically from infected cells by infecting with amber mutants defective in the appropriate genes. This aspect of a well-characterized phage system provides a method for the genetic identification of the phage structural proteins which form the target of the phage-neutralizing bodies. In these experiments, serial dilutions of amber mutant lysates, which lack known phage proteins, are incubated with dilute antiserum for a time sufficient for antibody-antigen binding reactions to go to comple-

Figure 7Kinetics of Inactivation of Phage P22 by Anti-
Phage and Anti-prohead Serum

Aliquots of P22 tester phage at 2×10^8 phage/ml were mixed with equal volumes of anti-phage serum (-x-x-) and anti-prohead serum (-■-■-) which had been diluted 21,000-fold and 4,200-fold, respectively, to give approximately the same final k values. A control sample (-o-o-) was incubated with broth only. Phage and antiserum samples (pre-warmed) were incubated at 37°C. The reactions were stopped by 100-fold dilutions prior to plating for surviving phage.



tion. The residual neutralizing activity of the serum is then measured by determining the rate of inactivation of subsequently added tester phage. The results of such experiments are expressed as the percentage of the neutralizing activity of the serum which is blocked by incubation with the lysate samples. I expect an amber mutant lysate to fail to completely block the serum's phage-neutralizing ability if the amber mutation occurs in a gene whose product is part of the neutralization target.

The final assay in these experiments is phage killing; thus, serum blocking power experiments detect only those antibodies which kill the phage on complexing with it. Data from serum blocking experiments are limited in that they provide a measure of the concentration of only those antigens which react with the phage-killing antibodies in the serum; the assay does not detect classes of antigenic phage proteins which bind antibodies, but whose combination with antibodies does not lead directly to phage inactivation. These antibodies are characterized in a later section.

Serum blocking power assays were done using anti-phage and anti-prohead sera, as these sera contain phage-neutralizing antibodies.

1) Serum blocking experiments with lysates lacking specific phage gene products

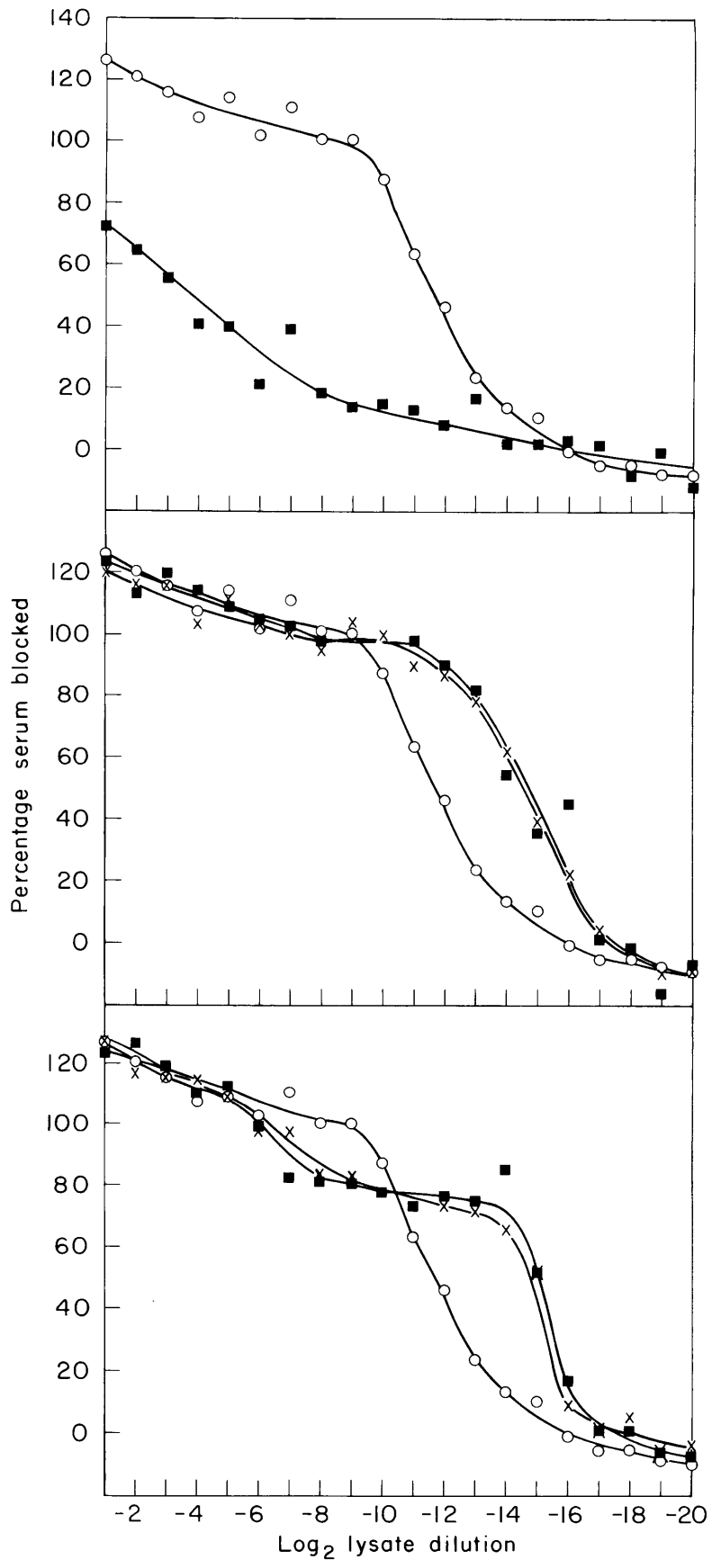
All P22 amber mutant lysates fell into one of four serum blocking categories. The first category is defined by the behavior of a wild-type lysate, which is shown as a reference curve in each panel of Figure 8. Incubation of anti-phage serum with a wild-type lysate, which contains all P22 structural proteins, completely blocks the ability of

Figure 8

Blocking of the Phage-inactivating Activity of Anti-
Phage Serum by P22 Amber Mutant Lysates

Lysates were prepared and serum blocking curves determined as described in Materials and Methods, Section h, using Protocol I. The k of the anti-phage serum was 0.025 min^{-1} at 48°C . The burst size of the wild-type lysate was 880 phage/input cell.

Panel a shows the blocking of anti-phage serum by a wild-type lysate (-o-o-) and a lysate which lacks the baseplate protein, $9 \cdot 13^{-}$ lysate (-■-■-). The serum blocking curve of the wild-type lysate is replotted in panels b and c for reference. Panel b shows blocking of anti-phage serum by a lysate which is blocked in DNA packaging and accumulates proheads, $2 \cdot 13^{-}$ lysate (-x-x-). Panel b also shows the blocking of anti-phage serum by a lysate which lacks one of the head completion proteins and which accumulates empty heads, $26 \cdot 13^{-}$ lysate (-■-■-). Panel c shows the serum blocking activity of two lysates which do not form appreciable numbers of structures and which contain several P22 structural proteins in soluble form. A $5 \cdot 13^{-}$ lysate (-■-■-) lacks the major capsid protein. An $8 \cdot 13^{-}$ lysate (-x-x) lacks the scaffolding protein and accumulates low levels of aberrant structures.



the neutralizing antibodies to kill phage. In a plot of percentage serum blocked against lysate dilution, the wild-type lysate generates a curve which starts around 100% serum blocked. The value stays close to 100% until dilution of the lysate reduces the amount of target antigen to a concentration below that capable of saturating the serum. At this point, the amount of serum blocking protein falls monotonically with lysate dilution, until finally no serum blocking antigen is detectable.

The second class of serum blocking curves is represented by the behavior of lysates made with amber mutants defective in gene 9, as shown in panel a of Figure 8. Such lysates lack gp9, the tail protein. Though the lysate shows considerable blocking activity at very high lysate concentrations, it contains less than 1% of the concentration of serum blocking protein in the control lysate. The serum blocking power at low dilutions of the lysate may be accounted for by the input phage particles used to generate the $9^{-}13^{-}$ lysate. Failure of the $9^{-}13^{-}$ amber mutant lysate to block a large percentage of the neutralizing activity of the serum suggests that it is missing most, if not all, of the target antigen classes. Therefore, the bulk of the inactivating antibodies in the anti-phage serum appears to be directed against the tail protein, gp9.

This hypothesis is supported by the behavior of all other P22 amber mutant lysates, each of which contains gp9 tail protein at concentrations equal to, or greater than, the wild-type level. Panel b of Figure 8 contains results representative of the third class of serum blocking curves. This category consists of amber mutant lysates which

contain fully potent serum blocking antigen in concentrations greater than that present in the wild-type lysate. Members of this category include amber mutant lysates in which assembly is blocked at the prohead stage. The behavior of a 2^{-13} amber mutant lysate, which produces only proheads, is plotted in panel b of Figure 8. Initially, the curve of a 2^{-13} amber mutant lysate parallels that of a wild-type lysate, blocking 100% of the serum. However, the serum blocking antigen in a 2^{-13} amber mutant lysate is more concentrated than the serum blocking antigen in a wild-type lysate. Quantitatively, the 2^{-13} amber mutant lysate in this experiment appears to contain about eight times as much target antigen as the wild-type standard lysate. Table 5, to be discussed, shows directly that gp9 is overproduced in a non-permissive infection with a 2^{-13} amber mutant phage. Thus, the presence of increased concentrations of serum blocking protein in lysates known to overproduce gp9 is consistent with the conclusion that the tail protein, gp9, is responsible for the bulk of the serum blocking protein present in lysates.

Panel b of Figure 8 also includes a plot of the data from the incubation of anti-phage serum with a 26^{-13} amber mutant lysate. This lysate is one of a class of amber mutant lysates which contains, in addition to proheads, empty head structures into which DNA has been unstably packaged. The curve shows a high degree of similarity with that of a 2^{-13} amber mutant lysate. This suggests, as discussed above, that gp9 is overproduced in 26^{-13} amber mutant infections.

The final class of serum blocking power behavior is exhibited by lysates prepared from amber mutants defective in genes 5 and 8. The common feature of these two lysates, which distinguishes them from all other P22 amber mutant lysates, is the absence of structure formation. A 5⁻ amber mutant lysate lacks gp5, the capsid protein. An 8⁻ amber mutant lysate lacks gp8, the scaffolding protein, which directs the proper assembly of gp5 into a capsid shell. A plot of the serum blocking activity of a 5⁻13⁻ and an 8⁻13⁻ lysate is shown in panel c of Figure 8. The curves at high lysate concentration block 100% of the serum because of the presence of input phage which were used to make the mutant lysates. With increasing dilution, a plateau level seems to occur in which 80-90% of the serum is blocked, leaving approximately 15% of the antibodies active. Furthermore, the serum blocking protein in these lysates, though lacking an antigenic species, appears to be present in concentrations higher than that which exists in a wild-type lysate, and more nearly equivalent to the concentration of serum blocking protein present in prohead-producing lysates. The 5⁻13⁻ and 8⁻13⁻ amber mutant lysates in this experiment may be diluted about eight times more than a comparable wild-type lysate before dilution reduces the amount of target antigen to levels no longer sufficient to saturate the neutralizing antibodies. The data in Table 5, to be discussed, show that gp9 is over-produced in a 5⁻13⁻ amber mutant lysate. SDS-gel experiments (unpublished experiments) show the same phenomenon for both 5⁻13⁻ and 8⁻13⁻ amber mutant lysates. Thus, the data from this final class of lysates are consistent with the hypothesis that the bulk of the phage-neutralizing antibodies in anti-

phage serum are directed against gp9, the tail protein. The data also identify a minority class of about 15% of the phage-inactivating antibodies which are directed against an antigenic determinant which is absent from 5⁻13⁻ and 8⁻13⁻ lysates.

We can probably exclude the gene 8 product itself as the target antigen of the 15% class of phage-neutralizing antibodies: the final assay in serum blocking power experiments is phage killing. Gene product 8, the scaffolding protein, is a catalytic structural protein which is not incorporated into the final assembled phage structure (King, et al., 1973). As such, gp8 itself cannot be part of the target antigen on the phage. This implies that the 8⁻ mutation exerts its influence indirectly in the serum blocking power assay by affecting the assembly of the target antigen. The serum blocking behavior of an 8⁻ amber mutant lysate is perhaps most easily interpreted as evidence of a structure-dependent antigen, i.e., a protein of the phage which is capable of binding antibodies against itself only when it exists as part of an organized structure. In an attempt to identify the target protein of the minority class of killing antibody, lysates made from amber mutants defective in each gene involved in phage assembly have been tested in serum blocking experiments with anti-phage serum. All remaining amber mutant lysates fell into either the first or third serum blocking power categories, that is, containing all species of target antigens at wild-type, or greater than wild-type, concentrations, respectively. Lysates defective in any of three genes, genes 16, 20 or 7, show wild-type serum blocking behavior, thereby falling into category I. These lysates produce non-infectious particles which are

morphologically identical to phage. The data for a 16⁻13⁻ amber mutant lysate are shown in Figure 9. Figure 9a also shows, for comparison, curves obtained by repeating the serum blocking assay for the 5⁻13⁻ and 8⁻13⁻ amber mutant lysates used previously in Figure 8. Data for a 20⁻13⁻ mutant lysate are in Figure 10, and for a 7⁻ amber mutant lysate, in Figure 12. All exhibit serum blocking power behavior very similar to that of a wild-type lysate. Two lysates which also fall into this category - 10⁻ and 4⁻ - produce tail-less heads which have lost their DNA. Such lysates usually have wild-type levels of gp9 tail protein (unpublished experiments). The serum blocking activity of a 10⁻13⁻ amber mutant lysate is shown in Figure 9b and the behavior of a 4⁻13⁻ amber mutant lysate in Figure 11.

The remaining prohead-producing lysates fall into category III of serum blocking behavior; all the serum blocking antigens are present at greater than wild-type concentrations. The behavior of a 1⁻13⁻ amber mutant lysate is shown in Figure 9b; the serum blocking activity of a 3⁻13⁻ amber mutant lysate in Figure 11. These lysates accumulate proheads and unassembled gp9.

Figure 12 graphs the results of an experiment investigating the role of gene 13 in antibody inactivation. Gene 13 product is required for bacterial cell lysis at the termination of phage infection, although it is not responsible for lysozyme production which is under the control of gene 19. It has not been identified on SDS gels and may or may not be a component of phage particles. Four 13⁺ lysates - 7⁻, 9⁻, 2⁻ and 5⁻ amber mutant lysates - were chosen to represent the first,

Figure 9

Blocking of Anti-phage Serum by 1^{-} , 10^{-} and 16^{-}
Amber Mutant Lysates

The lysates were prepared and the serum blocking experiment done as in Materials and Methods, Section h, Protocol I. The anti-phage serum in this experiment had a k at 48°C of 0.02 min^{-1} .

Panel a shows the blocking serum activity of a lysate which lacks one of the proteins involved in DNA injection. A $16^{-}13^{-}$ lysate (-o-o-) produces phage-like particles which are non-infectious. The serum blocking experiment included as a reference the $5^{-}13^{-}$ lysate (-□-□-) and the $2^{-}13^{-}$ lysate (-x-x-) used in the experiment of Figure 8. Panel b shows the serum blocking activity of a lysate defective in head completion which accumulates empty heads, $10^{-}13^{-}$ lysate (-x-x-), and a lysate defective in DNA packaging which accumulates proheads, $1^{-}13^{-}$ lysate (-□-□-). The $16^{-}13^{-}$ curve has been re-plotted for comparison.

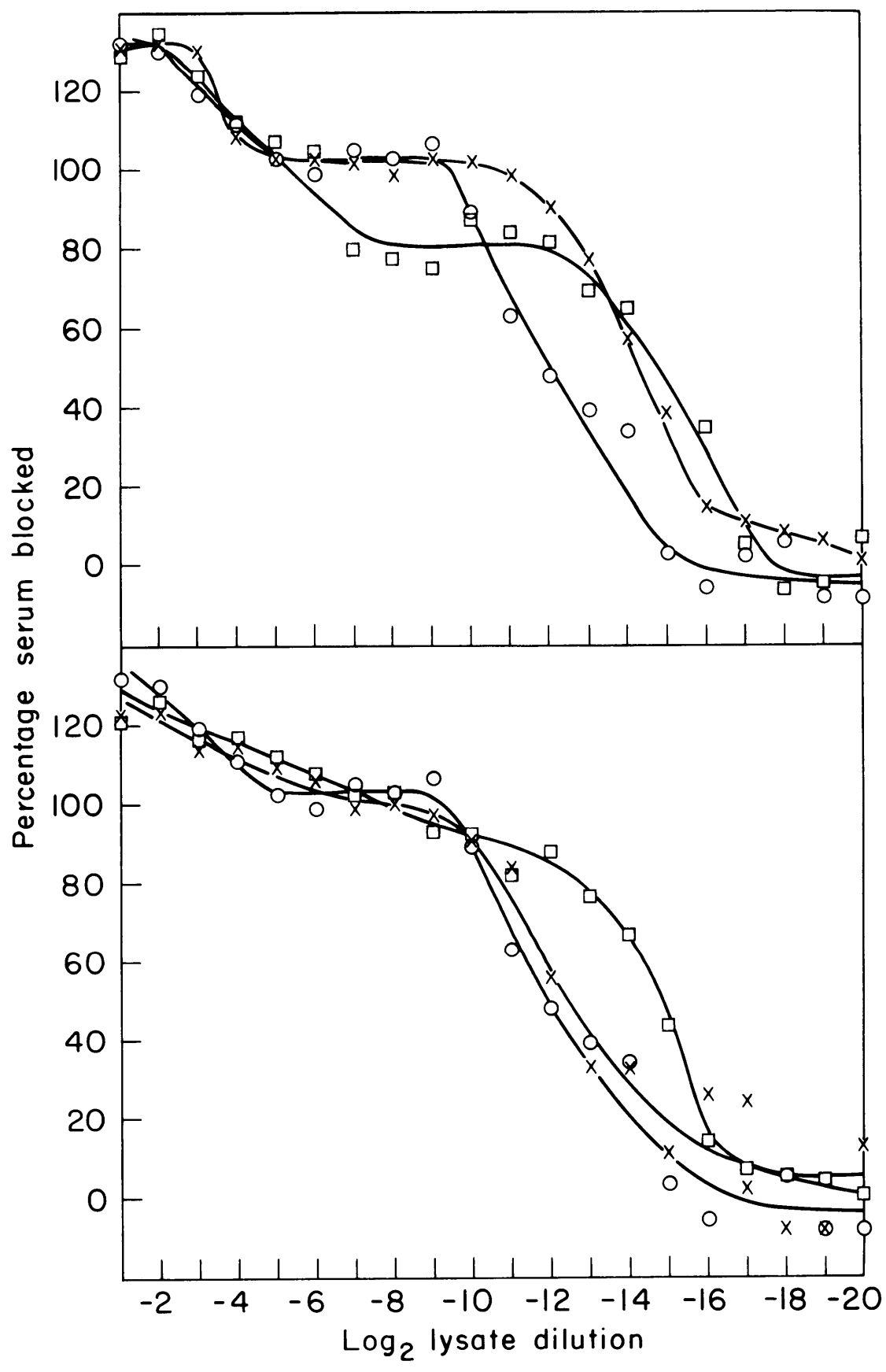


Figure 10Blocking of Anti-phage Serum by a Lysate Lacking the
Gene 20 Product

Lysates were prepared and serum blocking curves determined as described in Materials and Methods, Section h, using Protocol II. The 13^{-} control lysate (-o-o-) and the $20^{-}13^{-}$ lysate (-x-x-) were prepared in parallel. The antiserum had a k of 0.04 min^{-1} at 47°C .

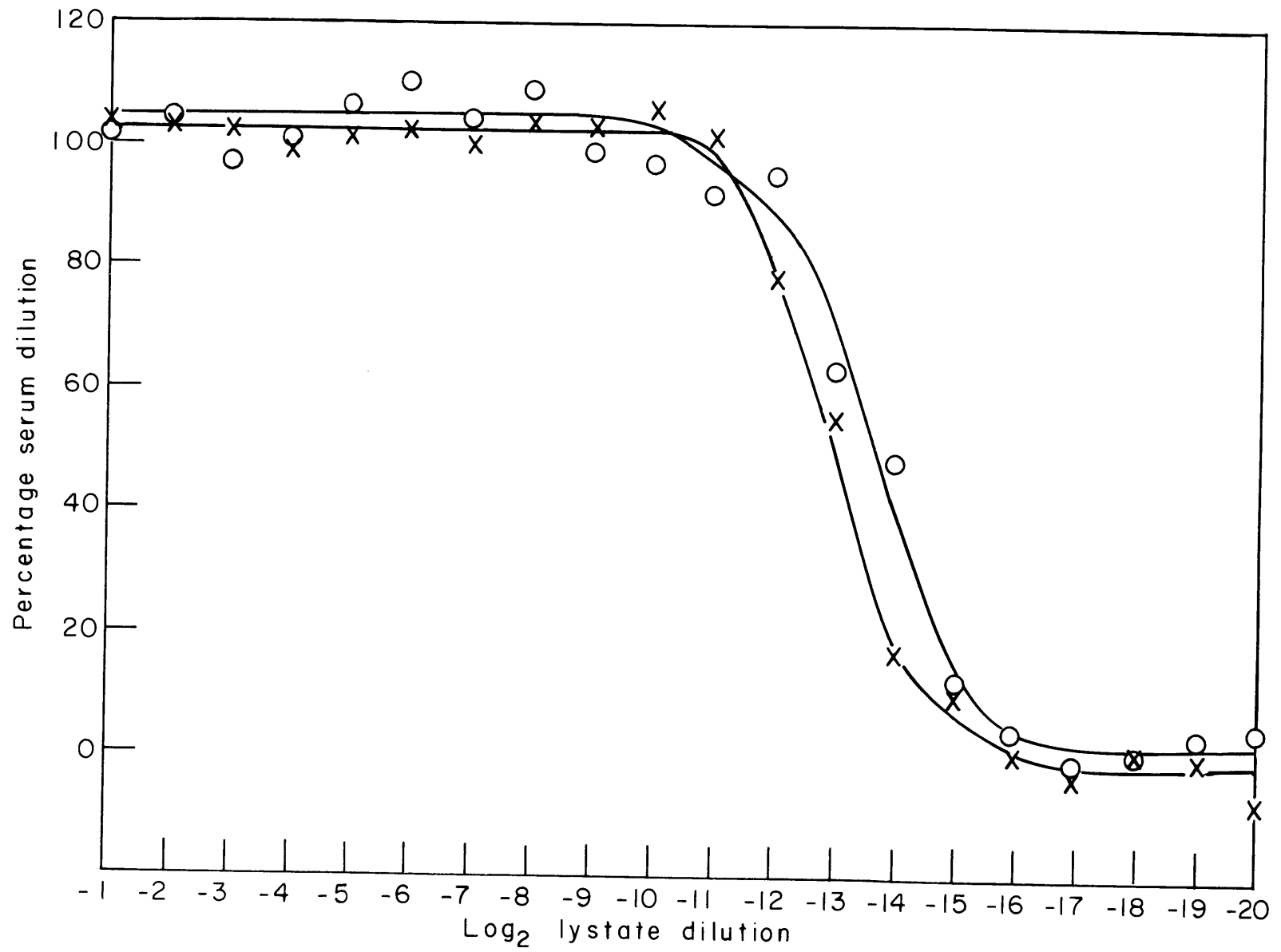
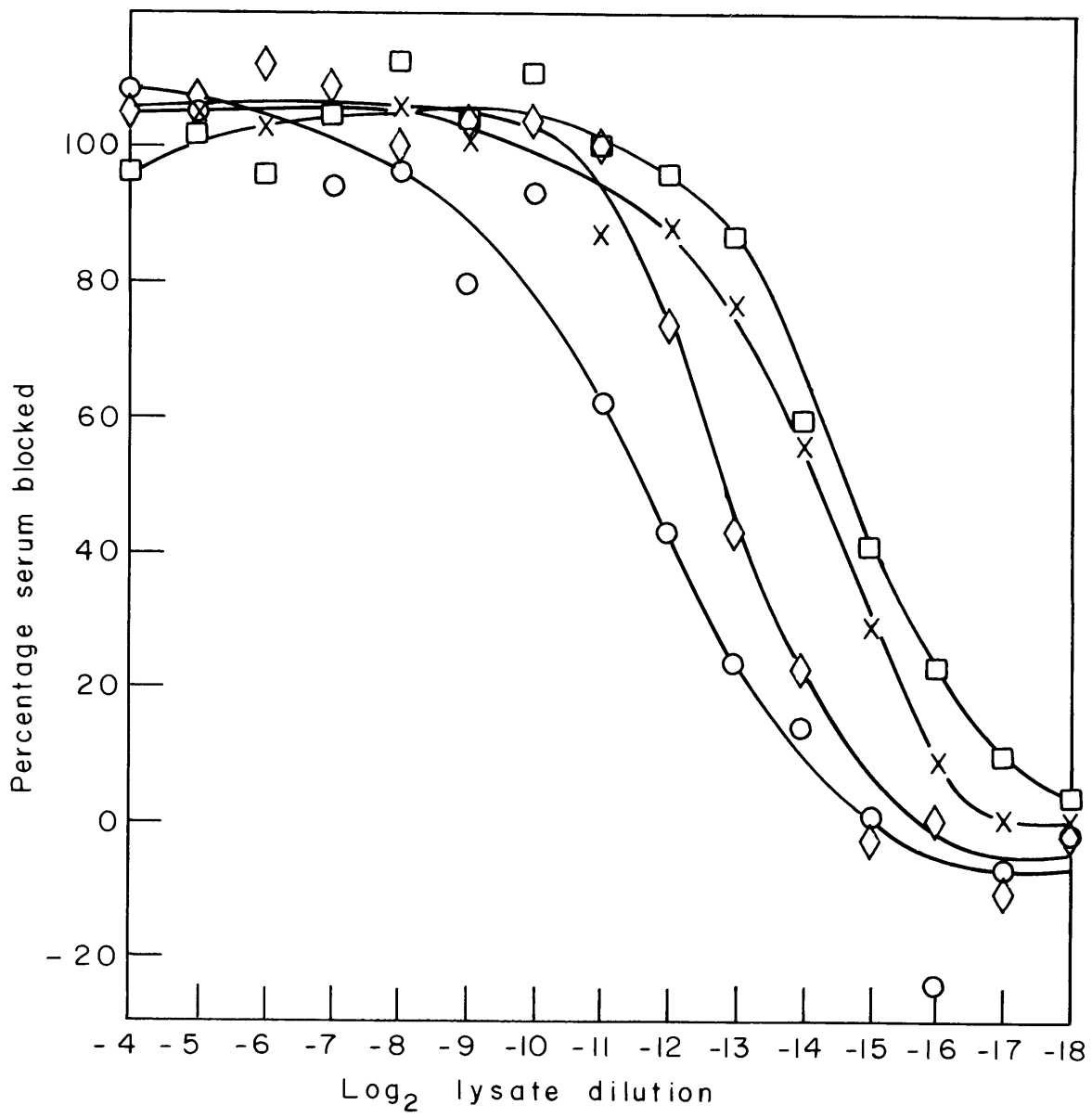


Figure 11Blocking of Anti-phage Serum by Lysates Lacking Gene
2 Product, Gene 3 Product or Gene 4 Product

Lysates were prepared and serum blocking curves determined as described in Materials and Methods, Section h, using Protocol II. The lysates included 13⁻ control lysate (-o-o-), 2⁻13⁻ lysate (-x-x-), 3⁻13⁻ lysate (-□-□-), and 4⁻13⁻ lysate (-◇-◇-). The wild-type 13⁻ lysate had a titer of 4.8×10^{11} \emptyset /ml. The k of the anti-phage serum at 47⁰C is 0.04 min⁻¹.



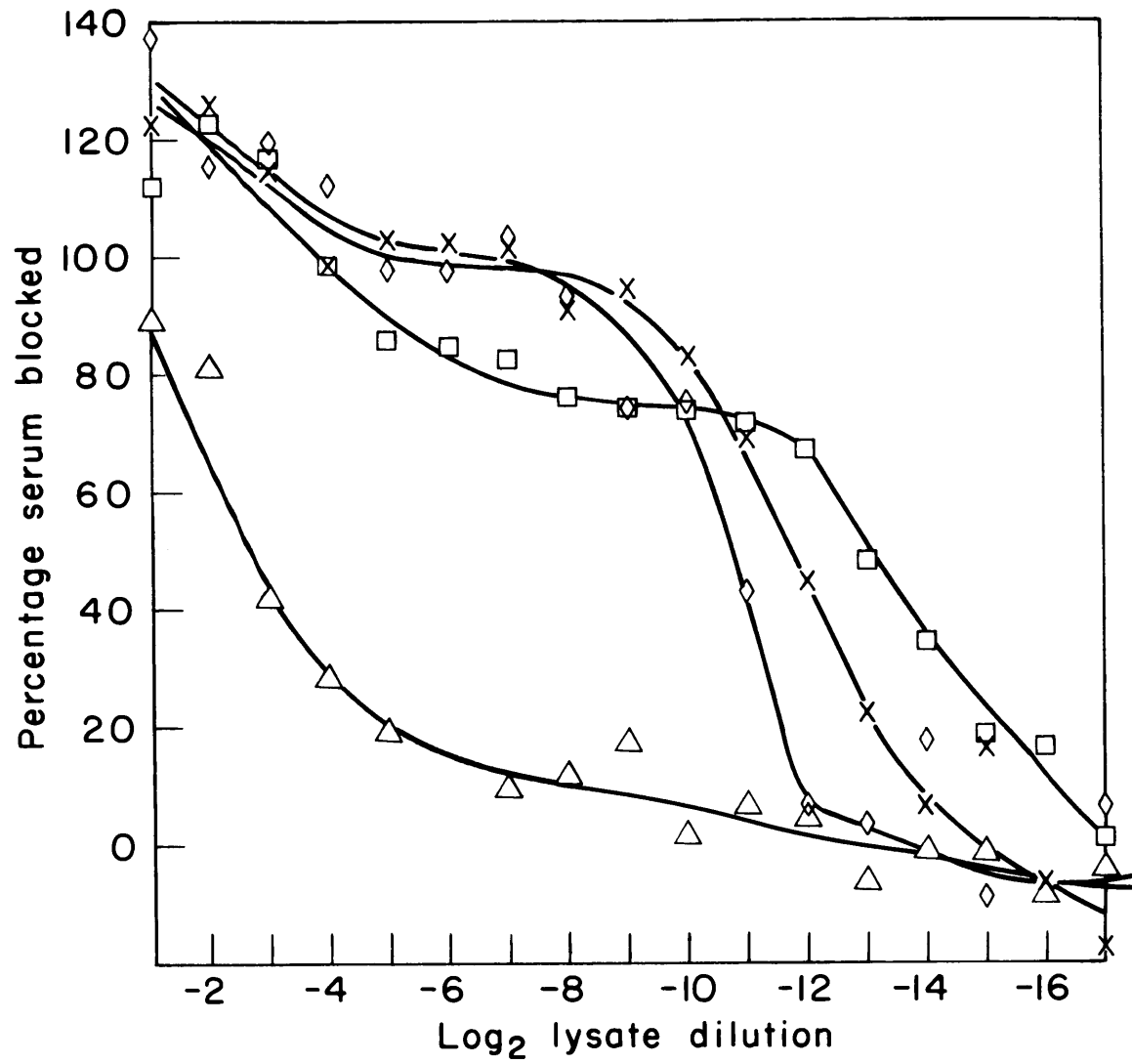
second, third and fourth categories of serum blocking activities, respectively, as had been determined by previous experiments using 13^- amber mutant lysates. The serum blocking curves described for the 13^+ lysates, shown in Figure 12, are very similar in nature to those obtained for lysates of the same class which were 13^- . These data indicate that the gene 13 product has no role in determining the antigenicity of the phage with respect to neutralizing antibodies. The data presented above eliminate all known minor phage proteins involved in assembly (with the exception of gp9) as targets of any portion of the neutralizing fraction of antibodies present in anti-phage serum.

In light of the gp5- and structure-dependence of the minority target antigen, the simplest hypothesis assigns some organized state of gp5, such as that which exists in phage or prohead structures, as the target antigen. Further relevant information on this question follows in the discussion of serum blocking power experiments using anti-phage serum in which purified structures serve as blocking agents. Results from these experiments contradict this simple interpretation of the lysate blocking data; rather, they suggest a complicated behavior for the target antigen of the minority fraction of the phage-neutralizing antibodies in the anti-phage serum.

Figure 12
Serum Blocking Curves With 13⁺ Lysates

Lysates were prepared with mutants defining each of the four serum blocking categories described previously, but all carrying the 13⁺ allele. The 9⁻ lysate (-△-△-), 7⁻ lysate (-◇-◇-), 2⁻ lysate (-x-x-), and 5⁻ lysate (-□-□-) gave curves similar to their 13⁻ counterparts.

Lysates were prepared from su⁻ cells at 2×10^8 cells/ml, infected at a multiplicity of 10 phage/cell and incubated at 30°C for 60 minutes. The burst size of a control wild-type 13⁺ lysate, prepared in parallel, was 490 phage per input cell. The serum blocking assay was as described in Materials and Methods, Section h, Protocol I. The anti-phage serum had a k of 0.02 min^{-1} at 48°C.



2) Serum blocking activity of the amber fragments of gp9

It is difficult to determine whether 9⁻ amber lysates block some small fraction of the phage-neutralizing activity of anti-phage serum (see Figures 8 and 12). The 9⁻ amber mutant chosen for the previous experiments produces the shortest gp9 amber fragment of several amber mutants mapping in gene 9. As larger amber fragments may contain a number of antigenic determinants, I examined several 9⁻ amber mutant lysates for their serum blocking activity.

Four amber mutant alleles of gene 9 were used to generate 9⁻ amber mutant lysates for serum blocking experiments. Two of the amber mutants map very close to the same site; however, they are not identical as they show unique patterns of suppression on several different amber suppressing hosts (P. Berget, unpublished experiments). SDS-gel electrophoresis experiments, using similar lysates, provide data on the molecular weight of the amber fragments in the lysates. A 9⁻amN110 lysate, which was used in previous serum blocking power experiments, contains the smallest gp9 amber fragment at a molecular weight of 7,000 daltons, 9% of the total mass of the polypeptide. A 9⁻amE1017 lysate contains a much larger fragment, with a molecular weight of 50,000 daltons, 66% of the mass of the complete polypeptide. Finally, lysates made from the two amber mutants which map very close together, 9⁻amN108 and 9⁻amH1014 contain 9⁻ amber fragments of similar molecular weight, approximately 59,000 daltons in molecular weight, which is 78% of the total mass of the gp9 molecule. The amber fragment from a 9⁻amN108 lysate is slightly smaller than the amber fragment from a 9⁻amH1014 lysate (C. Hall and J. King, unpublished experiments). The

relative lengths of these polypeptides are consistent with the data which exist on the relative ordering of the alleles by genetic mapping techniques (K. Lew, thesis results).

The results of the serum blocking experiments using these four 9⁻ amber mutant lysates are graphed in Figure 13. Though the lysates contain four different size amber fragments, none shows increased serum blocking ability.

3) Serum blocking experiments with purified particles and tail protein

In an effort to refine the characterization of the anti-phage serum, serum blocking experiments were done with components which were purified from amber mutant lysates. In these experiments, the purified structures include wild-type phage, 9⁻ tail-less heads, 2⁻ proheads, purified gp9 (P. Berget and A. Poteete, unpublished experiments), and phage which were purified after their formation in vitro by the addition of purified gp9 to purified 9⁻ tail-less particles. The results of serum blocking power experiments with these purified components are shown in Figure 14.

The data from the serum blocking behavior of purified wild-type phage particles are graphed in each panel of Figure 14 as a reference curve. As expected, purified phage block the anti-phage serum 100%. This plateau level is maintained until dilution lowers the concentration of target antigen below saturating amounts. With dilution beyond this point, serum blocking power decreases monotonically with dilution, until, finally, no serum blocking activity is detectable.

Figure 13Blocking of Anti-phage Serum by gp9 Amber Fragments

The lysates were prepared from DB7000 su⁻ cells in LB, infected at a multiplicity of 5 phage/cell, and incubated at 30°C for 60 minutes. The serum blocking procedure is described in Materials and Methods, section h, protocol II. The k of the anti-phage serum was 0.085 min^{-1} .

The 9⁻ amber mutant lysates contain different-sized amber fragments. The 9⁻amN110 lysate (-△-△-), used in previous experiments, contains the smallest gp9 amber fragment. The 9⁻amE1017 lysate (-□-□-) contains a gp9 amber fragment of intermediate molecular weight. The 9⁻amN108 (-◇-◇-) and 9⁻amH1014 (-x-x-) lysates contain larger amber fragments of approximately the same size. A 16⁻13⁻ lysate (-o-o-) serves as a reference curve.

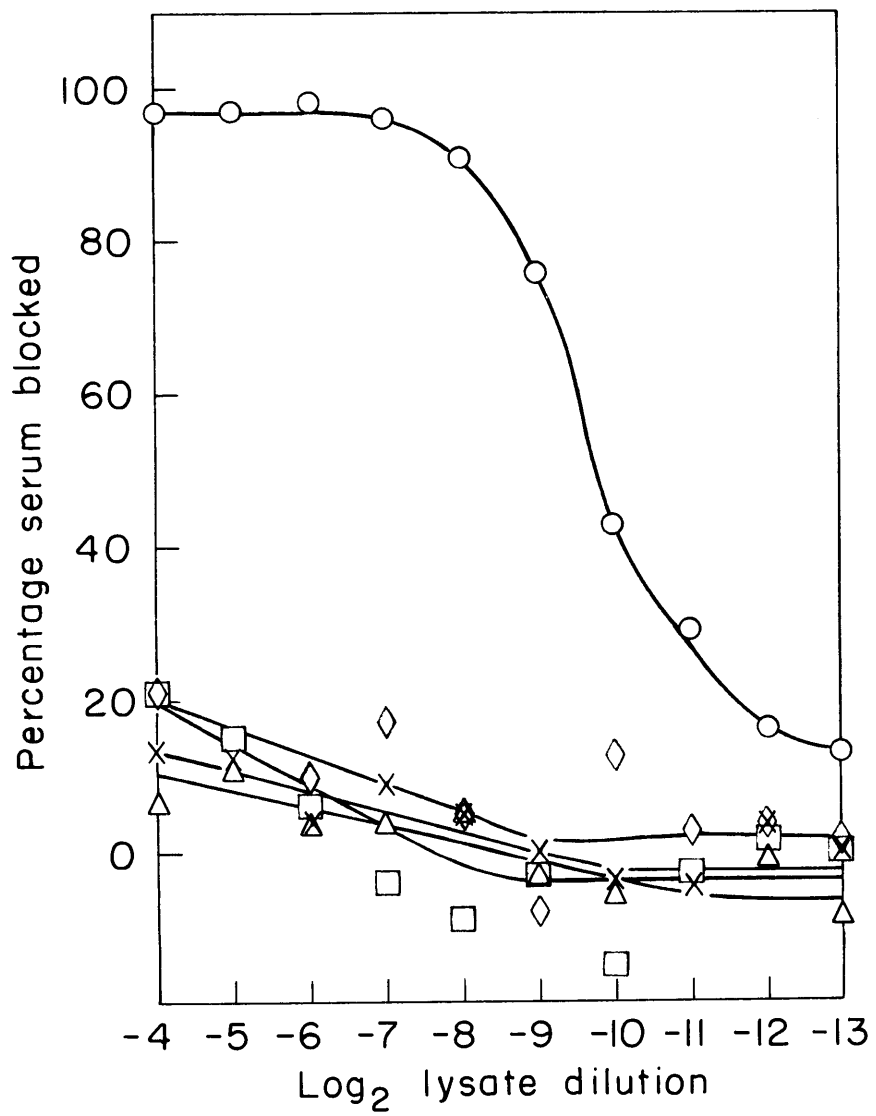


Figure 14

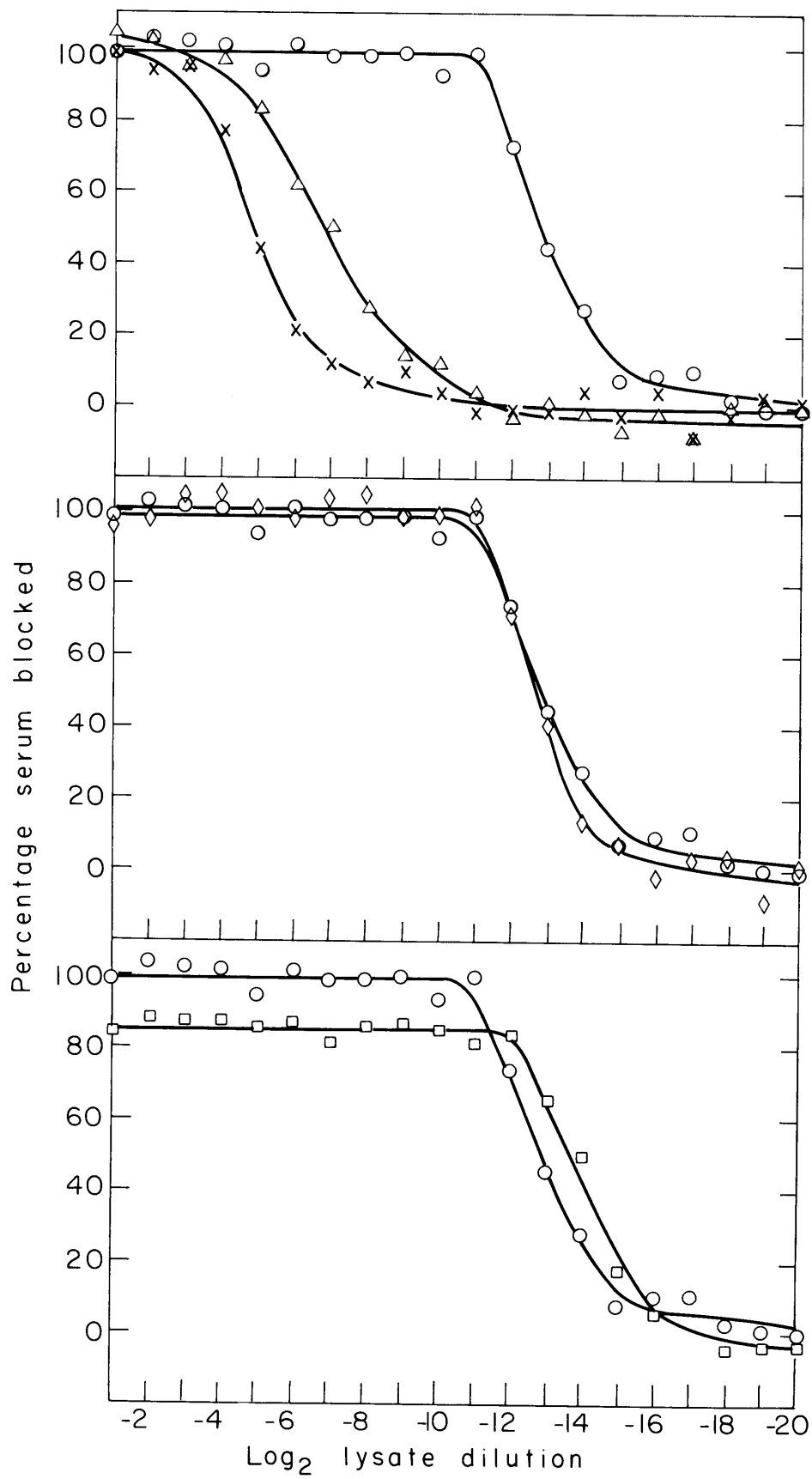
Blocking of Anti-phage Serum by Purified
Particles and Tail Protein

The serum blocking assay was done as in Materials and Methods, Section g, Protocol II. The k of the anti-phage serum was 0.04 min^{-1} . The preparation and purification of these particles are described in Materials and Methods, Section h, iii.

Panel a shows the serum blocking activity of purified phage (-o-o-), purified tail⁻ heads (-△-△-) and purified proheads (-x-x-). The viable titer of the phage at the first data point is 4.6×10^{12} phage/ml. The titer of the tail⁻ heads, is approximately 5×10^{12} heads/ml. The titer of the proheads was estimated by comparison of the proheads with the phage and heads above on SDS-gels. The titer of the proheads at the first data point is approximately 2×10^{12} proheads/ml. The serum blocking curve of purified phage is re-plotted in panels b and c for reference.

Panel b shows the serum blocking activity of purified phage particles (-◇-◇-) generated in vitro by the addition of purified gp9 to purified tail⁻ heads, as described in Materials and Methods, Section h, iii, 2c. The titer of the phage at the first data point is 2.7×10^{12} phage/ml.

Panel c shows the serum blocking activity of purified gp9 (-□-□-), provided by P. Berget and A. Poteete. The titer of tails, at the first data point is 5×10^{12} phage equivalents/ml.



The serum blocking power data for 9⁻ particles are also graphed in panel a of Figure 14. These particles, which lack the tail protein, gp9, are at approximately the same concentration as the purified wild-type phage in this experiment, as determined both by O.D.₂₆₀ measurements and by the titer of viable phage produced after tail addition. Despite their similar particle concentration, 9⁻ have only about 2% of the concentration of the serum blocking protein of the wild-type phage, as measured at the point where 50% of the serum is blocked. This substantiates the identification of the gp9 tail protein as the main target of the neutralizing antibodies. The background level of blocking probably represents input particles used for the infection. SDS-gel electrophoresis of the 9⁻ particles, at a concentration of 2.5×10^{12} particles/ml, did not reveal contaminating gp9 in the preparation, although levels less than about 10% would not be detected by this method. If these phage-density particles account for the low level of fully potent serum blocking protein present in the 9⁻ particle preparation, only about 0.0001% of them are viable phage. The viable phage present could account for only 30% serum blocking at the first data point. The remaining residual serum blocking antigen in this preparation is probably due to non-viable particles which contain less than the three equivalents of gp9 required for infectivity. Note that in the range of 2^{10} - 2^{12} -fold dilution, the 9⁻ particles block 0% of the neutralizing activity of the serum. In the same range of concentration, the wild-type particles block 100% of the phage-inactivating antibodies. If 9⁻ particles displayed the antigenic determinants miss-

ing from 5⁻ and 8⁻ lysates (Figures 8c and 12) we would expect them to block 15-20% of the serum. They do not; the curve goes to zero. The lack of serum blocking by the head particles indicates that the target antigen of the minor neutralizing antibody species is not located or is not available on phage heads.

Therefore, all of the phage-neutralizing antibodies in the anti-phage serum are apparently directed against antigenic determinants which are gp9-dependent. In the simplest interpretation of the results, all phage-neutralizing antibodies in the anti-phage serum are directed against the tail protein itself, gp9, though a subset may react only with the assembled state.

Particles which lack gp9 may be tailed to form viable phage by the in vitro addition of purified gp9. Immunologically, this same operation may be expected to provide the target antigen which is missing from tail-less heads, thereby generating full serum blocking power in the 9⁻ particle preparation. Panel b of Figure 15 shows the resultant shift in the serum blocking curve of 9⁻ particles after the addition of purified gp9. The serum blocking power of phage generated in vitro (and subsequently purified) compared with that of purified phage generated in vivo is virtually identical. This provides independent evidence that gp9 may be the sole agent responsible for blocking all of the phage-inactivating antibodies in anti-phage serum. Although the in vitro derived phage are, by viable titer, two-fold less concentrated than the in vivo phage, they show similar amounts of serum blocking. SDS-gel analysis (data not shown) indicates that the in vitro preparation of phage, formed in the presence

of excess gp9, contains roughly three times as much gp9 as the wild-type phage preparation, which accounts for their higher concentration of serum blocking protein.

Additional information of the characterization of the neutralizing antibodies in anti-phage serum is provided by the serum blocking behavior of purified proheads, which is included in panel a of Figure 14. SDS-gel analysis indicated that the proheads are about four times less concentrated than the 9⁻ particles. Therefore, proheads and tail⁻ heads are similarly poor blocking agents against anti-phage serum.

The small amount of gp9 which seems to be present in the pro-head preparation, as indicated by the serum blocking data, was not detectable on SDS-gels by protein staining. The tail protein was probably contributed by empty phage heads which came from the original input phage population which was used to generate the pro-head-producing lysate. Empty heads sediment similarly to proheads (King, et al., 1973) and proheads purified through a sucrose gradient, particularly in preparative scale purification procedures, are contaminated by the low levels of empty heads present in the input phage stocks.

Final proof for the hypothesis that gp9 is the target antigen of the majority of the phage-inactivating antibodies in anti-phage serum is shown in panel c of Figure 14. The purification of gp9 from a 5⁻13⁻ amber mutant lysate by biochemical methods (P. Berget and A. Poteete, unpublished results) provides the putative target antigen in a form which is approximately 95% pure. The purified gp9 was in-

cubated with the anti-phage serum and tested for its ability to block the phage-killing antibodies. As the results in panel c of Figure 14 show, purified gp9 blocks 85% of the phage-neutralizing antibodies present in anti-phage serum. The direct conclusion from these data is, therefore, that gp9 itself, as purified from a 5⁻¹³ amber mutant lysate, is the target of 85% of the phage-killing antibodies present in anti-phage serum.

C. The Neutralizing Activity of Anti-prohead Serum

(1) The serum blocking activity of purified components

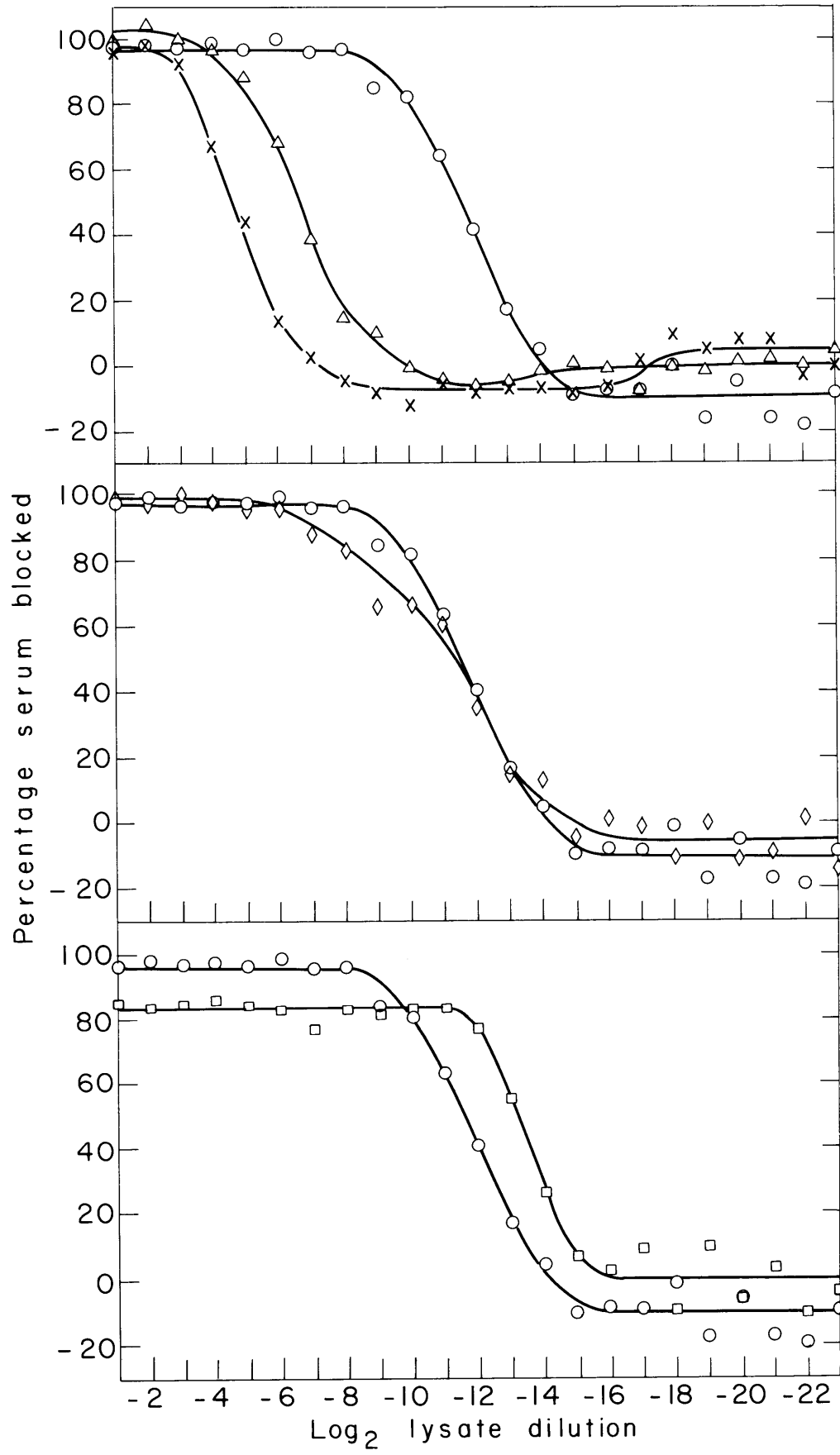
Anti-prohead serum kills P22 phage at a rate about five times slower than anti-phage serum. However, the shape of the two killing curves are very similar. In order to determine the target of the neutralizing activity of anti-prohead serum, I did serum blocking experiments with purified particles, as described previously. The same preparations of particles used with the anti-phage serum were used to block the anti-prohead serum. The results are shown in Figure 15.

The serum blocking curve of wild-type phage is plotted in each panel. As expected, the phage block 100% of the neutralizing species. The concentration of phage which blocks 50% of the neutralizing species in anti-prohead serum is very similar to that which blocks 50% of the anti-phage serum, at equivalent k values. This suggests that the neutralizing antibodies in both sera are very similar.

The serum blocking curve of purified proheads, at approximately the same concentration as the phage, is shown in panel a. As the serum was originally made against proheads, I was somewhat surprised that the proheads were very ineffective antigens against the neutralizing antibodies. This suggested that a species of immunogen present at very low concentration in the preparation was, nevertheless, responsible for the induction of a large fraction of the antibodies capable of killing phage. The most likely contaminants are phage ghosts. These derive from the input particles used to make the lysate from which the proheads were isolated. Empty heads sediment similarly to proheads and are

Figure 15Blocking of Anti-prohead Serum by Purified
Particles and Tail Protein

The serum blocking assay and purified components are as described in the Legend to Figure 14. The k of the anti-pro-head serum was 0.07 min^{-1} .



not easily fractionated by the procedure (King, et al., 1973).

Tail⁻ heads also showed virtually no serum blocking activity, as shown in panel a. This result indicates that the tail protein is the target of the neutralizing activity in anti-prohead serum, as well as in anti-phage serum. This can be seen more clearly in panel c, which shows blocking by purified gp9. The purified protein blocks more than 85% of the neutralizing species in the anti-prohead serum, similar to its blocking behavior against anti-phage serum.

The central panel shows that assembling the purified gp9 onto tail-less particles regenerates full serum blocking activity. Thus, all of the serum blocking activity of phage particles is gp9-dependent.

The serum blocking curves resulting from the incubation of purified components with anti-prohead serum are practically superimposable on those obtained using anti-phage serum. Consequently, the two sets of experimental data generate the same conclusions as to the nature of the phage-killing antibodies in both sera. Despite the fact that the prohead immunogen preparation contains^{ed} tail protein only as a contaminant, at least 85% of the phage-neutralizing antibodies in both anti-phage and anti-prohead sera are directed against the tail protein, gp9. The similarity in the serum blocking data may indicate that the minority antibody fractions of the two sera are directed against the same target, as well. The most likely target antigen for this antibody fraction is gp5, the capsid protein, as previously discussed for the anti-phage serum.

(2) Blocking of anti-prohead serum by P22 amber mutant lysates

Anti-prohead serum and anti-phage serum behaved almost identically

in response to serum blocking by purified components. In order to examine whether the analogous behavior of the two sera extended to interactions with crude lysates, I did additional serum blocking experiments using several P22 amber mutant lysates to block the anti-prohead serum.

The results of one such experiment are shown in Figure 16. The serum blocking curve for a wild-type lysate, shown in panel a, and re-plotted in panels b and c for reference, is particularly striking. At high lysate concentrations, the lysate blocks all of the phage-neutralizing antibodies in the anti-prohead serum. With increasing lysate dilution, the percentage serum blocked starts to fall; however, at intermediate lysate dilutions, this trend reverses itself, and increasing lysate dilution leads to increased serum blocking. Finally, at very high lysate dilutions, this effect ceases, and serum blocking by the lysate decreases monotonically with dilution. The serum blocking curve of a 2⁻ lysate, shown in panel b, exhibits a very similar shape, except that the target antigen appears to be present in higher concentration.

A 9⁻ lysate, shown in panel a, has no detectable serum blocking activity. In fact, the serum blocking curve may show negative values. Panel a also shows the serum blocking curve of a 5⁻9⁻ amber mutant lysate. This curve is very similar to that of the 9⁻ lysate.

Only a 5⁻ lysate, shown in panel c, shows a constant, positive level of serum blocking activity of about 85%. Presumably, the soluble tail protein present in this lysate accounts for its serum blocking activity.

Figure 16

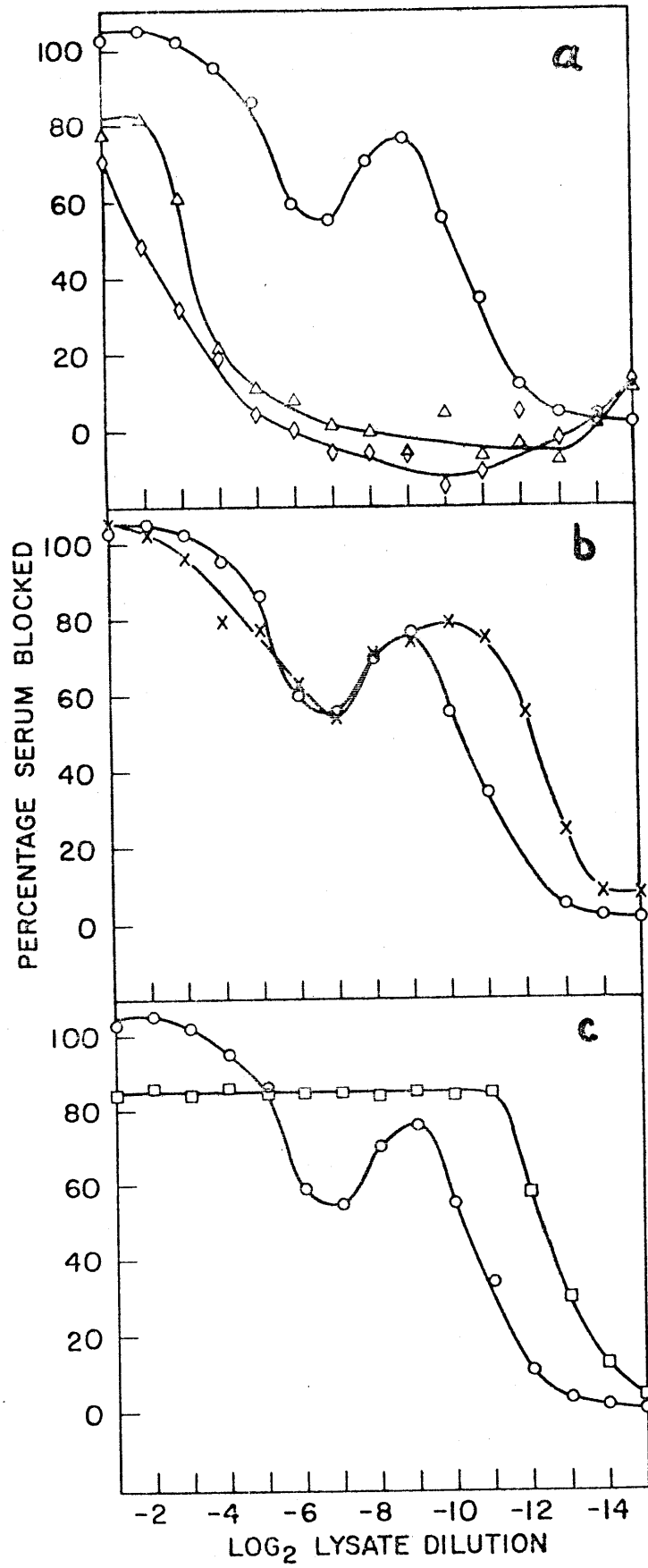
Blocking of Anti-prohead Serum by P22 Amber Mutant Lysates

The lysates were prepared from DB7000 su^- cells in LB, infected at a multiplicity of 5 phage/cell and incubated for 60 minutes at $30^{\circ}C$. The wild-type burst was 300 phage/input cell. All lysates are 13^- . The serum blocking protocol is described in Materials and Methods, Section h, Protocol II. The k of the anti-prohead serum was 0.06 min^{-1} .

Panel a shows serum blocking curves for wild-type lysate (-o-o-), 9^- lysate (-◇-◇-) and 5^-9^- lysate (-△-△-). The wild-type curve is re-plotted in each panel for reference.

Panel b shows the serum blocking curve of a 2^- lysate (-x-x-).

Panel c shows the serum blocking of a 5^- lysate (-□-□-).



Discussion - Serum Blocking

The Neutralizing Activity of Anti-phage Serum

The experiments with purified phage and phage precursors clearly show that the gp9 tail protein is the major target of the neutralizing antibody present in anti-P22 serum. Purified phage block all of the neutralizing antibody present in the serum. Deletion of a single protein species, gp9, from the phage particles removes all their serum blocking power. Addition of purified gp9 to tail-less particles, which alone do not block any fraction of the neutralizing antibody, restores full serum blocking activity. Therefore, antigens are composed of or depend upon the gp9 tail protein.

However, purified gp9 blocks only 85% of the neutralizing antibody species, not 100% as might be expected. This discrepancy might be accounted for if some of the antigenicity of the complete phage particle represented the assembled six-fold form of the tail protein and was not displayed by soluble tail subunits. Unfortunately, experiments with defective lysates are only partially consistent with the model. Lysates prepared with amber mutants of gene 9 did not block any substantial fraction of the serum, confirming that the major target is the gene 9 product. In addition, 5⁻ and 8⁻ lysates, which are blocked in shell assembly and accumulate the unassembled tail subunits block 85% of the neutralizing species, just like the purified protein. However, lysates blocked in DNA packaging - 1⁻, 2⁻, or 3⁻ - which also contain only the unassembled form of the tail subunits, block 100% in contradiction with the model. These lysates accumulate organized pro-heads, in contrast to the 5⁻ and 8⁻ lysates.

The lysate experiments suggest that the residual 15% of the neutralizing activity is directed against an antigen which only exists on an organized shell. Since the defective lysates containing proheads block all of the serum, the minor target could be a minor protein of the prohead. These include, gp1, gp7, gp16, and gp20. However, lysates made with mutants defective in each of these genes still block all of the killing antibody of the serum. This eliminates the minor proteins as candidates for the minor antigenic target. Only lysates defective in coat or scaffolding protein synthesis fail to block all of the killing species.

The scaffolding protein, gp8, is not a structural protein of the mature phage (Botstein, et al., 1973). Therefore, it cannot be a part of the target of killing antibody. This leaves as the best candidate for the target of the minor killing antibody species, the organized form of gp5, the major coat protein. If this is the case, proheads or tail-less heads should block 15% of the neutralizing species of the serum. The data shown in Figures 14 and 15 indicate that this was not the case; these particles had no detectable serum blocking power. The relevant observations are summarized below:

<u>Component</u>	<u>Serum Blocking</u>	<u>Component</u>	<u>Serum Blocking</u>
tail ⁻ heads	0%	proheads	0%
soluble tails (5 ⁻ lysate)	85%	soluble tails (5 ⁻ lysate)	85%
<hr/>		<hr/>	
phage (tail ⁻ heads + soluble tails)	100%	2 ⁻ lysate (proheads + soluble tails)	100%

These data point out the paradox which exists: the serum blocking activity of antigens in combination is greater than the sum of the serum blocking activities of the antigens alone. No simple model can account for this behavior. The non-additivity of the serum blocking activities implies a complicated situation in which events affecting serum blocking do not occur independently. Perhaps, the serum blocking activities of the antigens reflect a non-additive interaction of their complementary antibodies. One possible model which explains the data is as follows: Experiments in the following chapters will show that anti-phage serum contains large quantities of precipitating anti-capsid antibodies. Given sufficient time, these antibodies will lead to a loss of phage titer in serum blocking experiments, because the phage will become aggregated into complexes which will titer as a single plaque forming unit. Alternatively, there may exist a killing class of anti-gp5 antibodies which requires several hits before inactivation results. These two classes of antibodies are indistinguishable and both lead to multiple hit kinetics. In the presence of anti-gp9 antibodies, these anti-capsid antibodies will not detectably contribute to the overall rate of phage-neutralization: in a vast majority of the cases, the phage will be killed by a single anti-gp9 antibody before enough anti-gp5 antibodies can bind to kill the phage; as a result, anti-capsid antibodies bound to dead phage are undetectable. It is only in the absence of anti-gp9 antibodies that phage-neutralization by the anti-capsid antibodies may be measured.

The key observations are summarized in Table 4. These can be explained by the above model as follows. The killing activity of whole

Table 4

Characterization of the Phage-neutralizing Activity of
Anti-phage Serum Using Non-additive Antibody Interactions

<u>Antigen</u>	<u>Antibodies Absorbed</u>		<u>Antibody Composition of Absorbed Serum</u>	<u>Serum Blocking</u>
	<u>Anti-capsid</u>	<u>Anti-tail</u>		
Phage	+	+	No phage-neutralizing antibodies	100%
Tail ⁻ heads	+	-	Anti-tail	0%
Proheads	+	-	Anti-tail	0%
Soluble gp9	-	+	Anti-capsid	85%
Wild-type lysate	+	+	No phage-neutralizing antibodies	100%
9 ⁻ lysate	+	-	Anti-tail	0%
5 ⁻ lysate	-	+	Anti-capsid	85%
8 ⁻ lysate	-	+	Anti-capsid	85%
All other P22 lysates tested	+	+	No phage-neutralizing antibodies	100%

serum is due to antibodies against the tail protein. If these antibodies and the anti-capsid antibodies are removed by absorption, there is no residual killing activity. If only the anti-capsid antibodies are removed, the serum remains just as active as the whole serum. However, if the antibody class against the tail is absorbed out, leaving the anti-capsid antibodies active, one then detects a low level of inactivation whose apparent k is 15% of the starting serum. Thus, when the whole serum is blocked by preparations lacking organized capsids, such as 5^- or 8^- lysates, or purified gp9, only 85% of the k of the serum is blocked. Actually all of the antibody species normally detectable in the serum were blocked, but the absorption effectively unmasked the multi-hit and anti-capsid antibodies.

In fact, the numbers are somewhat misleading. The 15% figure was calculated from the survival of the tester phage after 2 hours incubation, assuming exponential inactivation. This was reasonable, since the starting serum displayed exponential inactivation. However, given that the residual inactivation was due to a multi-hit process, this apparent k is not comparable with that determined from exponential inactivation.

I attempted to prepare serum specifically absorbed with gp9, to characterize the residual antibody species in more detail. As a control, one sample was absorbed with 9^- particles. This absorption should leave behind all of the anti-gp9 antibodies, the dominant killing species. The resulting serum retained had an apparent k of about 120% the starting titer. However, the sample absorbed with 5^- lysate had a residual k value much lower than the 15% I had expected. However,

at that time I did not understand that the residual killing activity inactivated phage in a multi-hit fashion. In titrating the absorbed serum, I measured the rate of inactivation as a function of time from 0-60 minutes. There was little inactivation over this period. However, the conditions of the two experiments were not identical. In the standard serum blocking assay, a single time point was taken after 120 minute incubation with tester phage. Presumably, had I extended the incubation period for the absorbed serum to 120 minutes, I would have detected a residual neutralizing species.

The results of the serum blocking experiments using 8⁻ lysates suggest that only a fraction of the antibodies directed against the coat protein have neutralizing activity. Electron microscopy experiments described in Chapter III showed that 8⁻ lysates contained aggregates of coat protein which bound anti-phage antibodies. However, these structures were unable to absorb the neutralizing anti-capsid species. Thus, they represent only a subset of the total anti-coat protein antibodies.

The Neutralizing Activity of Anti-prohead Serum

The blocking of anti-prohead serum by purified components was similar to the blocking of anti-phage serum by purified components. This suggested that both sera inactivate infectious phage by similar mechanisms. Thus, one might have thought that the phage-neutralizing antibodies in anti-prohead serum would consist of anti-gp9 antibodies which inactivate with single-hit kinetics, and anti-capsid antibodies which display multi-hit inactivation.

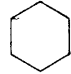

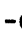

However, this relatively simple model is not sufficient to explain the blocking of anti-prohead serum by P22 mutant lysates. The

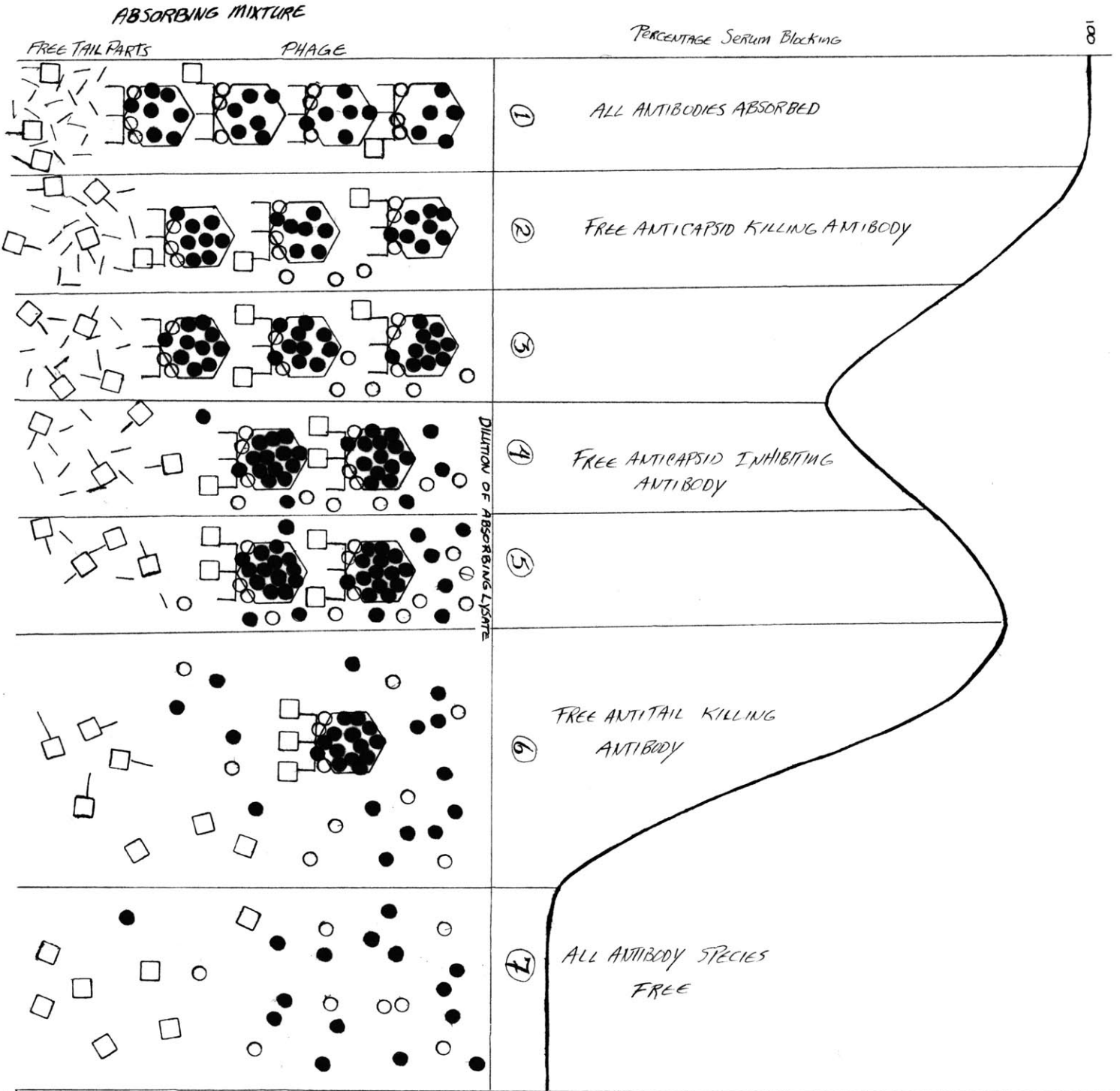
complex shapes of those curves indicates that the serum also contains antibodies which inhibit inactivation. The differential absorption of the inhibiting versus the inactivating antibodies then generates the complex blocking curves.

A model which accounts for the results is as follows: Assume that, in addition to the anti-tail neutralizing species and anti-capsid neutralizing species, the serum contains non-neutralizing anti-capsid antibodies which compete for the targets of the neutralizing anti-capsid species. When these antibodies bind to phage, they prevent the killing species from binding and inhibit phage inactivation. (As will become clearer later, this probably stems from the fact that the synthesis of most of the antibodies in the serum were induced by proheads. However, the inactivating species were probably induced by low levels of contaminating empty heads. When the whole serum is incubated with phage particles, the anti-prohead species react with sites close to the target sites for inactivation).

Lysates contain high levels of tail protein which block the anti-tail antibodies over a wide concentration span. The residual 15% inactivation by serum incubated with relatively high lysate concentrations is due to the anti-capsid species. Diagram 2 shows schematically what happens. At high lysate concentration all antigens are in excess, and all antibody species are absorbed. As the particle concentration decreases, one class of antigenic sites become limiting, and a class of neutralizing anti-capsid antibodies, directed against these targets, remains after absorption. For example, the killing anti-capsid antibodies may be bound only in the

Diagram 2: Schematic Illustration of the Blocking of
Anti-prohead Serum by a Wild-type Lysate

The symbols below the graph describe the state of the absorbing antigens and the neutralizing antibodies after overnight incubation with samples of lysate dilutions. The hexagonal symbols () represent the phage in the lysate; the short dashes (/->), the soluble gp9. The antibody species of interest, which include anti-gp9 antibodies (), killing anti-capsid antibodies (), and inhibiting antibodies () which interfere with phage neutralization by the killing anti-capsid antibodies, are either bound to the particles or remain free in solution, as indicated. Only free antibodies are active in neutralizing tester phage which are added after the binding reactions have gone to completion.



vicinity of the tail while targets for the non-neutralizing antibodies may be distributed over the entire capsid surface. According to this model, at lysate dilutions of 16-128 fold on the wild-type curve in Figure 16, or in Region 2 of Diagram 2, neutralizing anti-capsid antibodies are free in the absorbed serum while the interfering antibodies are bound. When tester phage are added, the free neutralizing antibodies in the absorbed serum do not have to compete for sites on the tester phage, and they kill phage at a rate even faster than when they are present in whole serum. Therefore in the initial part of the wild-type curve, increasing lysate dilution leaves more and more killing anti-capsid antibodies free in the serum.

Eventually, however, increasing the dilution of the antigens causes the number of binding sites for the inhibiting anti-capsid antibodies to become limiting (Region 3, Diagram 2). Beyond this point, more and more inhibiting anti-capsid antibodies remain in the serum after absorption. These inhibit the killing anti-capsid antibodies, and the rate of phage-killing decreases. This is reflected by the portion of the wild-type curve, from 128-512 fold in Figure 16, or Region 4 in Diagram 2, in which decreasing antigen concentration results in decreased serum neutralizing activity after absorption.

This trend continues until dilution of the lysate beyond 500-fold in Figure 16, or Region 5 in Diagram 2, finally reduces the concentration of the soluble gp9 in the lysate to a level where all of the anti-gp9 antibodies can no longer be absorbed (Region 6,

Diagram 2). Once anti-gp9 antibodies exist free in the absorbed serum, they are the primary antibody species responsible for phage-killing because they kill with single-hit kinetics. Thus, the final portion of the wild-type curve reflects the concentration of the anti-gp9 antibodies which are free in the absorbed serum. Lysate dilution increases the concentration of free anti-gp9 antibodies until, finally, all species of antibodies are free, and the percentage serum blocked falls to zero (Region 7, Diagram 2).

This model also accounts for the serum blocking behavior of the other P22 lysates tested. Prohead-containing lysates - 1⁻, 2⁻, and 3⁻ - and empty head-containing lysates - 4⁻, 10⁻ and 26⁻ - and lysates containing phage-like particles - 7⁻, 16⁻ and 20⁻ - contain organized capsid shells which presumably absorb the anti-capsid antibodies in more or less the same fashion as the phage particles. Therefore, the initial and intermediate portions of the serum blocking curves of these lysates are similar to those of the wild-type lysate. The anti-gp9 antibodies are absorbed by the soluble gp9 which is present in these lysates until high lysate dilution reduces the concentration of soluble gp9 to less than saturating amounts. Thus, the latter portions of the serum blocking curves of these lysates are also similar to the wild-type curve, except that the serum blocking curves of the prohead-containing lysates, which overproduce gp9, extend over a wider range of lysate dilutions.

With 5⁻ and 8⁻ lysates, none or very few of the anti-capsid antibodies are removed from the serum whereas all of the anti-gp9 antibodies should be removed. Therefore, 5⁻ and 8⁻ lysate-absorbed sera presumably contain the full complement of the killing and non-killing

anti-capsid antibodies. Thus, they provide an estimate of the rate of phage-killing by the minority fraction of the antibodies as it exists in whole serum.

I expected the residual rate of phage-killing by 9^- lysate-absorbed anti-prohead serum to be indistinguishable from the rate of phage-killing by the whole serum, because anti-gp9 antibodies would be solely responsible for phage-inactivation in both sera. Although the results are in general agreement with this prediction, it appears that negative values of serum blocking are actually obtained at several lysate dilutions. Apparently, at these lysate concentrations, high concentrations of neutralizing anti-capsid antibodies are free in the serum in the absence of significant concentrations of inhibiting antibodies. Under these conditions the contribution to phage-killing by the uninhibited anti-capsid antibodies becomes measurable. Eventually, at higher lysate dilutions, the inhibiting antibodies are free in solution, and the serum blocking level returns to zero.

The serum blocking curves of the wild-type or 2^- lysates against anti-prohead serum may be duplicated by mixing purified phage, or purified proheads, respectively, with purified gp9 (D. Smith, R. Griffin Shea, and J. King, unpublished experiments). These results confirm that the curves are generated by interactions solely between these structures and gp9.

Attempts to absorb anti-prohead serum with lysates or purified components were unsuccessful (D. Smith and J. King, unpublished experiments). The residual k values of the absorbed sera were so low

that further characterization of the sera was impossible. Although, the reasons for the inability to regain substantial neutralizing activity are ^{not} clear, it is possible that the high concentrations of serum and of the lysates or purified components used for absorption produces effects not present in the dilute conditions of the serum blocking experiments.

Note that the anti-prohead serum can be thought of as the rabbit's response to two classes of immunogens: 1. proheads, which induce a high concentration of precipitating antibodies, including anti-gp5 and anti-gp8 antibodies, as will be shown in the following chapters; and 2. contaminating empty heads with tails (from the infecting phage used to generate the proheads) which induce anti-gp9 antibodies. These empty phage presumably also induce anti-capsid antibody that slowly inactivates phage, as described for the anti-phage serum. However, the proheads in the preparation seem to have induced an additional class of anti-gp5 antibodies which may well compete for similar sites, or interfere sterically with the binding of this killing anti-capsid fraction. These interfering species apparently were not generated by the injection of phage particles, as there is no indication of an inhibiting antibody class in the anti-phage serum. I will show evidence in Chapters II and III that the population of antigenic coat protein sites on proheads contains determinants not present on phage, a result consistent with this model.

D. Comparison of the Level of Serum Blocking Activity with Concentration of Tail Parts

Comparison of the serum blocking curves of wild-type lysates with those of purified phage reveals a consistent feature: the lysates always display substantially more serum blocking antigen than can be accounted

for by the number of phage in the lysates. For example, using purified phage, as in Figure 15, 2.4×10^9 phage/ml are required to block 50% of the anti-prohead serum. Using a wild-type lysate, as in Figure 16, only 1.5×10^8 phage/ml are sufficient to block an equivalent amount of serum. (The values were normalized for the difference in the k values of the two sera). Thus, phage alone cannot account for the serum blocking activity of the lysate.

Previous SDS-gel electrophoresis experiments using radioactively labelled P22 lysates showed that tail protein is heavily overproduced relative to wild-type levels in all lysates in which DNA is not packaged - 5⁻, 8⁻, 1⁻, 2⁻ and 3⁻ (S. Casjens and J. King, unpublished experiments). However, the results of the serum blocking experiments suggest that, even in the wild-type lysate, amounts of gp9 are produced in excess of that needed to tail the phage which are present.

In order to examine this possibility, I compared the serum blocking activity and the concentration of soluble tail parts in wild-type, 5⁻, and 2⁻ lysates. Serum blocking curves, similar to those which have been presented were obtained (data not shown). The concentration of functional tail subunits in these same lysates was measured by assaying their ability to convert tail-less heads to viable phage (Israel, et al., 1967). First, phage and phage-sized particles were removed from the lysates by high-speed centrifugation so that only soluble tail parts remained. Then, serial dilutions of the lysates were incubated with a constant number of purified heads, and the numbers of viable phage produced were measured. The dependence of phage forma-

tion on lysate dilution (gp9 concentration) had the third power character described by Israel, et al. This indicated that all three lysates contained unassembled tail subunits. A summary of the results is shown in Table 5. Also included for comparison are similar data for purified gp9 and two samples of purified phage, one produced in vivo; the other, in vitro.

The results from the tailing assay of the wild-type lysate shows that, as expected, a considerable amount of excess soluble gp9 is produced. Comparing the tail parts/ml with the phage/ml in this lysate, soluble gp9 is present in almost 3-fold excess over that which would be needed to put 6 tail parts on every phage present in the lysate. In addition, in agreement with the radioactive labelling experiments mentioned previously, the number of tail parts/ml in 5⁻ and 2⁻ lysates is about 5-fold higher than in the wild-type lysate.

If we now compare the number of tail parts at 50% serum blocking for the three lysates, the values are similar for both sera. (The value for the 2⁻ lysate using anti-prohead serum was uncharacteristically high in this experiment). This is consistent with the neutralizing activities of the two sera being very much alike.

A significant difference appears to exist between the serum blocking activity of soluble gp9, whether purified or as it exists in lysates, and gp9 which has been assembled into tail structures. For example, the soluble tail subunits in the purified gp9 preparation are 6-9 times more effective in blocking the sera than tail protein present in the tails of phage made in vivo. This is also true of phage made in vitro by mixing the gp9 preparation with tail-less heads.

Table 5

Comparison of Serum Blocking Activity with Concentration of Tail Parts

Preparation	Viable Titer (phage/ml)	Tail Parts/ml ¹	Anti-phage Serum ³		Anti-prohead Serum ⁴	
			Fold Dilution at 50% Serum Blocking	Tail Parts/ml at 50% Serum Blocking ⁵	Fold Dilution at 50% Serum Blocking	Tail Parts/ml at 50% Serum Blocking
Purified phage	9.2×10^{12}	5.5×10^{13}	5,714	9.6×10^9	4,096	1.3×10^{10}
Purified <u>in vitro</u> phage	5.4×10^{12}	3.2×10^{13}	5,714	5.6×10^9	4,096	7.8×10^9
Purified gp9 ⁶	-	5.9×10^{11}	585	1.5×10^9	405	1.5×10^9
Wild-type lysate	4.8×10^{10}	$5.9 \times 10^{11^2}$	288	3.0×10^9	204	2.9×10^9
5 ⁻ lysate	-	3.3×10^{12}	-	-	319	4.0×10^9
2 ⁻ lysate	-	2.9×10^{12}	1,638	2.7×10^9	409	7.3×10^9

¹ Determined for lysates as described in Materials and Methods, Section h, iv. For purified viable phage, we multiplied the viable phage titer by six.

² The phage-sized particles were centrifuged out of these lysates prior to the tailing reaction.

³ Data taken from experiment in Figure 14.

Table 5 (Contd.)

Comparison of Serum Blocking Activity with Concentration of Tail Parts

Data taken from experiment in Figure 15.

These values have been multiplied by the ratio of the k of the anti-prohead serum (0.07 min^{-1}) to that of the anti-phage serum (0.04 min^{-1}) to adjust for the difference in the concentration of the two sera.

Provided by P. Berget and A. Poteete.

In this case, it takes 3 1/2 to 5 times as many assembled phage tail parts to block the sera as it does phage equivalents of the same preparation of soluble tail protein. Actually, the discrepancies are probably larger than those indicated here because the estimates for the number of tail parts in the phage preparations do not include tails present on non-infectious particles.

There are two possible explanations for why soluble gp9 appears to be a more active serum blocking species than assembled tail parts. First, there may be tail protein in the lysates and in the purified gp9 preparation which is not active in tailing but which is, nevertheless, antigenic. A second explanation is that free tail subunits have more antigenic sites available than subunits bound to phage. This seems likely because assembly of the tail may involve subunit-subunit interactions which mask determinants on the unassembled proteins.

The neutralization of P22 phage by anti-phage serum is caused primarily by the reaction of anti-gp9 antibodies with the tail protein, with one hit sufficient to cause inactivation. None of the minor proteins of the phage appears to be ^atarget of inactivation. Antibodies against determinants only present in the assembled shell also inactivate phage, but with multi-hit kinetics. The target of this antibody is unknown, but perhaps certain capsid sites at the site of head-tail attachment play a role in the infectious process.

As expected from the above, antibody induced by tail-less heads do not directly neutralize phage at any substantial rate.

Serum prepared against proheads does inactivate phage. The neutralizing antibody species are similar to those in anti-phage serum;

anti-tail antibodies which inactivate with single hit kinetics, and anti-capsid antibodies which inactivate with multi hit kinetics. In addition, the serum contains a species which inhibits the latter antibody. The data indicate that the neutralizing antibodies were induced by low levels of contaminating empty phage particles present in the prohead preparation. The targets of the neutralizing antibodies may represent particularly potent immunogens.

The inactivation by anti-tail protein may act either at the level of a sorption to the host cell, or at later stages of the infectious process (Israel, et al., 1972). In general, the inactivation resembles that of bacteriophage lambda and T4, where the neutralizing antibodies are also directed against the absorption organelles.

I had expected to identify a class of antibodies directed against the fiber that projects from the P22 tail plate. This looks morphologically like an attachment organelle. Either (1) the fiber is coded for by an unknown gene, and is therefore present in all mutant lysates or (2) it is not essential for phage infection or (3) it is not an effective immunogen.

CHAPTER II

Chapter II: Investigation of the Total Specific Antibody Composition of Anti-P22 Sera by Immunelectrophoresis

In the preceding Chapter, I described the inactivation of phage P22 by anti-phage and anti-prohead sera. I then utilized serum blocking experiments to characterize the species of antibody which were responsible for the neutralizing activity of the sera. This phage-neutralizing fraction of the antibodies may represent only a small subset of the total antibody population directed against P22 structures. For example, the sera may contain anti-phage antibodies which bind to the surface of the phage but which do not inactivate it. In addition, sera made against proheads or tail⁻ heads may contain antibodies which bind exclusively to these structures but not to mature phage.

In this section I employ immunelectrophoresis experiments to define antibodies in the sera which react with P22 proteins, but which may not directly inactivate phage particles.

A. Characterization of Precipitating Antibodies by the Technique of Immunelectrophoresis

Antibodies which are capable of forming a precipitin network with P22 antigens can be detected by immunelectrophoresis, whether or not they inactivate phage directly. Immunelectrophoresis is a two-stage process. In the first step, macromolecular species in the antigen sample are fractionated by electrophoresis through a buffered agarose matrix. The separation of the antigens depends both on their net charge and on their hydrodynamic properties. Species that are uncharged under the conditions of electrophoresis, or that are too

large to migrate through the agarose, remain in the sample well. In the second step of the procedure, antibody is added to troughs cut parallel to, but well separated from, the track of electrophoretic separation. The slide is incubated, allowing antibody and antigen to diffuse in the absence of electrophoresis. At positions where antibodies meet their target antigens, immune precipitates form. These have the form of an arc, since the antigens during electrophoresis were distributed in spherical or ellipsoidal zones. The precipitation arcs are visible directly in the agarose gel between the antibody trough and the antigen track. In these experiments, unreacted proteins are removed by simple washing. The immune precipitates, which remain fixed in the gel during washing, are then stained using a conventional protein stain.

Immuno-electrophoresis requires both antibody and antigens in much higher concentrations than were used in the phage inactivation and serum blocking experiments. The antisera were diluted only 2-15 fold before addition to the slides in all experiments not dealing specifically with the effects of antiserum dilution on immune precipitation. Purified structures were used as antigens at concentrations in the range of 10^{12} - 10^{14} particles/ml. When lysates served as the antigen sample, the infected cells were concentrated 200-fold prior to lysis for use as antigens.

All the antisera used in the immuno-electrophoresis experiments have been absorbed with whole, uninfected Salmonella typhimurium (DB7000) to remove anti-Salmonella antibodies. These antibodies arise due to contamination of the original particles injected into the rabbits with highly

immunogenic Salmonella cell envelope and flagellar debris.

In many experiments antisera have been absorbed with phage or phage-precursor particles in order to generate sera specific to an antigen or a set of antigens on a particular structure. For example, incubation of anti-prohead serum with phage, under conditions of antigen excess, leaves behind antibodies specific for determinants present on proheads but absent from phage.

The amber mutants of P22 were exploited in two ways in the immunoelectrophoresis experiments. Although there may be multiple antigenic species in a virus particle, these are all associated with a single, physically-diffusing species which generates a single precipitin band. If, however, we prevent particle assembly by infecting with an amber mutant of the coat or scaffolding protein gene, we increase the chances of structural proteins accumulating as soluble species. I hoped that this would allow me to detect minor structural protein antigens of the phage, if they existed.

In addition, I have used amber mutant lysates to absorb the sera. These lysates lack, in general, only the product of the mutant gene. Therefore, sera absorbed with lysates prepared with an amber mutant in a particular gene should contain antibody directed solely against the product of that mutant gene (Edgar and Lielausis, 1965). This is somewhat of a simplification. The antigenicity of some structural proteins may depend upon their organizational state, as suggested in Chapter I. For example, 5⁻ lysates which lack coat protein subunits also lack organized shell structures. If minor particle proteins are antigenic only as structural components of a

capsid shell, they will not be precipitated from a 5⁻ lysate.

The absorption experiments were done in the following way: undiluted sera were mixed with concentrated lysates or high titers of purified particles, and incubated overnight in the cold. These absorbed sera were used in immunoelectrophoresis experiments after low-speed centrifugation. The ratios of antiserum to antigen used in these absorptions were determined in pilot immunoelectrophoresis experiments. In all cases, the extent to which the antiserum had been absorbed was checked by immunoelectrophoresis.

In general, experiments using absorbed antisera are presented in the following manner: whole antiserum is added to one antiserum trough, absorbed serum to the other. The outer flanking antigen wells contain the absorbing antigen. In this arrangement, the reaction of absorbed serum with the absorbing antigen may be compared directly with the normal pattern obtained from the reaction of whole serum with the same antigen. This set-up provides the control reactions necessary to gauge the extent to which the serum has been absorbed. Finally, an antigen of interest is added to the central well. In this position, the behavior of a single sample of antigen may be compared against both unabsorbed and absorbed serum simultaneously.

B. Immunoelectrophoresis of Structure-containing Lysates and Purified Structures

1. Anti-phage serum

Despite the large size of P22 structures (approximately 50 million daltons), phage and precursor particles migrate appreciable distances from the antigen well during electrophoresis. The immunoelectrophoretic behavior of P22 phage and proheads against anti-phage serum is shown in Figure 17a. Purified wild-type phage have been added to the upper antigen well, and

Figure 17

Identification of P22 Antigenic Structures Using
Anti-phage Serum

For all immunoelectrophoresis experiments: the immunoelectrophoresis procedures are as described in Materials and Methods, Section j; the antigen samples are described in Materials and Methods, Table 3; the antiserum samples are from pools as described in Materials and Methods, Table 2. Volumes of antigen added are between 1.5 and 2.0 μ l; of antiserum, 100 μ l. The figures are presented so that the anode is to the right.

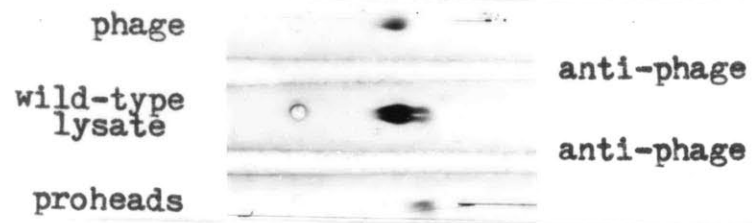
Every antiserum, unless otherwise indicated, has been absorbed with whole uninfected Salmonella cells, strain DB7000, concentrated 200-fold. The dilutions in these procedures, described in Materials and Methods, Section j, i, were negligible. Salmonella absorption removed 3-4 precipitin arcs from the immunoelectrophoretic patterns of P22 lysates.

(a) Undiluted anti-phage serum is from series 7. (b) and (c) Anti-phage serum from series 7 was diluted 1:10 and 0.2 ml of 5⁻ lysate from batch 1 (see Materials and Methods, Table 3) was added. The mixture was incubated at 37°C for approximately 30 minutes and was stored overnight in the cold. The absorbed serum was centrifuged at 15,000 rev/min for 2 hours in an SS-34 Sorvall rotor. Aliquots of the supernatant fraction were added to the antiserum troughs as indicated. Whole anti-phage serum from series 7 was diluted 1:10 to roughly match the concentration of the absorbed sera.

The pattern in the center of panel a is referred to as a "double-humped precipitin arc". Moving from the cathode to the anode, the precipitate has two distinct arcs, one very dense, one considerably lighter, which fuse to give a double-humped appearance. Phage are present in the inner more dense arc, while the proheads, present in the lower concentration are present in the arc to the right at the electrophoretically more negative position. Because the same serum is diffusing in from both troughs, the precipitate is symmetrical about its long axis, resulting in what will be termed mirror image precipitin arcs.

Absorption of the serum with a 5⁻ lysate is complete as shown in panel c. The gp9 precipitin arc, present in the reaction of whole serum with the 5⁻ lysate (lower section) is missing from the reaction of the absorbed serum with the same 5⁻ lysate (upper section). The anti-gp5 antibodies in the absorbed serum continue to precipitate the phage and prohead structures.

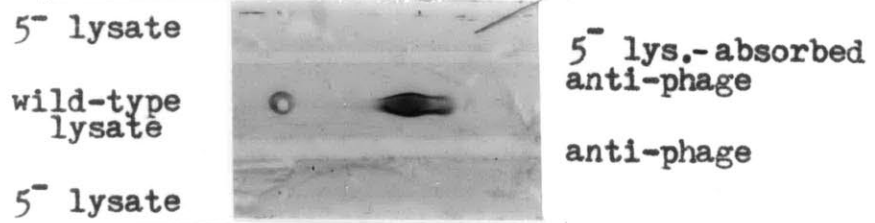
a)



b)



c)



purified proheads to the lower antigen well. Anti-phage serum filled both antiserum troughs. Phage and proheads migrate from the antigen well to the anode with the proheads moving faster than the phage. Immunoelectrophoresis of a wild-type lysate, in the central well of Figure 17a, with anti-phage serum results in a dense, slowly-diffusing, precipitin arc. It appears to be double-humped along its length (moving from the antigen well to the anode) because the structures, though antigenically related, electrophorese differently. The dense inner arc of the doublet, closest to the antigen well, migrates to the same position as purified phage; the outer arc shows immunoelectrophoretic behavior similar to the purified proheads. Therefore, the immunoelectrophoretic pattern of a wild-type lysate against anti-phage serum appears to be due to phage particles and prohead precursor structures which are present in the wild-type lysate.

Anti-phage serum has been shown by serum blocking experiments to contain anti-gp9 antibodies. Reaction of the anti-gp9 antibodies, present in the anti-phage serum, with the tail ^{subunits} of phage particles may be expected to contribute to the precipitation of phage particles. However, as proheads do not contain tails, prohead precipitation by the anti-phage serum must be the result of a reaction between anti-phage antibodies and some other antigen present on the proheads. The most likely antibodies responsible for prohead precipitation are anti-coat protein antibodies. The precipitation of phage by anti-phage serum is also probably not merely a result of anti-gp9: gp9 interactions, but anti-capsid: gp5 interactions as well.

The presence of anti-capsid antibodies is suggested by precipitation experiments with tail-less heads. These particles are

efficiently precipitated by anti-phage serum, as shown in Figure 17b. As these particles completely lack the gp9 tail protein, this precipitation cannot be due to the anti-gp9 antibodies in the serum, and must be due to another antibody species.

The non-essential role of the tail in the precipitin reaction is further demonstrated by removing anti-gp9 antibodies from the serum. To do this, I absorbed the anti-phage serum with a 5⁻ lysate, which lacks coat protein, but which contains large amounts of tail protein, as shown in the serum blocking experiments. Figure 17c shows an immunoelectrophoresis experiment using this 5⁻ lysate-absorbed serum. This serum should contain only anti-capsid antibodies. The absorbing lysate has been added to the upper and lower antigen wells. Anti-phage serum fills the lower trough; the 5⁻ lysate-absorbed serum fills the upper trough. The absence of precipitin bands in the upper region shows that the serum is fully absorbed. As will be discussed further below, the reaction of whole sera with 5⁻ lysate, in the lower region of Figure 17c, results in a single faint precipitin arc, which represents precipitation of soluble tail protein by anti-gp9 antibodies.

The central well of Figure 17c held wild-type lysate. The reaction with the whole anti-phage serum shows the typical double-humped precipitin arc, due to the precipitation of proheads and phage from the lysate. The 5⁻ lysate-absorbed serum, which is most likely composed of specific anti-coat protein antibodies, shows a very similar precipitation pattern. Thus, the precipitation of both phage and proheads does not depend on the presence of anti-tail antibodies.

In Figure 17b, this same 5⁻ lysate-absorbed antiserum, present in the lower antiserum trough, also precipitates tail⁻ heads. As will be shown directly by immunoprecipitation experiments described below, these precipitations are due to anti-coat protein antibody.

2. Anti-prohead serum

In preparing antibody against proheads, I was interested in two general questions: 1) Could I detect proteins in proheads which were not present or not antigenic in phage, such as the scaffolding protein, or other minor proteins? 2) Did antibody prepared against the precursor proheads efficiently precipitate phage? (This question may be of interest with respect to the general problem of vaccine production).

The reaction of anti-prohead serum with phage and proheads is shown in Figure 18a. Purified phage were added to the top well, purified proheads to the bottom well, and wild-type lysate to the center well. Anti-prohead serum was in both troughs. The reactions of the serum with the structures are very similar to the patterns found with anti-phage serum. The lysate shows the typical double-humped precipitin arcs due to proheads and phage particles. In addition, the anti-prohead serum reacts with a soluble protein in the wild-type lysate producing a precipitin arc between the antigen well and the structure-related precipitin arcs. As will be shown below, this is due to precipitation of soluble gp8 by anti-gp8 antibodies present in the anti-prohead serum.

The serum blocking experiments described in Chapter I showed that anti-prohead serum contained anti-gp9 antibodies at

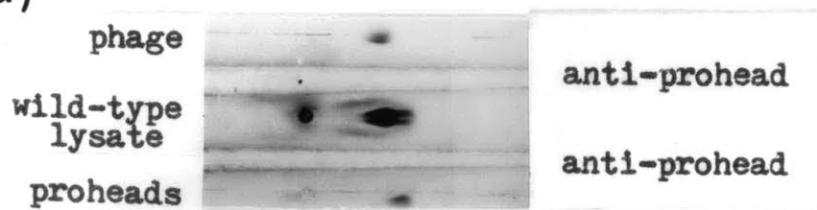
Figure 18

Immunoelectrophoresis of P22 Proheads and Phage Using Anti-prohead Serum

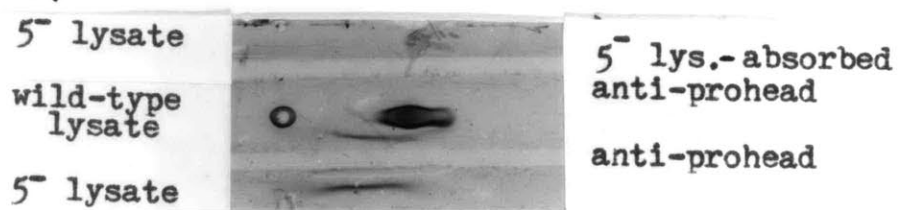
- (a) Undiluted anti-prohead serum is from series 7.
- (b) Anti-prohead serum from series 7 was absorbed with a 5⁻ lysate as described in the legend to Figure 17b. Whole anti-prohead serum has been diluted 1:10.

The pattern in the center of (a) is composed of precipitin arcs containing phage and proheads, flanked in precipitin arcs representing a soluble component by the lysate. Absorption of the sera with 5⁻ lysate, as in panel b, most likely leaves only anti-gp5 antibodies. These still precipitate the structures present in the wild-type lysate, but not the soluble component, gp8.

a)



b)



about 20% the level found in anti-phage serum. In order to determine if the precipitation of mature phage by anti-prohead serum was caused by anti-gp9 antibodies, I absorbed the anti-prohead serum with 5⁻ lysate to remove anti-gp9 and anti-gp8 antibodies. The reactions of the absorbed and whole antisera with 5⁻ lysate and wild-type lysate are shown in Figure 18b. Samples of 5⁻ lysate were added to the outer wells. The whole serum was added to the lower trough and the 5⁻ lysate-absorbed serum to the upper trough. The precipitin arc present in the bottom reaction is absent from the top, indicating that the serum is fully absorbed. No structures are present since the lysate is missing the major coat protein. The only antibodies remaining should be directed against the coat protein or structure-dependent antigens.

Examination of the central section of the slide shows clearly that the 5⁻ lysate-absorbed anti-prohead sera still efficiently precipitates both proheads and phage from a wild-type lysate. Thus, anti-capsid antibodies are most likely responsible for particle precipitation by anti-prohead serum.

3. Anti-head serum

P22 heads are identical to P22 phage except that they lack the tail protein, gp9. Consequently, though anti-head serum probably did not contain anti-gp9 antibodies, it might otherwise have been quite similar to anti-phage serum. In fact, this was the case.

The reaction of anti-head serum with the structures present in a wild-type lysate, shown in Figure 19, is very much like that obtained using anti-phage serum as shown in Figure 17. Precipitation of a wild-type lysate, in the central antigen well, by whole anti-head serum, in the lower serum trough, causes a typical double-humped precipitin arc due to phage and proheads.

The pattern remains essentially the same even after the anti-head serum has been absorbed with a 5⁻ lysate, as is present in the upper serum trough. Therefore, anti-capsid antibodies are most likely responsible for the precipitation of phage and proheads by anti-head serum.

C. Immuno-electrophoresis of Soluble P22 Antigens

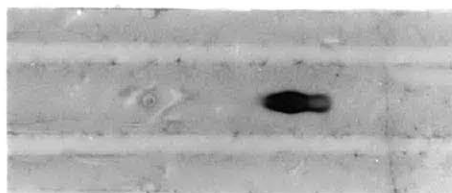
Immuno-electrophoresis of structure-containing lysates, though informative as to the immunological behavior of P22 structures as a whole, gives limited information as to the actual number and identity of P22 antigens which may exist in these structures. These may include, in addition to the major capsid protein and the tail protein, a number of minor phage proteins which participate in phage assembly (see Introduction). Antiserum generated against proheads, tail⁻ heads, and phage may contain antibodies against these minor structural proteins.

Only one protein, gp8, the scaffolding protein, was detected in soluble form in the immuno-electrophoresis of structure-containing lysates. Results from several immuno-electrophoresis experiments (data not shown) suggest that a pool of soluble gp8 subunits is present in every P22 amber

Figure 19Immunoelectrophoresis of P22 Phage and Proheads Using Anti-head Serum

Anti-head serum from series 7 was absorbed with a 5⁻ lysate as described in the legend to Figure 17b, except that 0.1 ml 5⁻ lysate was added to 1.0 ml anti-head serum. Whole anti-head serum has been diluted 1:10. The serum precipitated only the phage and prohead particles present in the wild-type lysate.

5⁻ lysate
wild-type
lysate
5⁻ lysate



5⁻ lys.-absorbed
anti-head

anti-head

mutant lysate, which reflects its unique properties as a catalytic structural protein. The other minor phage structural proteins may not exist in appreciable concentration in soluble form in lysates containing structures. As structural components of the phage or prohead capsid, these P22 antigens would be electrophoresed and precipitated as a single antigenic unit.

In the immunoelectrophoresis experiments to be described, 5⁻ and 8⁻ amber mutant lysates, which do not accumulate structures, are used as potential sources of antigens in their soluble form. Not all P22 antigens may be detected by this method. Some P22 antigens may be trapped in membrane debris or be otherwise insoluble in 5⁻ or 8⁻ amber mutant lysates, and remain inside the antigen well. Alternatively, as antibodies were originally generated against P22 antigens as they existed in particles, some proteins may not display their mature antigenicity in soluble precursor form. Therefore, immunoelectrophoresis of 5⁻ and 8⁻ amber mutant lysates provides a minimum estimate of the number of anti-P22 antibody classes that exist in the different anti-P22 antisera.

1. Anti-phage serum

(a) Identification of the gp9 precipitin band

Serum blocking experiments have shown that anti-phage serum contains anti-gp9 antibodies. These experiments detected antigenically-active gp9 in 5⁻ amber mutant lysates which was capable of blocking almost all of the phage-neutralizing antibodies in the anti-phage serum. Therefore, at the least, I expected to detect an anti-gp9: gp9 reaction in the immunoelectrophoresis of a 5⁻ lysate against anti-phage serum.

The results of such an experiment are shown in panel a of

Figure 20. Anti-phage serum filled both antiserum troughs; a 5⁻ amber mutant lysate was added to the central antigen well. A single precipitin arc is detectable. As this band was most likely the result of the precipitation of soluble gp9 by anti-gp9 antibodies, I constructed a double amber mutant phage, carrying amber mutations in both gene 5 and gene 9, to genetically identify the antigen in this reaction as gp9. This phage was used to generate a 5⁻9⁻ mutant lysate which was added to the top antigen well and immunoelectrophoresed. No precipitin band formed. Therefore, these results genetically identify the antigen responsible for the single, detectable precipitin band as the gene 9 tail protein.

Results from serum blocking experiments and tailing assays using wild-type lysate, and 5⁻ 8⁻, and 2⁻ amber mutant lysates (see Table 4) indicated that gp9 was over-produced in the latter three lysates relative to wild-type amounts. A 2⁻ amber mutant lysate has been added to the lower antigen well in panel a of Figure 20. The 2⁻ amber mutant lysate shows a precipitin band very similar in character to, and at the precise electrophoretic position of, the gp9 precipitin band in the 5⁻ amber mutant lysate. This is in contrast to a wild-type lysate, which shows no soluble bands against anti-phage serum (see Figure 17a and c). These data provide additional support for the genetic identification of gp9 as the antigen involved in these precipitation reactions.

The experiment in panel b of Figure 20 shows that purified gp9, in the central antigen well, produces a precipitin arc similar in character and electrophoretic position to the single precipitin band produced by the 5⁻ amber mutant lysate in the upper antigen well. No such band was

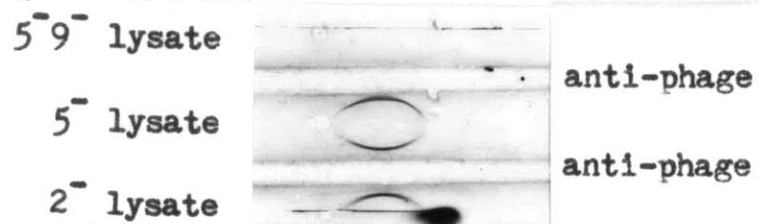
Figure 20

Identification of the gp9 Precipitin Arc Using
Anti-phage Serum

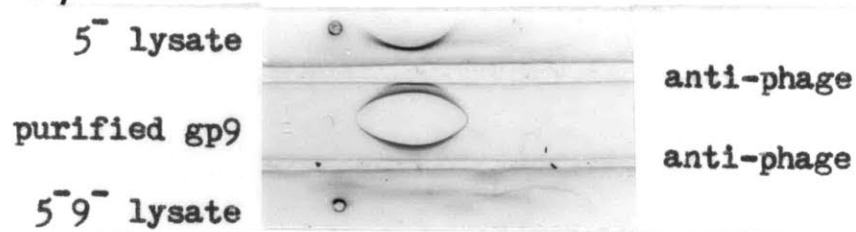
(a) Anti-phage serum, undiluted, is from series 7. (b) Anti-phage serum, undiluted, is from series 15. This serum has not been absorbed with Salmonella cells, and shows several faint bands due to Salmonella antigens in the lysates. (c) Sera are as described in the legend to Figure 17b.

The sharp precipitin arcs represent soluble gp9 tail subunits. The dense precipitate in the bottom of panel a represents prohead structures.

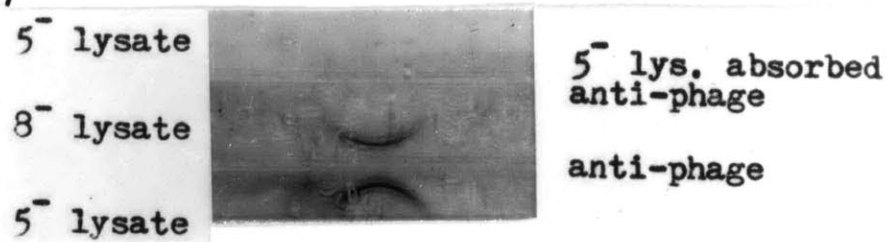
a)



b)



c)



detectable in a 5⁻9⁻ amber mutant lysate, present in the bottom antigen well. (The faint bands present in the 5⁻ and 5⁻9⁻ amber mutant lysates are the result of anti-Salmonella precipitation reactions, present because the antiserum had not been fully absorbed with bacterial cells). These results establish conclusively that gp9: anti-gp9 interactions are responsible for the single precipitin arc which results from immunoelectrophoresis of a 5⁻ amber mutant lysate against anti-phage serum.

(b) Absence of a coat subunit precipitin band

An 8⁻ amber mutant lysate provides the best potential source of soluble gp5, the capsid protein. Previous immunoelectrophoresis experiments of 5⁻ lysate-absorbed anti-phage serum against particles suggested that anti-phage serum contains anti-gp5. Therefore, I expected that immunoelectrophoresis of an 8⁻ lysate, would show an additional band due to the reaction of soluble gp5 with anti-gp5 antibodies. This was not the case as is shown in panel c of Figure 20. An 8⁻ lysate, in the central antigen well, has a single precipitin band against whole anti-phage serum, present in the lower serum trough. This band is virtually identical in appearance to the gp9 precipitin band present from a 5⁻ lysate in the lower antigen well. However, it was possible that the gp5 precipitin band was coincident with the gp9 precipitin band. Therefore, I absorbed the anti-phage serum with a 5⁻ lysate to remove the anti-gp9 antibodies. The absorbed serum, which should retain anti-capsid antibodies, was added to the upper antiserum trough in Figure 20c. All anti-gp9 antibodies were removed from the serum by the absorption, as is shown by the absence of a precipitin band against a 5⁻ amber mutant lysate in the upper antigen well. The

reaction of the absorbed serum with the 8⁻ lysate in the central antigen well shows that no precipitin arc was uncovered by the removal of the anti-gp9 antibodies. These results suggest that gp5 in an 8⁻ amber mutant lysate does not react with anti-capsid antibodies in the anti-phage serum. However, electron microscopic experiments described in Chapter III indicate that there is antigenic coat protein in 8⁻ lysates. A discussion of the paradoxical behavior of gp5 in an 8⁻ lysate will be taken up in that chapter. It may be that the coat protein accumulating in 8⁻ lysates is too heterogenous in electrophoretic behavior to give a detectable precipitin band; or, under the experimental conditions involved in immunoelectrophoresis, gp5 may be insoluble and remain inside the antigen well.

In summary, immunoelectrophoresis of soluble P22 antigen with anti-phage serum detected only anti-gp9 antibodies. Anti-capsid antibodies, shown by several other methods to be present in the anti-phage serum, were not detected by the immunoelectrophoresis of an 8⁻ amber mutant lysate. Finally, immunoelectrophoresis of 5⁻ and 8⁻ amber mutant lysates did not provide any evidence for the existence of antibodies in anti-phage serum against minor P22 structural proteins other than gp9. Either antibodies against them do not exist, at least in concentrations high enough to be detected by this assay; or P22 minor structural proteins are not antigenic in soluble form.

2. Anti-prohead serum

Proheads contain, in addition to the gp5 capsid protein, the scaffolding protein, gp8, and several of the minor proteins present in phage. If gp8 were exposed in the prohead immunogen preparation,

at 250 copies per prohead, it may reasonably be expected to have evoked an antibody response. In addition, some of the minor proteins may be more suitably disposed to induce antibody formation in proheads than in phage.

(a) Presence of the gp9 precipitin band

Serum blocking experiments have shown that anti-prohead serum contains anti-gp9 antibodies. As expected, then, immunoelectrophoresis of a 5⁻ lysate with anti-prohead serum, shown in the central portion of Figure 21a, shows a sharp precipitin arc at the position, and with the appearance, characteristic of the gp9 precipitin band. The pattern also contains a second, more diffuse precipitin arc whose identification will be discussed presently. When this experiment was repeated in the lower portion of Figure 21b, the two arcs became coincident with one another, although the sharp band remains somewhat distinguishable. No such precipitin arc is detectable in the immunoelectrophoretic pattern of a 5⁻⁹⁻ lysate, which was present in the top antigen well. However, one can generate the immunoelectrophoretic pattern of a 5⁻ lysate from a 5⁻⁹⁻ lysate by adding purified gp9 to the 5⁻⁹⁻ lysate and immunoelectrophoresing the mixture, as is shown in the central portion of Figure 21b. Panel c shows the reaction of two different pools of anti-prohead serum with purified gp9. From the serum blocking results, we know that the k of an antiserum reflects its concentration of anti-gp9 antibodies. Anti-prohead serum with a high k value, in the upper antiserum trough precipitates purified gp9 very strongly; anti-prohead serum which contains approximately one-third the number of anti-gp9 antibodies, as in the

Figure 21Precipitation of gp9 and a Second Soluble Antigen by
Anti-prohead Serum in Immunoelectrophoresis

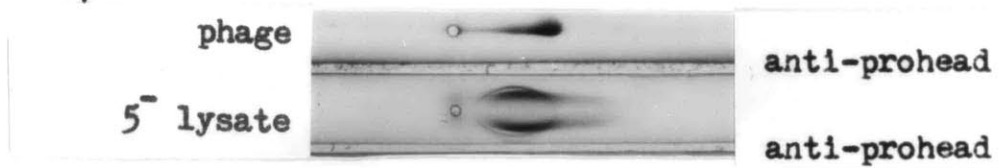
(a) Undiluted anti-prohead serum is from series 15. The lower antiserum trough contains serum which has been only partially absorbed with purified phage from batch 2 (see Materials and Methods, Table 3). Seven aliquots of 0.2 ml purified wild-type phage at 7.7×10^{12} phage/ml were added to 16.5 ml of serum over 4 1/2 hours at 47°C. The mixture was stored overnight at 4°C. The absorbed serum was centrifuged at 10,000 rev/min for 10 minutes in a Sorvall SS-34 rotor, and the supernatant fraction used in this experiment. Note that addition of 1.1×10^{13} phage particles to 16.5 ml of serum diminishes only slightly the intensity of the gp9 precipitin band. This experiment was done initially to monitor the extent of phage absorption of the serum. However, this is of no relevance to the conclusions of the present experiment as discussed in the text.

(b) Undiluted anti-prohead serum is from series 15.

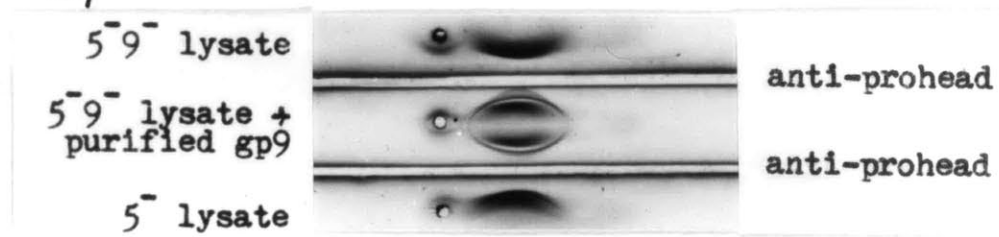
(c) Anti-prohead serum ($k = 1700 \text{ min}^{-1}$) is from series 15. Anti-prohead serum ($k = 500 \text{ min}^{-1}$) is from series 7.

The fine, sharp precipitin arcs represent soluble tail protein gp9. The dense precipitin arcs (other than the phage precipitate in the top of panel a) involve soluble scaffolding protein, gp8.

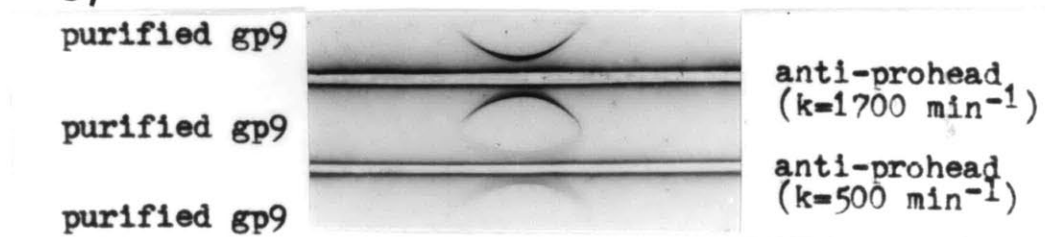
a)



b)



c)



lower serum trough, shows a very faint and diffuse precipitation reaction with purified gp9. Therefore, immunoelectrophoresis experiments detect the presence of anti-gp9 antibodies in the anti-prohead serum with a k greater than, or equal to, 500 min^{-1} .

(b) Identification of anti-scaffolding protein antibodies (anti-gp8)

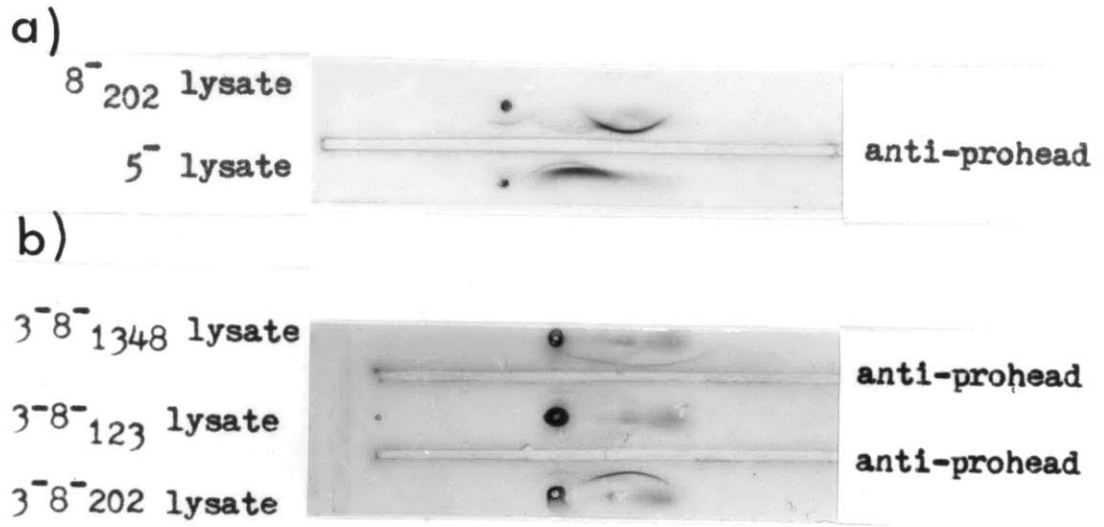
i. gp8 and its amber fragments show different immunoelectrophoretic behavior

As noted above, anti-prohead serum contains a second class of antibodies which reacts with a soluble protein in 5^- lysates to give a diffuse precipitin reaction. This precipitin arc is also present in the reaction of anti-prohead serum with a 5^-9^- lysate (Figure 21b) and with a wild-type lysate, as well (Figure 18). In fact, using anti-prohead serum, this precipitation reaction is present in all the morphogenetic mutant lysates (data not shown). Therefore, the antigen involved must be present in soluble form in fairly high concentrations in all such P22 lysates. One prime candidate for this antigen is gp8, the scaffolding protein. As a catalytic structural protein, gp8 is released from proheads during DNA encapsulation, creating a pool of re-usable gp8 subunits within the cell. If the precipitin arc is caused by gp8, it should be missing from the immunoelectrophoretic pattern of an 8^- amber mutant lysate. This is shown in panel a of Figure 22. Immunoelectrophoresis of a 5^- lysate, in the lower antigen well, gives the sharp gp9 precipitin band and the second, more diffuse band. The immunoelectrophoretic pattern of an 8^- amber mutant lysate, in the central antigen well, contains the gp9 precipitin arc; however, the diffuse band has virtually disappeared. However, a new band appears at an electro-

Figure 22Immunoelectrophoretic Behavior of gp8 and its Amber Fragments

(a) The anti-prohead serum is described in the legend to Figure 21a. The precipitin arc around the antigen well, present in the reaction of the 8⁻ 202 lysate, is variably present in this and other lysate reactions (see Figure 20b, 5⁻9⁻ lysate). It is most likely the result of the precipitation of Salmonella antigens by residual anti-Salmonella antibodies.

(b) The anti-prohead serum, from series 15, was diluted 1:5. The dark reaction around the antigen wells and the very faint and slowly-diffusion precipitates are probably caused by the reaction of the aberrant gp5-containing structures (spirals and shells) in these 8⁻ lysates.



phoretically more negative position. The disappearance of the precipitin band indicates that the antigen involved is gp8-dependent; the coincident appearance of a new band suggests that the anti-prohead serum may be precipitating a gp8 amber fragment from the 8⁻ amber mutant lysate.

In support of this theory, you may observe that the antigen in the 8⁻ lysate has precipitated closer to the antiserum trough than the antigen in the 5⁻ lysate. As the lysates were prepared similarly, the relative proximity of the 8⁻ lysate precipitin arc to the serum trough is consistent with the antigen's being a fragment of the full gp8 polypeptide in the 5⁻ lysate. According to this model, the fragment lacks determinants present on the full polypeptide chain; therefore, the effective concentration of antibodies in the serum against the antigen is decreased, and the antigen diffuses farther before being precipitated.

The full gp8 polypeptide has a molecular weight of 42,000 daltons. The 8⁻amH202 lysate used in Figure 22 contains a gp8 fragment of approximately 18,000 daltons. To test the idea that the new band represents an amber fragment, 8⁻ lysates were prepared with amber mutants at other sites in gene 8. These were 8⁻amH1348 lysate which yields a gp8 amber fragment of about 12,000 daltons; and 8⁻amN123 lysate, in which an amber fragment is not detectable by SDS-gel electrophoresis (J. King and C. Hall, unpublished experiments). Genetic mapping data are consistent with the observations on fragment sizes from SDS-gel electrophoresis and they suggest that the amber fragment in an 8⁻amN123 lysate would be quite small (F. Winston and D. Botstein, unpublished experiments).

If the precipitations in question are caused by anti gp8: gp8 interactions, anti-prohead serum may be expected to show a somewhat weaker reaction with the shorter gp8 fragment, most likely at a new electrophoretic position, and to show no band against the lysate which lacks a detectable gp8 fragment by SDS-gel electrophoresis. The results were as predicted, as shown in Figure 22b. (The lysates in this experiment are also 3⁻, but this has no effect on the precipitation pattern). I mention here two technical points to avoid confusion: in these experiments, the anti-prohead serum has been diluted to a k of less than 500 min⁻¹ so that the gp9: gp9 precipitin band is no longer detectable. Also, the proteins have not migrated during electrophoresis as far from the antigen well as they had in the experiments of Figure 22a. Therefore, the precipitin arc from an 8⁻amH202 lysate, in the bottom antigen well of Figure 22b, is present very close to the antigen well. The 8⁻ lysate, 8⁻amH1348, which contains the shorter gp8 amber fragment, has been added to the upper antigen well. Using this lysate as antigen, a weak band was detectable. The antigen in this reaction electrophoresed to a more negative position and diffused farther before being precipitated than the antigen in the 8⁻amH202 lysate. This is consistent with the hypothesis that we are seeing the precipitation of a shorter, more negatively charged, gp8 fragment which carries fewer determinants than the fragment present in the 8⁻amH202 lysate.

An 8⁻amN123 mutant lysate has been added to the central antigen well of Figure 22b. No new precipitin arc was found with this 8⁻ amber mutant lysate which lacks a detectable gp8 amber fragment.

The combined results show that not only does the precipitin arc

present in a 5⁻ lysate disappear from the pattern of an 8⁻ lysate, but the presence, position, and intensity of a new precipitin band in the 8⁻ lysates depends upon the presence and size of the gp8 amber fragment involved. Thus, I conclude that anti-prohead serum contains anti-scaffolding protein antibodies.

(ii) gp8 and its amber fragments show reaction of partial identity

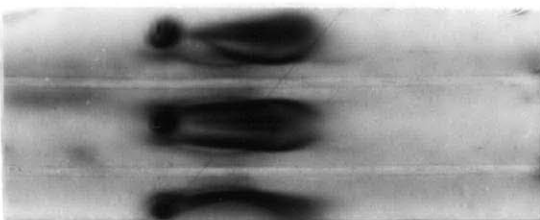
If the precipitin arc in a 5⁻ lysate is caused by the complete gp8 molecule, and the precipitin arcs in the 8⁻ lysates by fragments of gp8, then, in immunoelectrophoresis experiments the antigenic relatedness of these species may be shown directly by examining mixtures of the lysates. These will show reactions of partial identity, in which precipitin arcs both fuse and show spurs. The arcs fuse because the antigens involved share common determinants. All antibodies directed against these common determinants are precipitated at the position of equivalence. Spurs form at the junction of two precipitin arcs if the antigens involved also possess unique determinants. In this case, a subset of antibodies can pass through the precipitin network caused by the reactions of the common antigenic sites, because they do not recognize the shared antigens. These antibodies continue to diffuse until they react with their unique target antigens and form an immune precipitate within the boundaries of the fused precipitin arcs. Lysate-mixing experiments are shown in Figure 23. The set-up of the experiments was as follows: 1:5 diluted anti-prohead serum was present in every antiserum trough. A sample of a 5⁻ lysate was added to the bottom antigen wells, and one of three 8⁻ amber mutant lysates to the top antigen wells. The central antigen wells contained

Figure 23

Reactions of Partial Identity
Between gp8 and its Amber Fragments

(a, b) The central reactions show the fusion of the 8⁻ amber fragment with the complete gp8 polypeptide. The darkly staining, central tear-shaped precipitates in the 3⁻8⁻ lysate samples represent precipitation of the aberrant coat protein aggregates present in the lysates. (c) No amber fragment was detected in the 3⁻8⁻123 lysate.

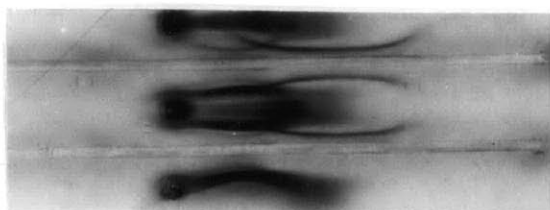
a)

 $3^{-8^{-}}$ 202 lysate 5^{-} lysate +
 $3^{-8^{-}}$ 202 lysate 5^{-} lysate

anti-prohead

anti-prohead

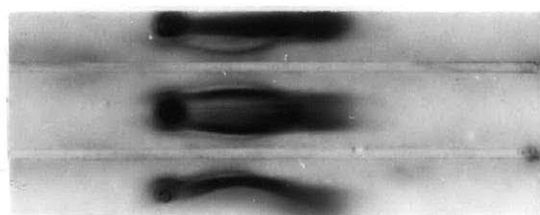
b)

 $3^{-8^{-}}$ 1348 lysate 5^{-} lysate +
 $3^{-8^{-}}$ 1348 lysate 5^{-} lysate

anti-prohead

anti-prohead

c)

 $3^{-8^{-}}$ 123 lysate 5^{-} lysate +
 $3^{-8^{-}}$ 123 lysate 5^{-} lysate

anti-prohead

anti-prohead

a 1:1 mixture of the 5⁻ and 8⁻ lysates present in the flanking antigen wells.

The anti-prohead serum in these experiments was diluted only 1:5 so as to maintain a sufficient concentration of antibodies to detect spur reactions. Consequently, immunoelectrophoresis of the 5⁻ lysates in these experiments shows a very dense diffuse gp8 band. The gp9 band is detectable as well. The gp9 band is present in every reaction and will not be discussed further.

Panel a of Figure 23 compares the immunoelectrophoretic pattern of a 5⁻ lysate with an 8⁻amH202 lysate. The 8⁻ lysate shows, as it had previously in Figure 22, a new band which is somewhat sharper than the band in a 5⁻ lysate, at an electrophoretically more negative position. When these two lysates are mixed together, the complete gp8 band and the amber fragment band fuse, showing that they share identical determinants. It is difficult to assess, because of the density of the precipitates, whether a spur extends from the inner precipitin arc, which corresponds to the full gp8 molecule; but, I think a weak, diffuse spur may be present. The low intensity of the spur reaction suggests that the full gp8 molecule contains very few unique antigenic determinants. Therefore, an amber fragment accounting for about 2/5 of the polypeptide chain, appears to contain almost all of the antigenic determinants present on a molecule more than twice its size.

Spur formation is much more clearly seen in the reaction involving the shorter gp8 fragment in an 8⁻amH1348 lysate, shown in panel b. As in the preceding reaction, the precipitin arcs fuse. For comparison, note the crossing of the unrelated gp9 and gp8 fragment bands in the 8⁻

lysate alone, in the upper portion of this panel. Also, as compared to the preceding experiment, a more dense spur extends from the precipitin arc of the full gp8 polypeptide. This is entirely consistent with the fact that the gp8 fragment in the 8⁻amH1348 lysate is shorter than the fragment in the 8⁻amH202 lysate. From these results, the shorter fragment appears to contain fewer determinants. Therefore, more antibodies recognize determinants as unique on the full gp8 molecule and cause a denser spur-related precipitate.

In panel c of Figure 23, the experiment has been repeated using an 8⁻amN123 lysate. As expected from previous experiments (Figure 22), no reaction against an amber fragment was detected.

In conclusion, these results confirm that the antigens in the 8⁻ lysates are portions of the larger gp8 molecule present in the 5⁻ lysate. Therefore, the reactions of partial identity observed in these experiments are derived from the interaction of anti-scaffolding protein antibodies with gp8 and its fragments.

The composition of the precipitating antibodies in anti-prohead serum, as shown by immunoelectrophoresis experiments, may be summarized as follows: the combined data provide strong evidence that anti-gp8 antibodies are present in anti-prohead serum. As expected from the serum blocking experiments, anti-prohead serum also contains anti-gp9 antibodies which may be detected immunoelectrophoretically using concentrated serum. As with anti-phage serum, anti-gp5: gp5 reactions were not detected by the immunoelectrophoresis of an 8⁻ lysate, although experiments in Chapter III suggest that they do occur. Finally, no

evidence exists for the presence of antibodies in anti-prohead serum directed against minor structural proteins other than gp8 and gp9.

3. Anti-head serum

Immuno-electrophoresis of a 5⁻ lysate with undiluted anti-head serum produced a single, somewhat faint, precipitin arc, as is shown in the central portion of Figure 24a; immuno-electrophoresis of a 5⁻9⁻ lysate produced a similar pattern. When an 8⁻amH202 lysate was used as an antigen, however, the original precipitin arc disappeared, and a new band, electrophoretically more negative took its place. This behavior, reminiscent of the anti-prohead precipitation patterns obtained using these lysates, suggested that anti-head serum might contain anti-gp8 antibodies. To test this hypothesis, 8⁻ amber mutant lysates containing different-sized amber fragments, were used as antigens. This experiment is shown in panel b of Figure 24. The results are very similar to the results of the same experiment with anti-prohead serum in Figure 22b. An 8⁻amH202 lysate produced a sharp band; an 8⁻amH1348 which contains a smaller gp8 fragment produced an electrophoretically more negative band which diffused farther before being precipitated; and an 8⁻amN123 lysate, which does not contain a detectable gp8 fragment, did not produce a precipitin arc specific to this lysate. In analogy with the identification of anti-scaffolding protein in anti-prohead serum, these results indicated that anti-head serum contained anti-gp8 antibodies. Tail-less heads ordinarily do not carry gp8; however, when the particles used to generate the anti-head serum were run in SDS-gel electrophoresis, a contaminating gp8 band was barely detectable by protein staining (data not shown). This probably repre-

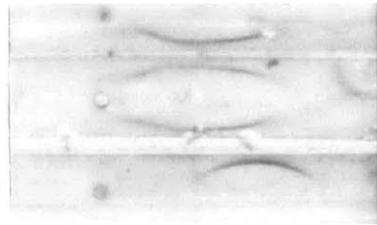
Figure 24Detection of gp8 and its Amber Fragments in
Immunoelectrophoresis by Anti-head Serum

The anti-head serum is from series 7.

(a) The lightly staining precipitin arcs in the 5⁻9⁻ and 5⁻ lysates represents soluble scaffolding protein, gp8. This arc is missing from the 8⁻202 lysate and has been replaced by a precipitate containing a more negatively charged antigen, the gp8 amber fragment.

(b) The dense darkly staining central precipitates, particularly prominent in the 3⁻8⁻1348 and 3⁻8⁻123 lysates, represents precipitation of the aberrant coat protein aggregates present in these lysates. The lengthy precipitin arc just outside the dense structure precipitate may also represent precipitation of gp5 in these lysates, but as this was not typically detected in comparable lysates, their identification is uncertain. The fast-diffusing precipitin arcs, involving the more negatively charged antigenic species in the top and central reactions show precipitation of the gp8 amber fragment. No amber fragment was detectable in the precipitin pattern of the 3⁻8⁻123 lysate.

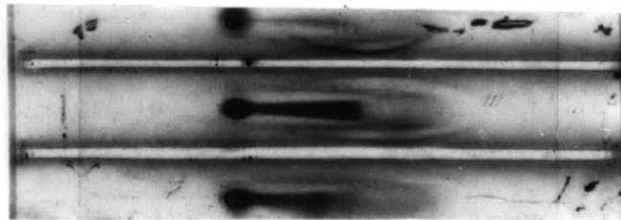
a)

5⁻9⁻ lysate5⁻ lysate8⁻₂₀₂ lysate

anti-head

anti-head

b)

3⁻8⁻₂₀₂ lysate3⁻8⁻₁₃₄₈ lysate3⁻8⁻₁₂₃ lysate

anti-head

anti-head

sents contamination of the tail⁻ heads used for immunization with a small number of proheads. (ca. 6%, see Fig. 3)

As anti-head serum was generated against phage heads which lacked tails, I had expected that I might find additional bands in the immunoelectrophoretic pattern corresponding to neck-specific antigens. If these antigens exist, they were not detectable by immunoelectrophoresis of soluble P22 antigens with anti-head serum.

D. Cross-reactivity of P22 Structures

1. Common antigens

The precipitin arcs from the immunoelectrophoresis of the phage and proheads in a wild-type lysate fuse, regardless of the anti-P22 serum involved (see Figures 17a, 18a and 19). As discussed previously, this phenomenon shows that these structures share a set of common antigenic determinants. Absorption of the sera with a 5⁻ lysate, designed to generate anti-capsid antibody, did not perceptibly affect the reaction of these structures with the sera. These results suggest, as will be shown directly in Chapter III, that proheads and phage share many gp5 determinants. Therefore, it appears that the transition from the prohead precursor structure to the mature phage particle does not involve a gross rearrangement of the capsid subunits.

2. Unique antigens

(a) Capsid determinants unique to phage as shown by spur formation

Anti-P22 sera appear to recognize unique antigenic determinants on phage and proheads, as shown by spur formation between the phage and prohead precipitin arcs. At high antiserum concentration, however, it is often difficult to see the spurs. Because P22 structures are so large,

they do not freely diffuse in this system so they remain localized in high concentration. In addition, not all unreacted structures are removed by washing. Even in the absence of serum, structures are stained, although the stained areas lack the sharp edges of structure immunoprecipitates (data not shown). Consequently, when structures are diffusing from the central antigen track against very concentrated antisera, the mirror-image precipitin arcs are very close together and very dense, making detection of spur formation nearly impossible. With more dilute antisera, however, spurs are more clearly either present or absent, depending on the nature of the antibody-antigen reaction.

These effects are illustrated in the experiments of Figure 17a and c in which I attempted to examine, using spur formation, whether anti-phage serum recognized a set of determinants unique to the phage capsid. As shown in Figure 17a, phage structures form such a dense, almost solid sphere of precipitate against concentrated anti-phage serum that it is extremely difficult to assess whether a spur actually extends from the phage precipitin arc. Presumably, one does because anti-gp9 antibodies in the anti-phage serum react with phage tails and not with proheads. However, in the experiment of 17c, when the anti-serum is 10-fold more dilute, even whole serum does not seem to form a spur extending from the phage precipitate. As will be discussed in section f of this Chapter, the k of the anti-phage serum, about 500 min^{-1} in this experiment, is such that soluble gp9 would give only a faint reaction with the serum. Apparently, in this situation, the k of the anti-prohead serum is, nevertheless, too low to detect the expected spur

formation. It seems unlikely, then, that a substantial additional class of determinants could be contributing to spur-related precipitation reactions. Thus, I conclude from these results that antibodies generated against phage capsids probably recognize the outer shells of the proheads as identical. Results from experiments using electron microscopy support this conclusion and will be discussed in Chapter III.

The reaction of concentrated anti-prohead serum with P22 phage and proheads, as in Figure 18a, produces a precipitin pattern very similar to that produced by concentrated anti-phage serum. However, as shown in Figure 18b, 10-fold dilution of the whole anti-prohead serum results in the definition of a faint precipitin arc extending from the phage precipitate. The k of the anti-prohead serum, about 50 min^{-1} in this reaction, would be much too low to see gp9-related spur formation, given the previous result that anti-phage serum at a k of 500 min^{-1} did not produce such a spur. Thus, these results suggest that there may be a significant number of determinants on phage, other than gp9 determinants, which anti-prohead serum recognizes as different from proheads.

This possibility may be tested by removing the anti-gp9 antibodies from the serum by absorbing with a 5^+ lysate. If a spur reaction persists, the precipitation may be most reasonably attributed to antibodies specific for the phage capsid. This experiment was done and the results are shown in Figure 18b. Despite absorption, the spur appears to persist. If the spur is real, then the experiments suggest that anti-prohead serum recognizes a class of capsid determinants as present on phage but not on

proheads. These phage-specific anti-capsid antibodies must have been generated against contaminating empty phage heads in the original prohead immunogen preparation, or some breakdown product of proheads which was antigenically similar to phage.

Will serum made against phage heads which lack gp9 recognize determinants as present on phage but absent on proheads? Results from immunoelectrophoresis confirm that anti-head serum lacks anti-gp9 antibodies (Figure 19). In the absence of anti-gp9 antibodies, phage-related spurs show directly that phage and proheads are different in some way other than that proheads lack tails. In the experiment of Figure 19, the reaction of anti-head serum with the phage and proheads in a wild-type lysate produced such a spur. Absorption of the serum with a 5⁻ lysate has little effect on the spur, as shown in the same figure; this is not particularly meaningful, however, because anti-head serum did not show a positive precipitation reaction in the first place with the 5⁻ lysate. If phage-specific antigens do indeed exist, they may include a special class of capsid subunits or some minor structural proteins of the phage which are either not present or not antigenic in proheads. However, these phage-specific antigens cannot be present in a part of the neck which is covered by the phage tails because they are detectable on phage particles.

(b) Capsid determinants specific to proheads as shown by spur formation

One might expect that antibodies made against phage would not recognize prohead-specific determinants. Indeed, as is shown in Figure 17a, no spur is detectable extending from the prohead precipitin arc.

Perhaps a more intriguing question is: does anti-prohead serum recognize antigenic determinants unique to proheads? Proheads contain approximately 250 copies of gp8, the scaffolding protein, which are not present in the mature phage. The exact location of gp8 within the prohead structure has not been determined, but Earnshaw, et al. (1976) have concluded from the results of electron microscopy and X-ray diffraction studies on proheads that gp8 is part of an inner shell structure within the prohead capsid. However, localization of all of the gp8 molecules to the inner shell of the proheads makes it difficult to explain how the gp8 protein is able to exit from the prohead shell during DNA encapsulation, fully intact, ready to be recycled in further prohead assembly reactions. Perhaps the gp8 molecule protrudes through the outer capsid shell. If gp8 molecules are exposed on the capsid of proheads, and if they elicited an antibody response during immunization of the rabbit, they may be expected to give rise to a class of prohead-specific antibodies which react exclusively with proheads and not with structures which do not contain gp8.

In fact, in contrast to the behavior of anti-phage serum, immunoelectrophoresis with anti-prohead serum of a wild-type lysate produced a spur extending from the prohead precipitin arc. This is shown in

Figure 18a. Therefore, antibodies exist in anti-prohead serum which do not recognize targets on phage but which do precipitate proheads.

In the upper portion of Figure 18b, the anti-prohead serum has been fully absorbed with a 5⁻ lysate; it no longer reacts with the soluble gp8 in either the 5⁻ or the wild-type lysate. If gp8 is the only antigen unique to proheads, the prohead spur should be removed by this absorption. However, a spur extending from the prohead precipitin band persists. Therefore, these results suggest that, unless there are structure-dependent determinants, gp8 antigens cannot be solely responsible for the antigenic difference between proheads and phage. In the simplest interpretation of the data, proheads probably carry gp5-determinants which are not present in the capsid shell of phage particles. This hypothesis is supported by experiments involving electron microscopy in Chapter III.

It is difficult to be absolutely sure because of the density of the structure precipitates, but anti-head serum does not seem to form prohead-related spurs. Thus, anti-head serum probably does not recognize determinants on proheads which it does not also detect in phage.

3. Investigation of prohead-specific antibodies by phage-absorption of the anti-prohead serum

(a) Residual activity of phage-absorbed anti-prohead serum against proheads

The existence of a prohead-specific class of antibodies in anti-prohead serum has been suggested by the formation of spurs in immunoelectrophoresis of a mixture of phage and prohead structures (see Figure 18). To establish this more clearly, I absorbed anti-prohead serum exhaustively with purified phage. The object of this absorption

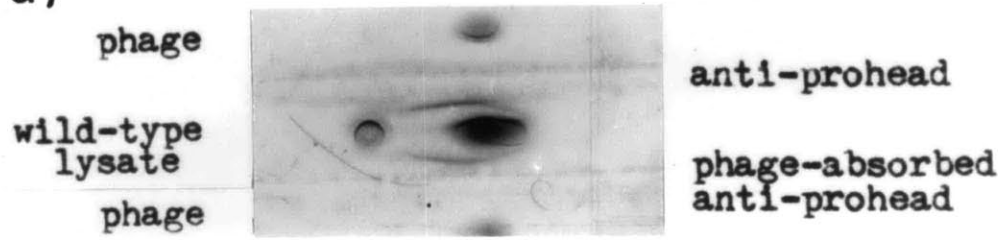
process was to isolate the reactions of prohead-specific antibodies from the high background of antibody reactions directed against determinants shared by proheads and phage. Once isolated, the residual activity of phage-absorbed anti-prohead serum could be examined by immunoelectrophoresis. The phage-absorbed sera should contain anti-scaffolding protein antibodies. In addition, the prohead-specific sera may include prohead-specific anti-capsid antibodies. These antibodies recognize gp5 as antigenic only in the particular structural conformation it assumes in proheads, and not as it exists in phage. Finally, phage-absorbed anti-prohead serum may contain antibodies against minor proteins of the prohead, if these proteins are not available in antigenic form on the phage structure during absorption.

The residual activity of phage-absorbed anti-prohead serum against proheads is examined in Figure 25a. Purified wild-type phage have been added to the outer antigen wells. Whole anti-prohead serum, present in the upper antiserum trough, precipitates the phage particles. Anti-prohead serum, after absorption with wild-type phage, present in the lower antiserum trough no longer precipitates wild-type phage, and thus has been fully absorbed. Whole anti-prohead serum precipitates phage, proheads and soluble gp8 from a wild-type lysate, present in the central antigen well. Phage-absorbed anti-prohead serum no longer produces the inner of the two structure-related precipitin arcs. This provides additional evidence that the anti-prohead serum is fully absorbed with phage. As expected phage-absorbed serum continues to precipitate the soluble gp8 in the wild-type lysate.

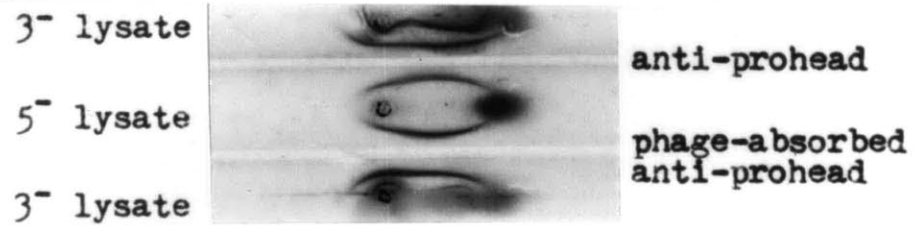
Figure 25Residual Activity of Phage-absorbed Anti-prohead Serum Against Proheads in Immunoelectrophoresis

(a) Anti-prohead serum from series 7 was absorbed as in the legend to Figure 17b except that purified phage from batch 1 were added. Complete absorption of the serum required several additions of phage. Whole anti-prohead serum from series 7 was diluted 1:15 to match the concentration of the phage-absorbed serum. (b) and (c). Anti-prohead serum was absorbed sequentially with phage six times as described in Materials and Methods, Section j. Whole anti-prohead serum was diluted 1:22.5 to match the dilution of the absorbed anti-prohead serum. Note the soluble gp8 precipitin band present in the reaction of the serum with the prohead preparation added to the central well.

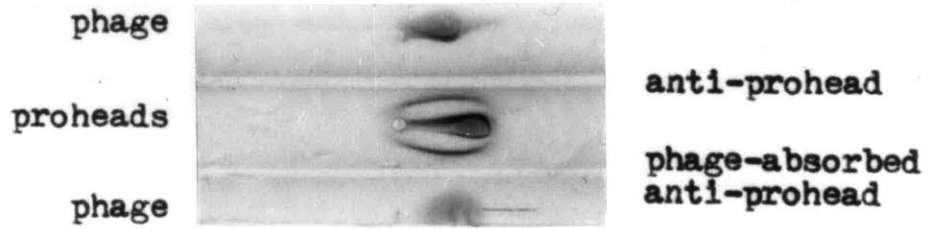
a)



b)



c)



Will phage-absorbed anti-prohead serum precipitate proheads?

The central precipitation reaction in Figure 25a shows that anti-prohead serum which has been exhaustively absorbed with phage particles continues to react, though more weakly, with prohead structures. A definite precipitin arc exists at the prohead position. This result yields two important pieces of information about the antigenic-relatedness of phage and proheads. First, the amount of precipitate formed against proheads by phage-absorbed anti-prohead serum is significantly less than that formed by whole anti-prohead serum. In addition, the antigen travels closer to the antiserum trough before being precipitated. The substantial diminution in the response of phage-absorbed anti-prohead serum to the proheads indicates that anti-prohead serum recognize a large number of determinants on phage and proheads as identical. Secondly, a low level of residual activity in the anti-prohead serum persists against proheads even after exhaustive absorption of the serum with phage. This result establishes the existence of a class of antigenic determinants on proheads which are absent from phage.

It is informative to compare spur formation in this experiment with that in the experiment shown in Figure 18b. In Figure 18b, spurs extended from both phage and prohead precipitin arcs after reaction with anti-prohead serum, suggesting that antigenic determinants exist on both phage and prohead structures which are not shared between them. In the actual experimental data of Figure 25, although it may be difficult to detect in the photographic reproduction of the data, a spur is again detectable extending from the prohead pre-

cipitin arc. Thus, the immunological phenomenon of spur formation serves to confirm the result of the cross-absorption experiment; that is, prohead-specific determinants exist which are not present on phage.

As expected, phage-absorbed anti-prohead serum also precipitates proheads from a 3⁻ amber mutant lysate, which accumulates only proheads. This is shown in Figure 25b. Whole anti-prohead serum, present in the upper antiserum trough, shows a strong precipitation reaction with the proheads in a 3⁻ lysate. Phage-absorbed anti-prohead serum in the lower antiserum trough, produces a very much weaker, but perceptible, response to the proheads. Both whole and absorbed anti-prohead serum precipitate soluble gp8 from the 5⁻ and 3⁻ lysate. Therefore, the results from this experiment are in agreement with the results of the preceding experiments: anti-prohead serum which had been fully absorbed with phage retained a small fraction of prohead-specific antibodies which continued to react with proheads. The proheads in the 3⁻13⁻ amber mutant lysate of Figure 25b appear to be electrophoretically heterogeneous. This effect, seen in several structure-containing lysates, is variable and may merely be indicative of the effectiveness of the DNase treatment of the concentrated lysates. Often, low-speed centrifugation of the lysate reduces considerably the electrophoretic variability of the structure and removes completely the precipitation reaction around the antigen well, as will be shown in Chapter III. The residual precipitating activity of phage-absorbed anti-prohead serum against proheads present in lysates is observed even more clearly when concentrated, purified proheads are used as antigens, as shown in panel c. These proheads are

roughly ten times more concentrated than the proheads in the wild-type lysate of panel a. After exhaustive phage absorption, anti-prohead serum continues to precipitate purified proheads, which have been added to the central antigen well. The residual response of the phage-absorbed serum is stronger here than in panels a and b because the proheads are more concentrated. Nevertheless, the precipitin arc caused by the phage-absorbed serum is significantly weaker than that caused by the whole anti-prohead serum. Therefore, in every instance, the experimental results indicate that proheads contain a limited number of determinants not present on phage.

In the experiment in panel c, I was surprised to find that the preparation of purified proheads contained appreciable amounts of a soluble antigen. This antigen, precipitated by both whole and phage-absorbed anti-prohead serum, was very similar in its immunoelectrophoretic behavior to gp8. Using anti-prohead serum as the precipitating antiserum, this band appeared in the immunoelectrophoretic patterns of several older preparations of proheads; however, the antigen was not precipitated by anti-phage serum. These results suggest that proheads progressively release gp8 from their capsid shells during storage, and that immunoelectrophoresis may be used to detect this release. This assay for released gp8 serves as an important control in immunoelectrophoresis experiments to follow which use prohead-absorbed anti-prohead serum absorption.

(b) Absence of prohead-specific determinants on the necks of tail-less phage

Particles which lack gp9 are morphologically very similar to phage except that they are missing a baseplate or tail structure. In the absence of a tail structure, a short cylindrical neck becomes visible protruding from the icosahedral head of the particle. Attached to the distal end of the neck is a single, fiber-like appendage, which is also partially visible on phage as a fiber extending downward from the tail structure (see Figure 34). Therefore, several sites become more accessible in the absence of a tail structure. This suggests the possibility that anti-prohead serum, generated in response to prohead determinants, may contain antibodies against these same determinants in the neck region of gp9⁻ particles which cannot be absorbed out by phage which carry tails.

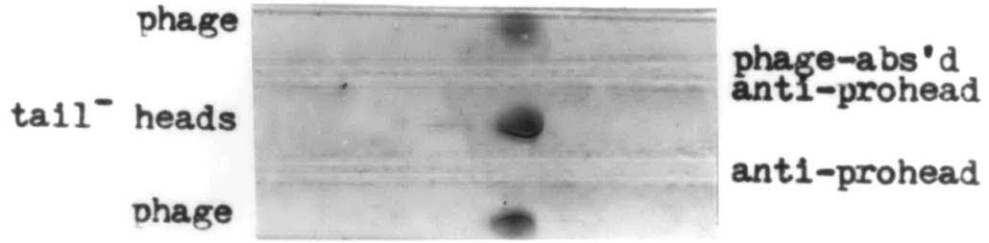
An experiment designed to detect neck-specific antibodies in the anti-prohead serum is shown in Figure 26a. Whole anti-prohead serum, in the lower trough, precipitates both phage and tail⁻ heads. Phage-absorbed anti-prohead serum, in the upper antiserum trough, no longer precipitates either phage or tail⁻ heads. These results suggest that there are no antigenic determinants on gp9⁻ particles which are not also recognized as being present on phage by anti-prohead serum; hence, absorption of anti-prohead serum by phage removes all precipitating activity against tail-less heads. Therefore, antibodies against proteins as they exist in the neck structure of tail-less phage have not been generated in response to the determinants present on proheads.

Figure 26

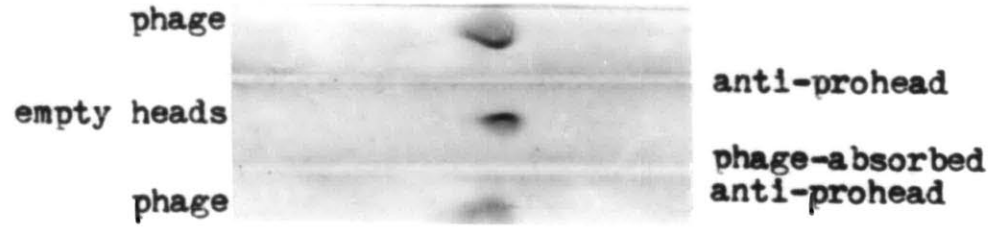
Absence of Prohead-specific Determinants
on Tail-less Phage and Empty Heads

- (a) Sera are as described in the legend to Figure 25a.
- (b) Sera are as described in the legend to Figure 25b.

a)



b)



(c) Absence of prohead-specific determinants on empty heads

Several amber mutant lysates, including 4⁻, 10⁻, and 26⁻ lysates, produce phage heads in which the DNA is unstably packaged. A large number of these heads appear to contain DNA when they are present inside the bacterial cell, as observed in thin-section electron microscopy experiments (Lenk, et al., 1975); however, the particles lose their DNA very rapidly at cell lysis (Botstein, et al., 1973). The resultant empty head structures have been purified from a 10⁻ 13⁻ amber mutant lysate (W. Earnshaw, et al., 1976). The experiment in Figure 26b examines the immunoelectrophoretic behavior of these empty head structures against whole and phage-absorbed anti-prohead serum. Whole anti-prohead serum, in the upper antiserum trough, precipitates the empty heads; phage-absorbed anti-prohead serum, in the lower antiserum trough, does not. Perhaps not surprisingly, these experimental results indicate that the process by which the mutant particles eject their DNA does not expose prohead-related determinants that are not also present on DNA-containing phage.

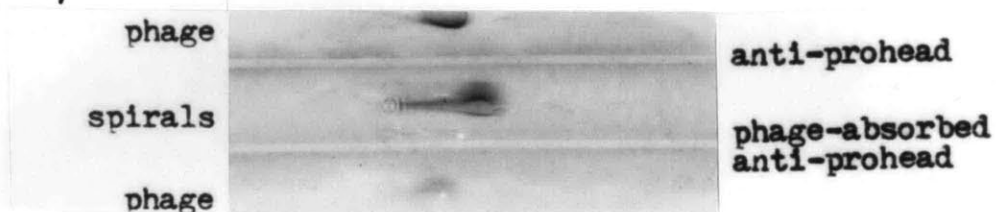
(d) Antigenicity of aberrant aggregates of gp5

Thus far, the phage-absorption experiments have established that a class of prohead-specific antibodies exists in anti-prohead serum, although their target proteins on the prohead have not yet been identified. One possibility is that these antibodies are anti-gp8 antibodies reacting with exposed gp8 on proheads; however, if the phage-absorbed anti-prohead serum can be shown to react with structures which do not contain gp8, then the presence of additional antibodies other than anti-gp8 antibodies is clearly indicated. These antibody classes may include

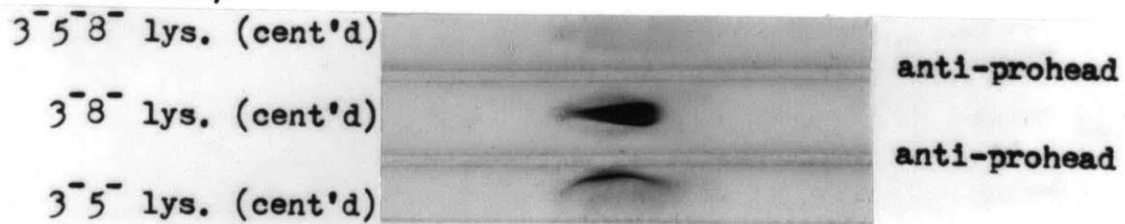
Figure 27Residual Activity of Phage-absorbed Anti-prohead Serum Against Organized P22 Coat Protein

(a) and (b) Sera are as described in the legend to Figure 25b. (c) The anti-prohead serum has gone through an additional cycle of phage absorption as compared to the phage-absorbed serum in panels a and b (see Materials and Methods, Section , Ø7). The central reaction in panel a shows the precipitation of purified spirals. The upper asymmetrical smudge is the result of spillover of the antigen during its addition to the well. The central reactions in panel b and c show the precipitation of the mixture of aberrant gp5 aggregates present in these lysates, which includes spirals and two size classes of closed shell structures.

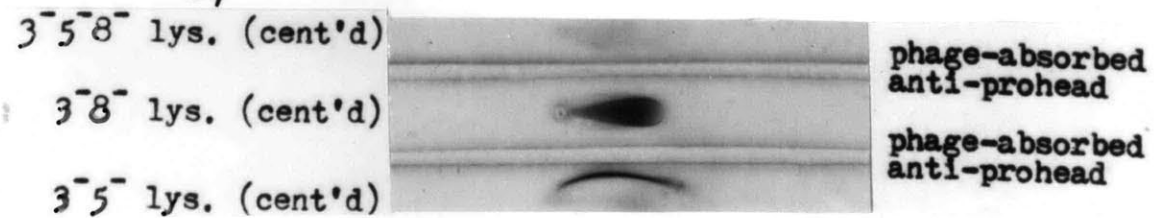
a)



b)



c)



effect often produced by antibody dilution.

Regardless of the fine points, the basic result of this experiment is clear: phage-absorbed serum continues to precipitate a class of gp5-containing structures which do not contain gp8. Therefore, the prohead-specific antibodies in the anti-prohead serum include antibodies against the coat protein as well as against the scaffolding protein.

The preceding experiment established that anti-capsid antibodies remained in the anti-prohead serum after phage absorption. However, the spirals used in the previous experiment were purified from an 8⁻amH202 lysate which contains a substantial amber fragment. If this gp8 amber fragment assembled onto some of the spirals, then the positive precipitation of spirals could have been produced, not by anti-capsid antibodies, but by anti-gp8 antibodies reacting with the gp8 amber fragment present on some of the structures. Therefore, I examined the reaction of phage-absorbed anti-prohead serum with the structures present in an 8⁻amN123 lysate, which does not contain a detectable gp8 amber fragment. The aberrant gp5-containing structures present in the lysate have been characterized (W. Earnshaw, unpublished experiments). They fall into one of three morphological classes: either the spiral structures which have been described, or, into one of two discrete size classes of shells. These shells have diameters either like that of the proheads or considerably smaller.

Panel b of Figure 27 examines the reaction of whole anti-prohead serum with these structures; an 8⁻amN123 lysate has been added to the central antigen well. (These lysates are also 3⁻ but that is irrelevant to this discussion). Precipitation of the structures in this lysate

results in a single, dense precipitin arc. As expected, this precipitation reaction is gp5-dependent; when a 5⁻ lysate is used as an antigen, as in the bottom antigen well, only the soluble gp8 band is detectable. When a lysate which lacks both gp5 and gp8 serves as the antigen, as in the upper antigen well, no precipitin bands are formed.

This same experiment has been repeated in panel c of Figure 27, except that the anti-prohead serum in both troughs has been fully absorbed with phage. Phage absorption of the serum significantly reduces the reaction of the gp5-containing structures from an 8⁻ lysate; however, a definite precipitin band persists which is much lighter and closer to the antiserum trough. Therefore, even in the absence of an antigenic gp8 amber fragment, phage-absorbed anti-prohead serum continues to react with structures principally composed of gp5. This result strengthens the conclusion from the previous experiment: after exhaustive phage absorptions, anti-prohead serum retains a class of anti-capsid antibodies.

4. Can proheads absorb anti-scaffolding protein antibody?

The immunoelectrophoresis experiments of this section focus directly on the question: is gp8 in proheads accessible to the environment? if so, absorption of anti-prohead serum with intact prohead structures would remove antibodies in the serum directed against the scaffolding protein. As a consequence, prohead-absorbed anti-prohead serum would no longer show a precipitin arc against the soluble gp8 present in P22 lysates. Alternatively, if gp8 were not accessible,

absorption of anti-prohead serum with proheads would not affect its precipitation of soluble gp8. Although this scheme is theoretically

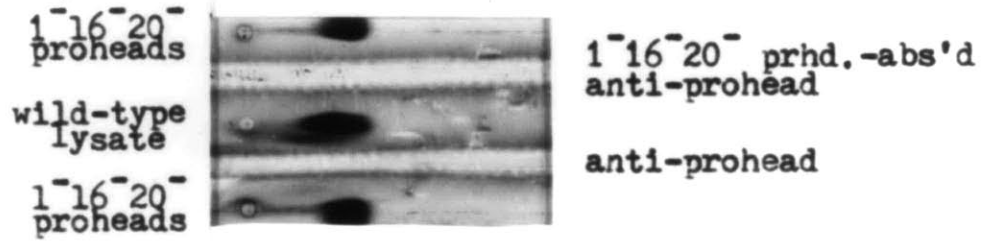
straightforward, it was technically difficult to prepare the large amounts of very concentrated proheads necessary to fully absorb the anti-prohead serum. As a result of this limitation in the availability of proheads, the sera in these experiments were not fully absorbed and they continued to precipitate prohead structures. However, as these experiments will show, even partial absorption of anti-prohead serum with proheads reduces the anti-gp8 titer sufficiently so that soluble gp8 is no longer precipitated from lysates.

Proheads were purified from a 1⁻16⁻20⁻13⁻ amber mutant lysate (W. Earnshaw, et al., 1976) and used as antigens in the experiment shown in Figure 28a. These proheads are missing the minor prohead structural proteins, gp1, gp16, and gp20, and are composed of only gp5, gp8, and a minor protein, gp7. In the lower portion of panel a, whole anti-prohead serum precipitates these proheads. It is important to note that there is no evidence of soluble gp8 being present in the prohead preparation. Whole anti-prohead serum precipitates soluble gp8 from a wild-type lysate, which was present in the central antigen well. The anti-prohead serum in the upper trough of this panel has been absorbed with 1⁻16⁻20⁻ proheads, although the absorption is far from complete, as evidenced by the strong, residual precipitation reaction by the absorbed serum against the proheads. Despite incomplete prohead absorption, the partially absorbed serum no longer precipitates the soluble gp8 from the wild-type lysate. These results indicate that prohead structures are very efficient in absorbing anti-gp8 antibodies from the anti-prohead serum. Therefore, the conclusion is that gp8 is accessible to the environment. Also, because of the complete lack of residual activity of the prohead-absorbed serum

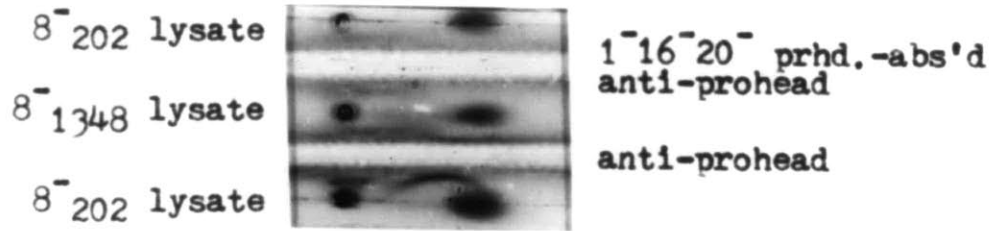
Figure 28Absorption of Anti-scaffolding Protein Antibodies
From Anti-prohead Serum by Proheads

(a) and (b) Anti-prohead serum from series 7 was absorbed with an equal volume of 1×10^{16} proheads and incubated for 90 minutes at 38°C . The suspension was stored overnight in the cold to promote precipitate formation. The absorbed serum was centrifuged at 10,000 rev/min for 10 minutes in a Sorvall SS-34 rotor. Whole anti-prohead serum from series 7 was diluted 1:2.

a)



b)



against soluble gp8, every determinant present on the soluble gp8 molecule appears to be accessible on the proheads.

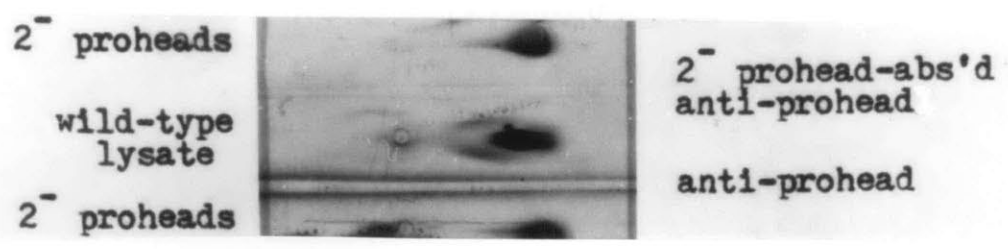
The experiment in Figure 28b provides an additional check that anti-gp8 antibodies have been removed from the anti-prohead serum by prohead absorption. While whole anti-prohead serum, in the lower trough, precipitates the gp8 amber fragment from an 8⁻amH202 lysate, which was present in the outer antigen wells, absorption of this serum with 1⁻16⁻20⁻ proheads causes the gp8 fragment precipitin arc to disappear, as shown in the upper portion of panel b. Once again, intact prohead structures have been able to absorb anti-gp8 antibodies from the serum. Thus, the determinants present on the gp8 amber fragment are also available in the prohead.

The accessibility of gp8 in 1⁻16⁻20⁻ proheads is not a result of the absence of several minor proteins from the structure. When 2⁻ proheads, which contain a wild-type complement of prohead proteins, are used to absorb anti-prohead serum, they also absorb anti-gp8 antibodies. Figure 29 has been included to show that the 2⁻ prohead preparation used to absorb the anti-prohead serum does not contain soluble gp8. Though the anti-prohead sera in both troughs (one has been only partially absorbed with 2⁻ proheads) precipitate soluble gp8 from a wild-type lysate, present in the central antigen well, neither serum shows a reaction against soluble gp8 when reacted with the proheads.

The possibility existed that the availability of ^{gp8} in 1⁻16⁻20⁻ proheads was a direct consequence of the absence of several of the minor proteins from the prohead shell. Therefore, in the following experiment, I examined the absorbing activity of 2⁻ proheads, which

Figure 29Absence of Soluble Scaffolding Protein in 2 Prohead Preparation

Anti-prohead serum was absorbed with 2⁻ proheads as described in the legend to Figure 28. The absorbed serum was diluted with buffer to yield a final dilution of 1:5. Whole anti-prohead serum was also diluted 1:5.



contain a wild-type complement of prohead proteins. In a control experiment, presented in Figure 30, I showed that the 2⁻ prohead preparation did not contain soluble gp8. There is no soluble gp8 precipitin arc present in the reaction of the whole anti-prohead serum present in the lower serum trough, and the prohead preparation, added to the outer antigen wells; however, this same serum precipitates the soluble gp8 in the wild-type control lysate, present in the central antigen well. This result establishes that the absorption of anti-scaffolding antibodies by this preparation must be accomplished by gp8 which is present as a structural component of the prohead.

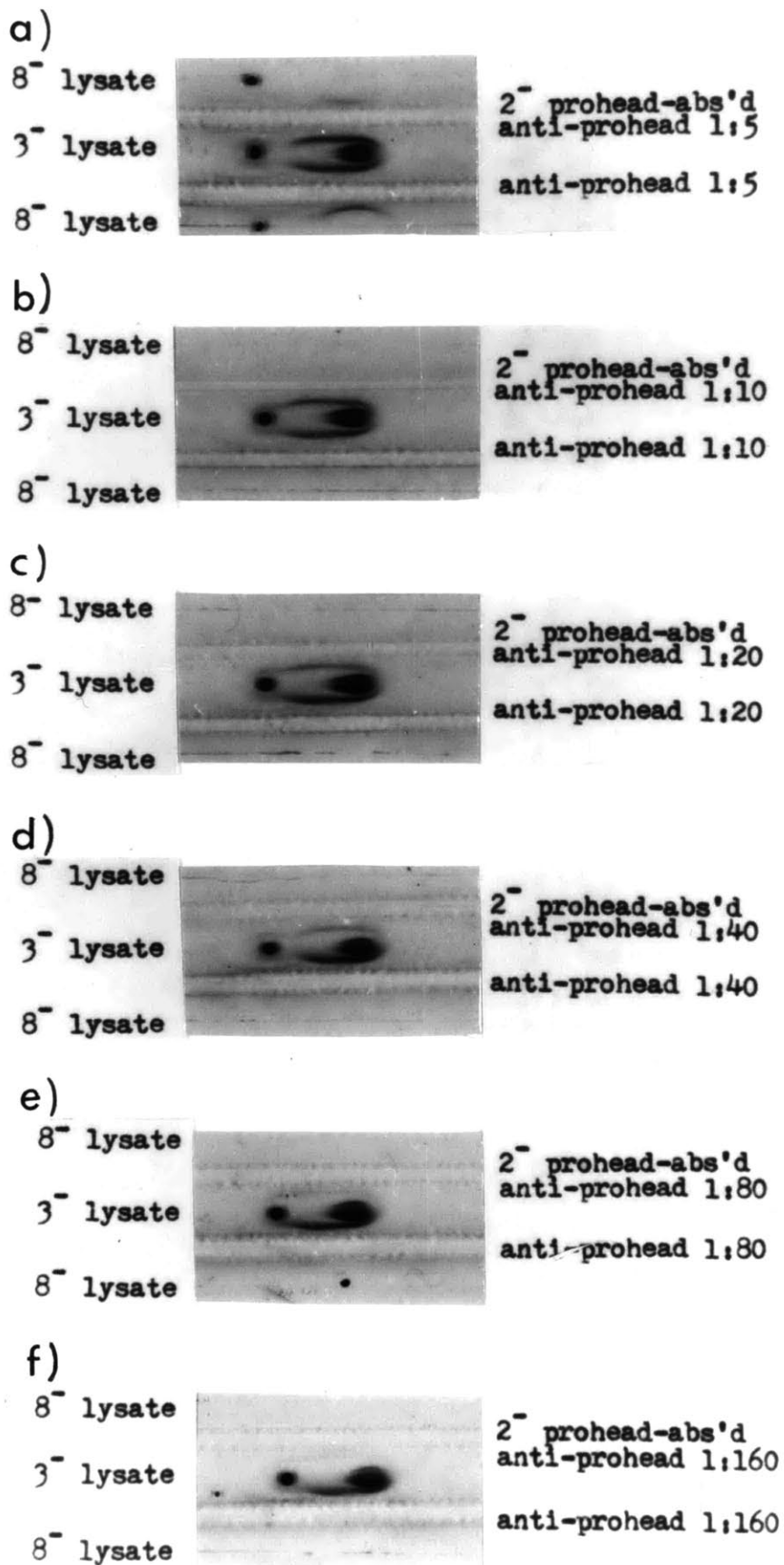
The upper antiserum trough of Figure 30 contains anti-prohead serum which has been incubated with the 2⁻ prohead preparation. The strong residual precipitation of the proheads by the absorbed serum shows that the absorption was very incomplete. In fact, at this relatively high concentration of antiserum, the prohead-absorbed serum appears to precipitate soluble gp8 from the wild-type lysate, as if the proheads had not removed anti-gp8 antibodies from the serum. However, appropriate dilution of the serum reveals that absorption of the serum with 2⁻ proheads actually does deplete the serum of its anti-scaffolding antibodies.

In this experiment, whole anti-prohead serum in the upper troughs, and 2⁻ prohead-absorbed anti-prohead serum in the lower troughs, have been 2-fold serially diluted. In each panel, the sera are reacted with an 8⁻amH202 mutant lysate in the outer antigen wells and a 3⁻ lysate in the central antigen well.

Figure 30

Absorption of Anti-scaffolding Antibodies by Proheads
Containing a Wild-type Complement of Proteins

Sera are dilutions, as indicated, of sera used in Figure
29.



I direct your attention to the immunoelectrophoretic patterns involving more dilute sera, presented in panels d, e, and f. At these serum dilutions, whole serum precipitates gp8 very efficiently from a 3⁻ lysate. At the same concentrations, however, prohead-absorbed serum displays a considerably weaker, and with increasing dilution, almost undetectable, reaction with the gp8 in the lysate. Thus, even proheads which contain all of the proteins normally found in wild-type proheads can absorb the anti-scaffolding protein antibodies from anti-prohead serum. The most likely conclusion from these results, then, is that gp8 is ^{accessible} Λ in all prohead structures.

Because the serum was incompletely absorbed by the proheads, anti-gp8 antibodies, though diminished, were still present in substantial numbers. Thus, at high antiserum concentration, as in panels a and b, large numbers of residual anti-gp8 antibodies give a precipitation reaction with the soluble gp8 of the 3⁻ lysate which is indistinguishable from that of whole serum. It is also only at high antiserum concentration, as in panel a, that the reaction of the anti-gp8 antibodies with the gp8 fragment is detectable. Both whole and prohead-absorbed sera produce a precipitin arc against the gp8 fragment; but, the band resulting from the reaction of the absorbed serum, which we expect to contain many fewer anti-gp8 antibodies, is indeed substantially weaker.

In retrospect, it is interesting to think that an experiment originally conceived of as a control experiment - prohead absorption of anti-prohead serum - would yield such important information on the structure of the prohead. In the simplest interpretation of the results of these experiments, the ability of proheads to absorb anti-

scaffolding protein antibodies from the serum indicates that gp8 determinants in the prohead are available for reaction with antibodies in the environment. I did not expect this result, in light of previous conclusions reached in studies using electron microscopy and X-ray diffraction (J. King et al., 1973; Earnshaw et al., 1976). Thus, I was eager to substantiate this finding using another approach. A set of experiments which lead to the same conclusion using electron microscopy are described in Chapter III.

E. Sensitivity of the Immunoelectrophoretic Assay

1. Effects of antigen dilution

Insoluble antibody antigen complexes appear in immunoelectrophoresis only if the antibody and antigen encounter each other in precise proportions corresponding to equivalence (Grabar, 1964). Too low a concentration of antigen may cause the precipitate to be located in the antigen well, and too high a concentration may push the position of equivalence into the antibody trough (J. Clausen, 1971).

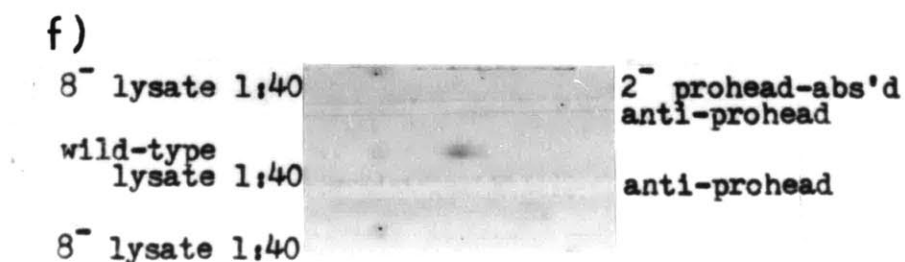
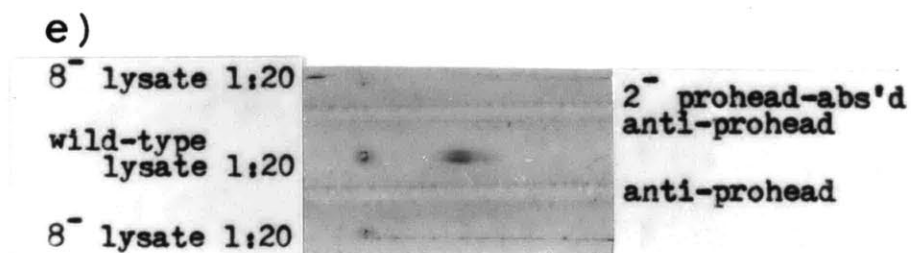
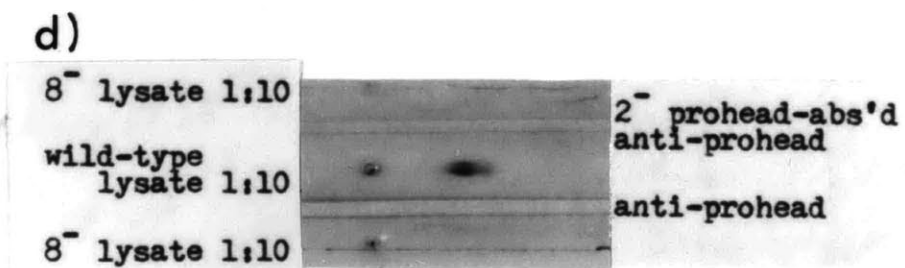
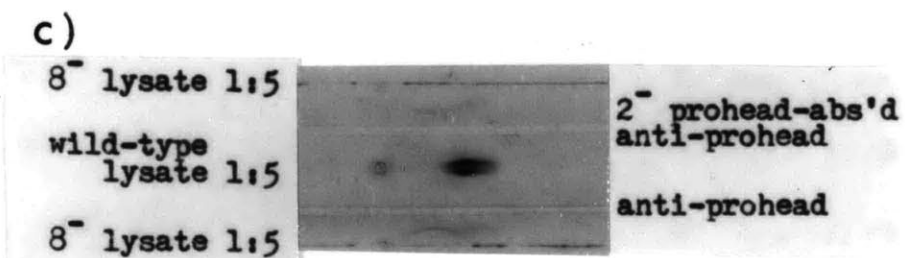
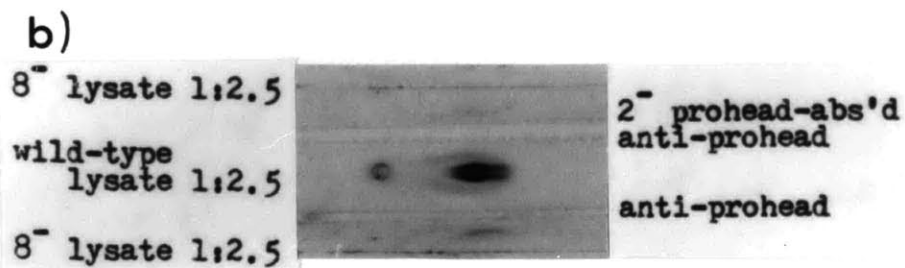
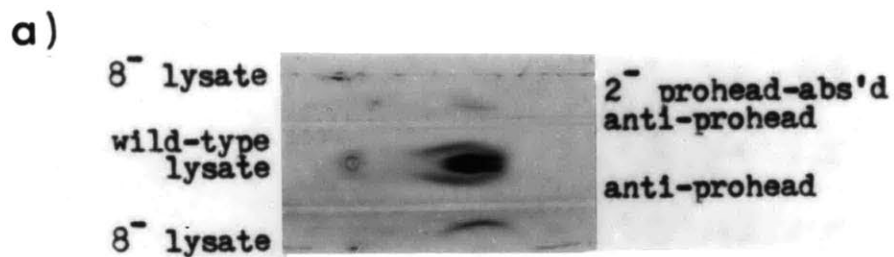
The effect of antigen dilution on the immunoelectrophoretic patterns of P22 wild-type and 8⁻ lysates is examined in Figure 31. In each panel, wild-type lysate filled the central antigen well, and 8⁻ lysate, the outer antigen wells. The lower antiserum troughs contained whole anti-prohead serum. The upper antiserum troughs contained anti-prohead serum which had been incompletely absorbed with 2⁻ proheads. This absorption seems mainly to have decreased the intensity of the reactions and will not be discussed separately.

Decreasing concentration of the antigen in Figure 31 has two obvious effects: the intensities of the precipitin reactions decrease and the extent to which the antigens diffuse before being precipitated also decreases. For example, the double-humped structure precipitin arcs become fainter and more localized with decreasing structure concentration. At dilutions greater than 10-fold, the precipitate becomes too faint to be of analytical use. At 10-fold lysate dilution, the phage titer in the lysate is approximately 10^{12} phage/ml. Thus, a high concentration

Figure 31

Effects of Antigen Dilution on Immunolectrophoretic
Patterns Using Anti-Prohead Sera

The serum is described in the legend to Figure 29.



of particles is required for immunoelectrophoretic analysis-

Precipitins of soluble antigens appear to be even more sensitive to dilution. For example, the precipitation of soluble gp8 from the wild-type lysate in Figure 31 disappears when the lysate is diluted 5-fold. In comparison, the gp8 amber fragment from the 8⁻ lysate shows a somewhat stronger precipitation reaction with the serum. Presumably, it is present in soluble form in higher concentrations than the gp8 in the wild-type lysate, some portion of which has assembled into prohead structures. Even so, at 10-fold dilution of the lysate, the precipitation reaction of the gp8 amber fragment disappeared.

Precipitation of gp9 from the 8⁻ lysate in Figure 31 provides the single instance in which dilution of the antigen appears to increase its precipitation. The gp9 precipitin arc was barely detectable when the lysate was concentrated. At 2.5-fold dilution of the lysate, the band is slightly stronger; and, at 5-fold lysate dilution, it reaches its maximum density. The precipitation optimum is very sharp. The reaction becomes barely detectable at 10-fold dilution of the lysate, and disappears entirely at 20-fold lysate dilution. This series of observations may be explained if gp9 is present in antigen excess in the undiluted lysate. Because antibody antigen complexes are typically soluble in antigen excess (Eisen, 1974) gp9 is not visibly precipitated at high lysate concentration. Lysate dilution reduces the concentration of gp9 to equivalence and a precipitate form. This precipitation falls off rapidly, however, with decreasing antigen concentration. The gp8 present in the lysate did not seem to be in excess of the number of anti-gp8 antibodies in the serum. There-

fore, I conclude that the concentration of anti-gp9 antibodies in the anti-prohead serum is lower than that of the anti-gp8 antibodies. This seems reasonable as anti-gp9 antibodies were presumably generated in response to contaminating tails in the prohead preparation, while anti-gp8 antibodies were produced against large numbers of gp8 subunits exposed on the prohead structure.

In general, the results indicated that only very narrow ranges of antigen concentrations produced visible precipitates, particularly in the case of the soluble antigens. Perhaps this explains why I have never detected soluble gp9 in immunoelectrophoresis of wild-type lysates (see, for example, Figure 17 and 18). The immunoelectrophoresis results seem to contradict the data presented in Table 5, which had shown that a wild-type lysate contained a considerable amount of soluble tailing activity. The results of the antigen dilution experiment suggest an explanation: the concentration of soluble gp9 in the wild-type lysate may be too low to yield detectable precipitation. Apparently, a 5-10-fold increase in the concentration of gp9, as occurs in 5⁻, 8⁻ and 2⁻ lysates which overproduce gp9, is sufficient to produce a visible precipitation reaction (compare Figures 20a and 17a for anti-phage serum, and see Figure 31 for anti-prohead serum).

2. Effects of antiserum dilution

Serum blocking experiments have shown that almost all of the phage-killing titer of anti-phage and anti-prohead serum results from the binding of anti-gp9 antibodies to the phage tail. Thus, for anti-gp9: gp9 precipitation reactions, the sensitivity of the system to antibody dilution may be expressed in terms of k equivalents. The experiment in

Figure 21c defines a lower limit for the k value of serum which will show visible precipitation of gp9. Soluble gp9, at a concentration of 6×10^{14} phage equivalents/ml, was precipitated strongly by a serum with a k of 1700 min^{-1} but shows only a very faint diffuse precipitation reaction with serum from an earlier bleeding, with a k of 500 min^{-1} . Similar limits of detection were found using dilutions from a single antiserum pool against the gp9 in 5^- , 8^- and 2^- lysates. The concentration of gp9 in these lysates, probably about 10^{15} phage equivalents/ml, is similar to that of the purified gp9 preparation of Figure 21c, discussed above. In Figure 17c, for example, anti-phage serum with a k of about 500 min^{-1} just barely precipitated gp9 from a 5^- lysate. In contrast to this weak precipitation behavior, anti-phage serum with a k about ten times higher precipitated purified gp9 and gp9 from 5^- , 8^- and 2^- lysates (Figure 20) very efficiently. Anti-prohead serum at a k of 50 min^{-1} (Figure 18b) or even 100 min^{-1} (Figure 32) did not precipitate gp9; anti-prohead serum with a k of about 500 min^{-1} precipitates gp9 (Figure 22); and anti-prohead serum with a k of about 1700 min^{-1} did so effectively (Figure 21).

The precipitation of structures appears to be somewhat less sensitive to antiserum dilution. In Figure 30, anti-prohead serum which is 160-fold diluted still precipitated structures quite strongly. The relative insensitivity of structure precipitation to antiserum dilution may simply reflect the high concentration of antibodies against proheads in the anti-prohead serum; however, the large size of P22 structures may also be a contributing factor. Molecules with molecular weight greater than about 200,000 daltons are too large to diffuse freely through the micelle structure of the agarose matrix (J. Clausen, 1971).

DISCUSSION

Considering that proheads contain six species of phage proteins, tail⁻ heads contain eight, and phage contain nine, the antisera made against each of these particle types contained relatively few classes of antibodies. Proheads induced antibodies against gp5 and gp8, the major prohead proteins; phage induced antibodies against gp5 and gp9, the major proteins of the phage; and tail⁻ heads induced antibodies against gp5, the major head protein.

It is difficult to ascertain whether the sera contain antibodies against the minor proteins and that these were not detected, or whether such antibodies were not induced in the rabbits in the first place. The sensitivity of the assay indicated that high concentrations of both antigen and antibody are needed to form detectable precipitin arcs in immunoelectrophoresis. Thus, minor antibody species would not be detected. On the other hand, the three antigens are also displayed as repeating arrays on the immunogenic particles, and may have been more effective immunogens than the minor proteins.

I originally started characterizing the antisera using Ouchterlony double-diffusion techniques (J. Clausen, 1971). However, I quickly switched to immunoelectrophoresis experiments because the interpretation of the data was made considerably easier by the extra dimension of separation given by electrophoresis of the antigens prior to their diffusion. In addition, the information obtained regarding the relative electrophoretic mobilities of gp8 and its amber fragments

greatly facilitated the identification of anti-scaffolding antibodies in the anti-prohead serum. Because immunoelectrophoresis also involves double diffusion, information as to the antigenic-relatedness of species by analyzing their fusion and spur formation behavior is also available. It is only in the area of the relative sensitivities of the two methods that immunodiffusion may have a slight advantage in that 10-30 times the volume of antigen is routinely used in immunodiffusion. Thus, given the sensitivity of the precipitation reaction to antigen concentration, immunodiffusion may be useful in detecting antibody-antigen reactions in which the antigen concentration would be too low for detection by immunoelectrophoresis.

Infection with P22 elicits a new somatic antigen on the infected cell surface (Levine, 1972). Antibody induced in the rabbit by contaminating cell envelope fragments would not be absorbed out by uninfected Salmonella cells. However, it is unclear whether this induced host antigen would be expected to yield a precipitin band.

The potency of the tail and the scaffolding proteins as immunogens is evidenced by the level of antibody against them induced by low levels of particles. Thus, the empty phage particles contaminating the prohead preparation represented only a few % of the total prohead particles injected, and yet they elicited a very substantial antibody response. Similarly, the tail-less heads were contaminated with only a few % proheads, yet they elicited a substantial concentration of anti-gp8 antibodies. In hindsight, I realize that the proheads should have been induced from a lysogen, to avoid contamination from input particles, and the tail-less heads should have been further purified.

However, at the time of the experiment, I was not aware of the potency of these particles as immunogens.

Phage heads without a tail show clearly a short neck structure with a thin projecting fiber. I had expected that antibodies would be induced against the proteins in this structure. Apparently either the antibodies are induced in too low a concentration to be identified, or the constituent proteins are not immunogenic. I tend to favor the latter model for the following reason. Reactions which involve the precipitation of whole phage are easily detected, because even a low concentration of antibodies, reacting with only a few determinants on the particle, still precipitates a high concentration of protein. In the experiment in which anti-head serum was absorbed with whole phage, the residual activity of the serum against tail-less heads was tested. As discussed above, this should have been a relatively sensitive test for the existence of neck-specific antibodies. The negative results indicate that the serum did not contain anti-neck antibodies, unless these are also available in mature phage particles.

The absence of a precipitin band in 8^- lysates corresponding to the reaction of gp5 coat subunits and anti-gp5 antibodies was unexpected. However, similar results had been found by Yanagida with phage T4 (1972). There is some evidence of a free pool of gp5 subunits in 8^- lysates, but this comes from labelling experiments (Casjens and King, 1974). The gp5 subunits might aggregate or precipitate in the concentrated lysates used under conditions for immunoelectrophoresis.

The induction of antibodies directed against scaffolding protein by proheads was somewhat of a surprise. However, the identification of these antibodies as anti-gp8 antibodies follows directly from the

immuno-electrophoretic patterns of the 8⁻ amber mutants in which the normal precipitin band disappeared and a new one appeared. Mixing experiments in which the new band fused with the old band confirms that the new band represents an amber fragment. The fact that at least two amber fragments of the scaffolding protein were antigenic and gave a discrete precipitin arc indicates that they are in a conformation similar to the mature protein. This is also consistent with in vivo experiments which indicate that these fragments still have the autoregulatory functions of the mature protein (King, Hall, and Casjens, personal communication).

It is not clear why amber fragments of gene 9 weren't detected. They may be unstable within the cell, or may not be antigenic. The gene 5 amber fragments are unstable and are degraded within the cell (King and Casjens, unpublished results).

Though the lysate experiments showed conclusively that anti-prohead serum contained anti-gp8 antibodies, it was possible that this was due to induction by scaffolding protein released from the proheads during preparation, or in the rabbit. The ability of proheads to remove anti-gp8 from the serum rules this out. Either gp8 is normally accessible in proheads, or it becomes accessible upon incubation with antiserum. The latter is not unreasonable, since detergent binding releases scaffolding protein (Casjens and King, 1974) and since the release must occur in the normal processes of morphogenesis. It is not clear whether such release takes place at a particular site on the prohead, for example, a site of DNA entry, or whether the scaffolding protein projects through the entire lattice. This question is taken up in the next chapter.

APPENDIXCalculation of Relative Surface Changes of P22 Structures from their Relative Electrophoretic Mobilities1. Comparative immunoelectrophoretic behavior of P22 structures

In previous immunoelectrophoresis experiments, P22 structures migrated different distances from their points of origin during electrophoresis. The migration behavior of several P22 structures are systematically compared in Figure 32. In panels a-c, purified wild-type phage have been added to the outer antigen wells to serve as electrophoretic standards. Whole anti-prohead serum has been added to each of the upper antiserum troughs, and 5⁻ lysate-absorbed anti-prohead serum, previously shown in Figure 18b to be fully absorbed, filled each of the lower antiserum troughs.

In panel a, a sample of tail-less heads has been added to the central antigen well. These tail-less heads electrophorese slightly faster than phage, a phenomenon also apparent in a comparison of the relative positions of phage and heads in Figure 26b. In panel b, the central antigen has been filled with purified proheads, which migrate considerably faster than either phage or tail-less heads. In panel c, purified 10⁻ empty heads (provided by W. Earnshaw) were added to the central antigen well. These particles, which characteristically lack tails, migrate more slowly than proheads, slightly faster than phage, and with approximately the same mobility as tail⁻ heads.

In panel d, the electrophoretic mobilities of empty heads, phage, and proheads are compared directly using whole anti-prohead serum. The actual measured distances which these particles have migrated from the center of the antigen well are shown in Table 6.

Figure 32

Comparative Immunoelectrophoretic
Behavior of P22 Structures

- (a) - (c) Sera are as described in the legend to Figure 18b. (d) Anti-prohead serum is from series 7.

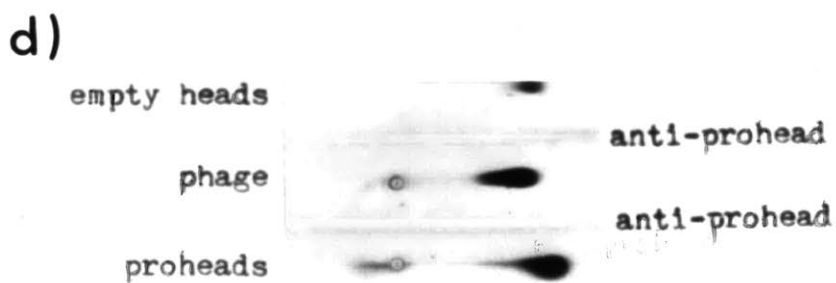
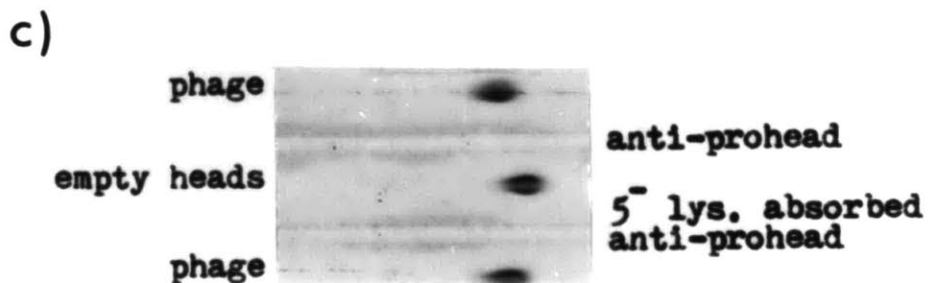
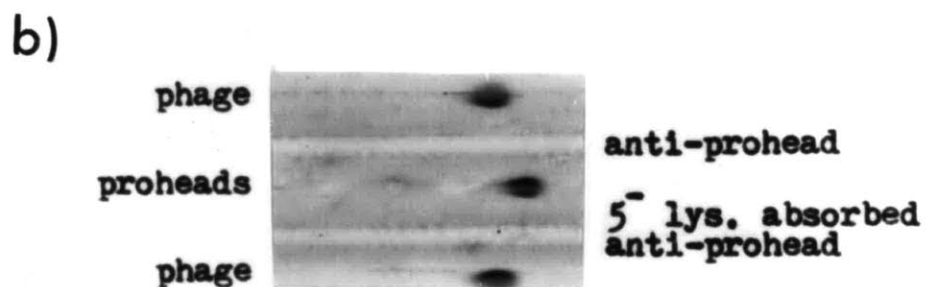
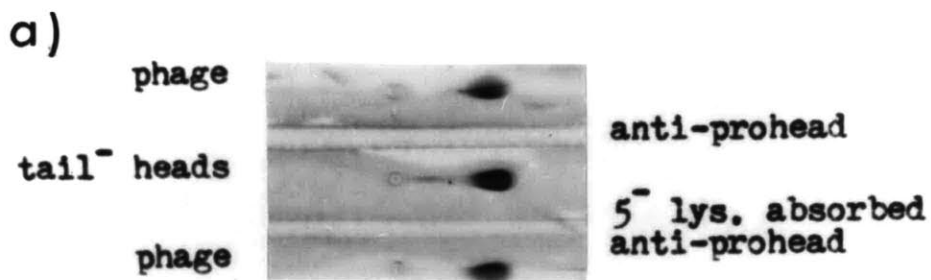


Table 6

Relative Electrophoretic Mobilities of P22 Structures

<u>Figure</u>	<u>Distance Migrated (cm)¹</u>				<u>Relative Electrophoretic Mobility (Distance Ratios)</u>			
	Proheads (PH)	Empty heads (EH)	Tail ⁻ heads (HD)	Phage (Ø)	PH/Ø	EH/Ø	PH/EH	HD/Ø
31d	1.9	1.6		1.5	1.27	1.07	1.19	
31a			1.1	1.0,1.05				1.08
31b	1.45			1.1,1.1	1.32			
31c		1.5		1.25,1.3		1.18		
26b			1.35	1.25				1.08
Average Relative Electrophoretic Mobility: →					1.3	1.13	1.15*	1.08
					PH/EH = 1.3/1.13 = 1.15*			

¹ To measure the distance migrated, I dropped a perpendicular from the summit of the arc of the structure precipitate to a line parallel to the axis of migration. I measured the distance from this perpendicular to a perpendicular dropped from the center of the antigen well. (In general, one measures the distance which the protein has migrated from the point of zero mobility, but an electrically neutral species was not included in the runs).

* As indicated, PH/EH ratios calculated from average PH/Ø and EH/Ø.

2. Relationship between electrophoretic mobility and surface charge

I wondered whether the differences in the electrophoretic mobilities of the P22 structures was simply a result of differences in their frictional co-efficients, or whether differences in their net surface charges might also be contributing. These variables are related in the following way (J. Cann, 1968): during electrophoresis, a uniform electric field of intensity E exerts a force qE on an isolated particle of charge q , assuming it is suspended in a perfect insulator. The particle is accelerated until the opposing frictional force, f , exerted by the surrounding viscous medium just equals the electrical force, after which time the particle moves with constant velocity, v , according to the relationship:

$$qE = fv$$

Therefore, the theoretical electrophoretic mobility, μ , of a particle of arbitrary shape is:

$$\mu = \frac{v}{E} = \frac{q}{f}$$

This calculation assumes that the electrophoresing particle exists in a perfect insulator. In reality, particles surround themselves with an ion cloud of opposite charge which tends to decrease their electrophoretic mobility. The perfect insulator assumption may be particularly inadequate in the following calculations which attempt to describe the relative electrical states of virus structures. These particles carry multiple charges dispersed over complex surfaces; thus, charge differences between two particle surfaces may affect the composition and distribution of their ion clouds, and so, their apparent

electrophoretic mobilities, in extremely complicated ways. Therefore, the theoretical calculations presented below provide only an approximation of the relative surface charges on the virus structures.

3. Experimental limitations: measurements of the relative electrophoretic mobilities

Had I designed the experiments to measure the absolute electrophoretic mobilities of the particles, I could have gotten an estimate for the absolute charge on the particles, which may have been of interest. However, the determination of absolute electrophoretic mobility depends upon experimental conditions such as the strength of the electric field, the duration of the run, the pH and ionic strength of the buffer, and the temperature (J. Uriel, 1964). At the time I did these immunoelectrophoresis experiments, I did not monitor or control these variables with the kind of precision which would be required to obtain meaningful data. Furthermore, the measurement of the absolute electrophoretic mobility of a particle requires knowing the point of zero mobility in the system. This defines the position to which an electrically neutral substance would migrate during the run. It is often different from the point of application because of the electro-osmotic flow of the liquid phase relative to the supporting medium (Grabar, 1964). As I did not include material known to be electrically neutral in the runs, such as glucose or dextrans, this variable could not be determined.

However, the electrophoretic mobilities may be expressed in relative values as well; and, in fact, they often are because of the difficulties involved in establishing and maintaining reproducible

conditions (J. Uriel, 1964). If μ_r is the mobility of a standard reference protein, and μ_x , the mobility of the protein under study, then the ratio μ_x/μ_r should be constant, regardless of the particular electrophoretic conditions, as long as the migration velocity of the proteins is constant. This is true for proteins in agar for the first 4-5 hours of electrophoresis (J. Uriel, 1958).

Values for the distances migrated by various P22 structures, taken from Table 6, were used to calculate relative electrophoretic mobilities for empty heads, proheads and tail-less heads, using mature phage as reference structures. The calculated values, and their averages are also presented in Table 6.

4. Calculation of the frictional co-efficients of P22 proheads and empty heads

(a) Calculations assuming proheads and empty heads are solid spheres

In order to determine the relative surface charges of proheads and empty heads (this choice of particles will be explained presently), I needed to know their frictional co-efficients. I estimated the frictional co-efficients in two ways. Each had its limitations, and I was interested in the range in values the two methods would generate.

First, I treated proheads and empty heads as solid spheres of known radius. Although we know from X-ray diffraction work (Earnshaw, et al., 1976) that empty heads and proheads are not solid spheres, the same data provides us with an accurate measure of their radii. With these measurements, we can calculate the frictional co-efficients of the particles from the equation:

$$f = 6 \pi \eta r$$

where η is the density of water (0.01 centipoise), and r is the radius in cm (J. Cann, 1968). Values for the radii of the particles and their calculated frictional co-efficients are shown in Table 7, Method I. The accuracy of these values depends upon the extent to which proheads and empty heads deviate from the behavior of solid spheres.

(b) Calculations using sedimentation behavior of proheads and empty heads

Perhaps a better estimate for the relative frictional co-efficients of the particles can be obtained from their relative sedimentation co-efficients as these are based on experimental measurements of the behavior of the particles during sedimentation. The relevant equation for the relationship between the frictional co-efficients of proheads (PH) and empty heads (EH) and their sedimentation behavior is (K.E. Van Holde, 1971):

$$\frac{S_{20, w} (\underline{\text{PH}})}{S_{20, w} (\underline{\text{EH}})} = \frac{M (\underline{\text{PH}}) (1-\bar{v}_p)}{f (\underline{\text{PH}})} \times \frac{f (\underline{\text{EH}})}{M (\underline{\text{EH}}) (1-\bar{v}_p)}$$

Because the partial specific volume, \bar{v} , for proteins is typically 0.73 (K.E. Van Holde, 1971), and because proheads and empty heads are composed of only protein, I am assuming that the term $(1-\bar{v}_p)$ cancels out. That is also why I am restricting this set of calculations to particles which do not contain DNA. Therefore:

$$\frac{f (\underline{\text{PH}})}{f (\underline{\text{EH}})} = \frac{M (\underline{\text{PH}})}{M (\underline{\text{EH}})} \times \frac{S_{20, w} (\underline{\text{EH}})}{S_{20, w} (\underline{\text{PH}})}$$

Table 7
Calculation of Relative Frictional Co-efficients
for Proheads and Empty Heads

Method I: assumes proheads and empty heads to be solid spheres

$$\text{Equation: } f = 6 \pi \eta r \quad \eta = \text{density of water} = 0.01 \text{ centipoise}$$

$r = \text{radius in cm}$

	<u>PH</u>	<u>EH</u>
radius ¹	295 Å	335 Å
f	5.56×10^{-7}	6.32×10^{-7}

$$\frac{f_{PH}}{f_{EH}} = \frac{r_{PH}}{r_{EH}} = \frac{295}{335} = 0.88$$

Method II: data from sedimentation behavior

$$\text{Equation}^2: \frac{f_{PH}}{f_{EH}} = \frac{S_{EH}}{S_{PH}} \times \frac{M_{PH}}{M_{EH}}$$

$$\frac{f_{PH}}{f_{EH}} = \frac{170}{240} \times \frac{3.7}{2.6} = 1.02$$

¹ Radii were taken from curves of Figure 7 in Earnshaw, et al., 1976, as the points at which the curves crossed zero density. A correction of 5Å was added to this number to adjust for a possible sphere of hydration about the particle.

² Molecular weights of the particles are taken from Table 8.

Values for the $S_{20, w}$ of P22 phage have been determined by a comparison of their sedimentation behavior in a 5-20% linear sucrose gradient with that of T₇ phage (Botstein, et al., 1973), for which a precise value of $S_{20, w}$ has been determined. Because the gradient is linear, a direct linear relationship exists between the distance traveled by one particle relative to another of the same density, and their sedimentation co-efficients. The values of 170S for empty heads and 240S for proheads (Botstein, et al., 1973) have been calculated by comparison of their sedimentation behavior with that of P22 phage. This estimation assumes equivalent densities, although phage contain DNA and empty heads and proheads do not; thus, the absolute values for the $S_{20, w}$ of empty heads may be different from 170S and 240S. However, the difference in the sedimentation co-efficients calculated in this manner is an accurate measure of the difference between their true $S_{20, w}$ values, because the particles being compared in this instance are of the same density. In this particular set of calculations, accuracy in the relative sedimentation co-efficients is sufficient because we are mainly interested in the relative frictional co-efficients of the particles.

The uncertainties in the calculation of the frictional co-efficients from sedimentation behavior derive mainly from uncertainties in the molecular weights of the particles, which may be substantial. I estimated the molecular weights for the proheads and empty heads by multiplying the molecular weight of the known structural components by the number of copies believed to be present in each structure (S. Casjens and J. King, 1974). The computation and its result are shown in Table 8.

Table 8
Molecular Weights of Proheads and Empty Heads¹

<u>Gene Product</u> ²	<u>No. of Copies</u> (1)		<u>Monomer Molecular Weight</u> (daltons) (2)	<u>Molecular Weight Contributed by Gene Products in the Structure (daltons)</u>	
	<u>PH</u>	<u>EH</u>		(1)	x (2)
				<u>PH</u>	<u>EH</u>
5	420	420	55,000	2.3×10^7	2.3×10^7
8	250	-	42,000	1.1×10^7	-
1	10	9	94,000	9.4×10^5	8.5×10^5
16	10	7	67,000	6.7×10^5	4.7×10^5
20	18	14	50,000	9×10^5	7×10^5
7	20	20	18,000	3.6×10^5	3.6×10^5
4	-	10	15,000	-	1.5×10^5
			Sums:	3.7×10^7	2.6×10^7

¹ Values for monomer molecular weights and the number of copies of gene product in the structure taken from S. Casjens and J. King, 1974.

Table 8 (Contd.)

Molecular Weights of Proheads and Empty Heads¹

- ² These calculations leave out figures for gp10 (MW = 50,000 daltons), (MW = approximately 10,000 daltons), believed to be minor components of the phage. Gene product 9 is not a component or 10⁻ empty heads.

Using the relative molecular weights and relative sedimentation co-efficients thus obtained, the relative frictional co-efficients of proheads and empty heads were calculated. The computation and its result are shown in Table 7, Method II.

According to this calculation, the frictional co-efficients of proheads and empty heads are very similar, differing only by a factor of 1.02. In the previous calculation, assuming proheads and empty heads were solid spheres, the frictional co-efficients differed by a factor of 0.88.

5. Calculation of the relative surface charges of proheads and empty heads

We have obtained a value for the relative electrophoretic mobilities of proheads and empty heads, and two estimates for their frictional co-efficients. Therefore, we can determine the relative surface charges of proheads and empty heads according to the equation:

$$\frac{q_{PH}}{q_{EH}} = \frac{\mu_{PH}}{\mu_{EH}} \times \frac{f_{PH}}{f_{EH}}$$

Values for the relative surface charges of the particles using the two methods outlined above are shown in Table 9. They vary from 1.03 to 1.19. Therefore, if we assume that empty heads and phage heads which contain DNA have the same surface charge, then these calculations suggest that there is no gross change in the relative surface charges of the capsid shells in the transformation from prohead to phage.

How good an assumption is it, though, that empty heads and phage have the same surface charge? The data in Table 6 actually suggest that empty heads migrate faster than phage by a factor of 1.08. However,

Table 9

Calculation of the Relative Surface Charges
of Proheads and Empty Heads

$$\text{Equation: } \frac{q_{PH}}{q_{EH}} = \frac{\mu_{PH}}{\mu_{EH}} \times \frac{f_{PH}}{f_{EH}}$$

q = surface charge
 μ = electrophoretic mobility
 f = frictional co-efficient

$$\text{Method I}^1: \frac{q_{PH}}{q_{EH}} = \frac{1.17}{1.17} \times \frac{0.88}{0.88} = 1.03$$

$$\text{Method 2}^2: \frac{q_{PH}}{q_{EH}} = \frac{1.17}{1.17} \times \frac{1.02}{1.02} = 1.19$$

- ¹ Relative frictional co-efficients taken from Table 7, Method I, assuming proheads and empty heads to be solid spheres.
- ² Relative frictional co-efficients taken from Table 7, Method II, using data from the sedimentation behavior of proheads and empty heads, and particle molecular weights as calculated in Table 8.

this difference may well be caused by the lack of gp9 in these 10^{-} empty heads, rather than some surface charge difference in the capsids. This is suggested by the fact that tail⁻ heads, which contain DNA but lack tails, electrophorese faster than phage by about the same amount as the tail-less empty heads.

Therefore, insofar as I can tell at this level of computation and with these data, the maturation of a P22 phage from a prohead precursor occurs without major changes in the surface potential of the capsid shell.

CHAPTER III

Chapter III: Electron Microscopy of Antibody-coated P22
 Structures

Previous experiments have shown that injection of P22 phage into rabbits induced the synthesis of antibody against the gene 5 major coat protein and the gene 9 tail protein. Injection of proheads primarily generated antibodies to the coat protein and also to the gene 8 scaffolding protein. A question arises, however, as to whether the induction of antibodies by these antigens actually indicates that the antigenic determinants are exposed at the particle surface. The possibility exists, for example, that internal proteins were released as a result of structure degradation either prior to injection, during mixture of the structures with the adjuvant, or afterwards, in the tissues of the rabbit. This question is particularly relevant in relation to the scaffolding protein. X-ray and electron microscopic investigations (Lenk, et al., 1975; Earnshaw, et al., 1976) had suggested that the scaffolding protein was primarily located within the particle. Yet, results from immunoelectrophoresis experiments have indicated that determinants on the scaffolding protein are available to the environment for reaction with anti-scaffolding protein antibodies. Thus, I felt it was important to pursue this question further. Secondly, although immunoelectrophoresis experiments showed that the antigenicity of the coat protein in the phage and its prohead precursor particle was very similar, there was also evidence for a set of unique gp5 determinants on proheads. These apparently became unavailable during maturation of the virus capsid. I was interested to see whether these unique capsid determinants might be

located at a limited number of sites on the prohead, such as those which give rise to the vertices of the viral icosahedral head, for example.

Using high resolution transmission electron microscopy and simple negative staining techniques, antibodies bound to phage structures can be visualized directly as fine, hair-like projections extending from the positions of the target antigens (M. Yanagida and C. Ahmad-Zadeh, 1970; S. Casjens and R. Hendrix, 1974; M. Tosi and Anderson, 1973). Thus, once the antisera have been characterized, electron microscopy of antibody-coated particles provides a method for determining the location of known antigenic proteins on the structures.

A. Experimental Approach

Rather than examining the binding of antibody molecules to each of the various classes of purified phage structures separately, I prepared a mixture of P22 proheads, phage, tail-less heads, and spirals (from 8⁻ infections provided by W. Earnshaw). The mixture also contained purified T4 phage (provided by Dr. P. Berget) as a negative control. This allowed me to examine on the same sample grid the specificity of antibody binding to several particle types at once. Electron micrographs of these mixtures are shown in Figure 33. Two phage are present in the upper right-hand corner of panel a. The phage carry small tail structures and the phage on the left shows a short, fine tail fiber projecting from the center of the tail. (The tail fiber, only occasionally visible, can be seen more clearly in the higher magnification electron micrograph of Figure 34.) A tail-less head is present in the center of the upper panel, showing the short neck and, vaguely, the projecting single

Figure 33Morphology of the Unreacted Antigen Mixture

(a) Electron micrograph of the negatively stained mixture of particles before incubation with antiserum. This antigen preparation, described in Materials and Methods, Section j, i and vi, includes P22 phage, proheads, and a tail-less head in the center of the micrograph. T4 phage are also present. The tail fibers of the T4 phage are in close proximity to the sheath in these experiments. The length of the T4 head, 100 nm, serves as an internal standard of measurement. Magnification is about 110,000 x.

(b) Electron micrograph of the negatively stained mixture as in (a), except that spiral structures are also present. The upper left aggregate of particles contains an empty shell structure which may represent one of the two aberrant shell classes contained in 8⁻ lysates. Note that the proheads in this figure exhibit inner dense material. Magnification about 110,000 x.

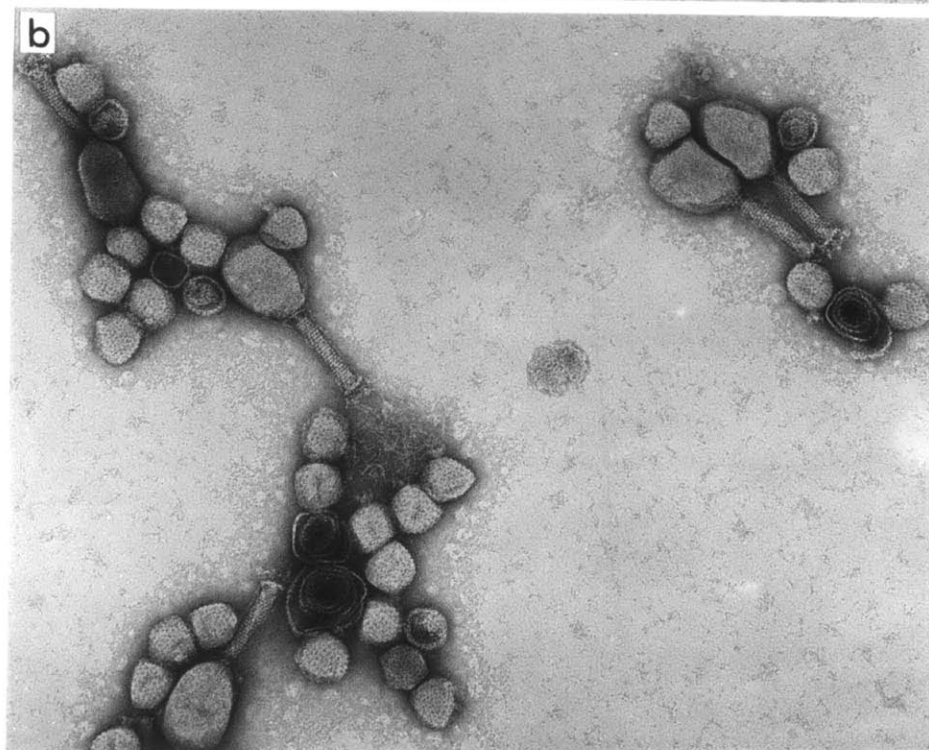
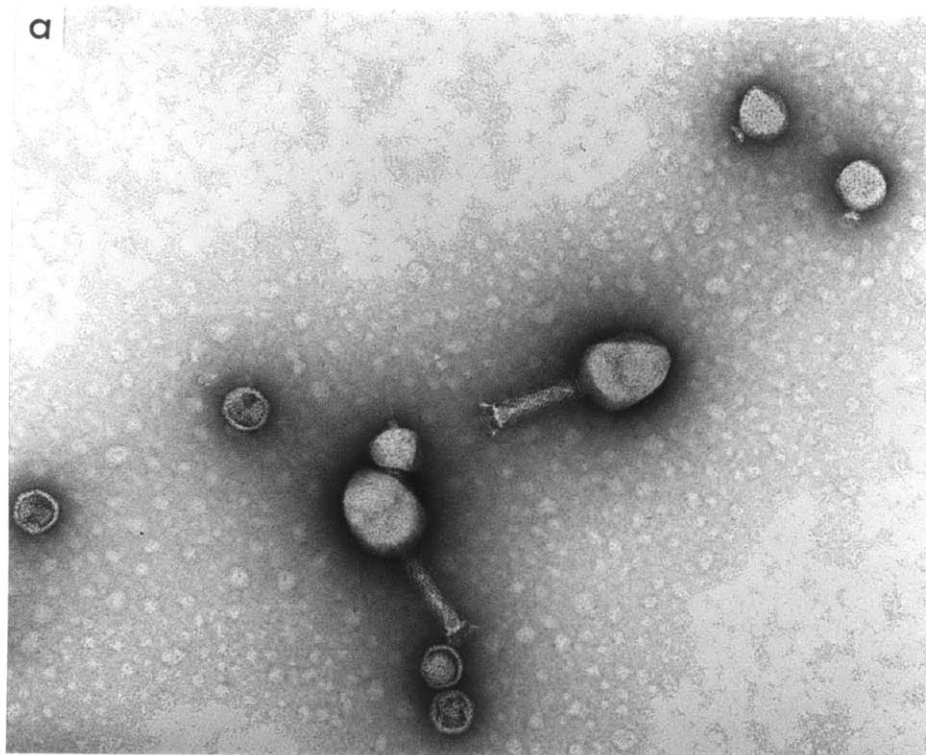


Figure 34

Morphology of the Tail and Neck Structures of P22 Phage

Electron micrograph of P22 phage which includes a tail-less head. The morphology of the phage tail and neck structure and fiber are particularly clear in the phage and tail-less heads which are in contact in the central area of the figure. Preparation and purification of the phage are described in Materials and Methods, Section j, i, 1.



fiber. Proheads are easily distinguishable by the partial penetration of stain which defines the outer shell and the inner stain-excluding scaffolding protein. The lower panel (b) shows a field with a number of spiral structures, also clearly distinguishable from both proheads and phage.

The experimental protocol in these experiments was as follows: First, the structures in the mixture were absorbed to electron microscope grids prior to their incubation with the antisera. Unabsorbed particles were washed off. Particles were incubated with antiserum by simply inverting the grids onto a drop of antiserum for 15 minutes or more at room temperature. Incubation was terminated by washing off the unreacted antiserum. Finally, the samples were stained according to standard negative staining procedures.

There are several advantages and disadvantages to this method. First, it is simple and efficient. By using a mixture of particles, one obtains many pieces of data from a single grid. Furthermore, the presence of experimental and control particles on the same grid facilitates their direct comparison. Of course, using this procedure, one must be able to identify the particles according to their morphology even after antiserum incubation. Pilot experiments showed that this was not a problem except, perhaps, in distinguishing antibody-coated empty heads from coated proheads. However, empty heads were not intentionally added to antigen mixture and would have been present only as contaminants of the prohead preparation or as phage breakdown products. Therefore, they represented only a small source of error. A second advantage is that a large number of antibodies can bind to the particles without causing their

aggregation because the particles have been previously absorbed to the electron microscope grid. However, in this procedure, unreacted antibody molecules also bind to the grid. Thus, all detail must be viewed against a protein saturated background, which actually appears granular. In addition, I found that particles in the mixture would desorb from the grid during incubation on the antiserum drop, unless the antiserum involved was specifically directed against that sort of particle. In fact, this actually worked to my advantage as this became a sort of assay for residual antibody activity. This effect is illustrated in the following experiments.

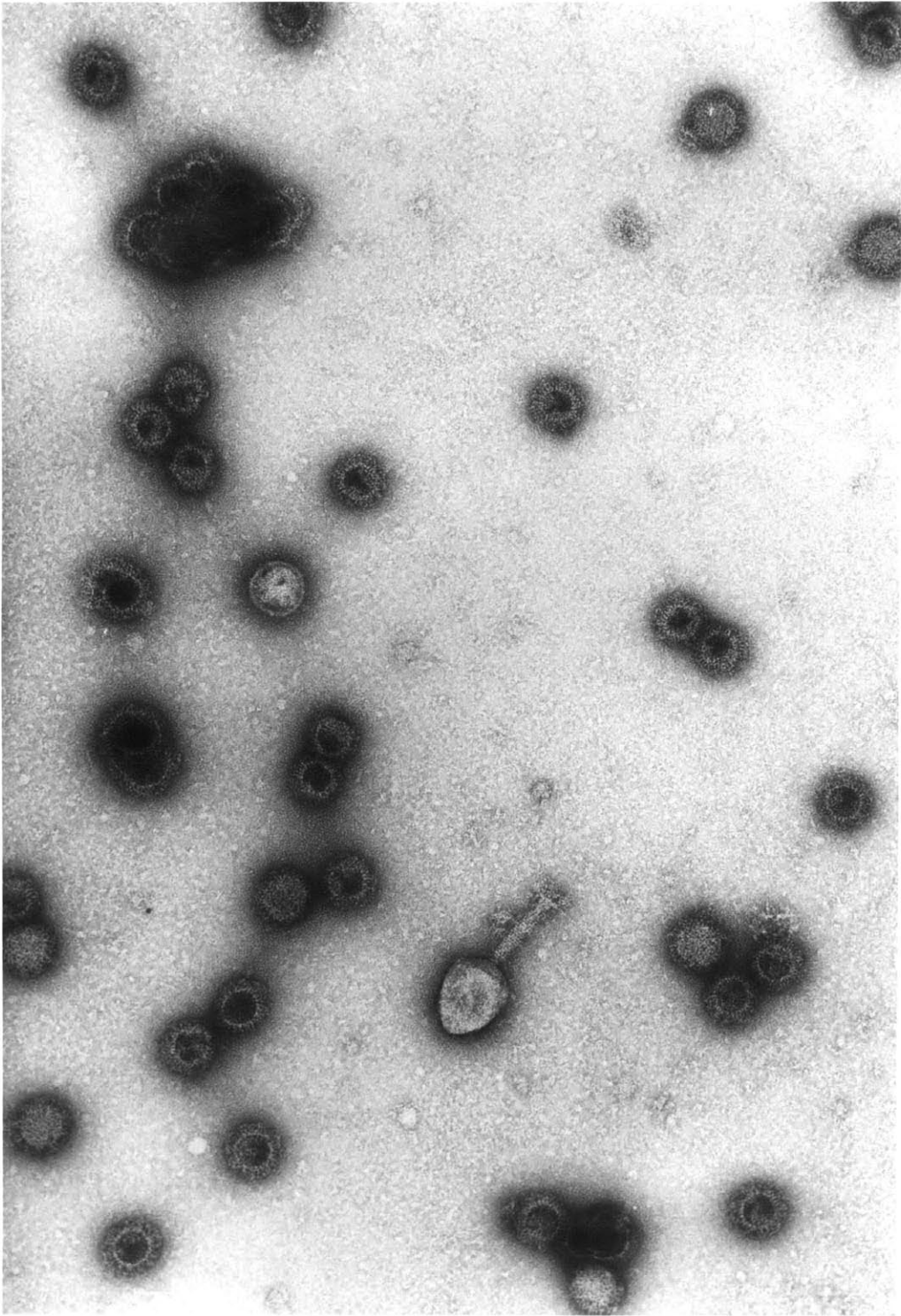
B. Coating of Particles by Anti-phage Serum

1. Whole serum

Immunoelectrophoresis experiments showed that anti-phage serum precipitated phage and proheads. Figure 35 shows the appearance in the electron microscope of these particles after reaction with anti-phage serum. The stain-excluding P22 phage particles are coated with fine hair-like appendages having the dimensions and appearance typical of bound antibodies (Yanagida and Ahmad-Zadeh, 1970; Casjens and Hendrix, 1974). Proheads appear as dark spheres and are also antibody-coated. The coated proheads do not seem to exclude the stain as strongly as uncoated proheads, as if there is some rearrangement of the inner proteins. The outside surfaces of spiral structures also appear coated. The edges of all these particles are easily distinguished from the well-defined boundaries of the corresponding uncoated particles in Figure 33 or the sharp edges of the T4 phage on the same grid. The T4 phage served as a negative control and showed that the antiserum was specific

Figure 35Specific Coating of P22 Particles by Anti-P22 Phage
Serum

Electron micrograph of the antigen mixture after incubation with anti-P22 phage serum showing antibody coating of the P22 particles. Note the fine, hair-like extensions at the edges of the P22 phage, proheads and spirals which are missing from the T4 phage. The large, round dense object in the left central portion of the figure probably represents a membrane component.



for P22 phage.

The coating of phage tails by anti-gp9 antibodies is not obvious. However, the phage tail protrudes from the capsid only by about the length of the antibody molecules themselves. The reaction of phage tails with anti-gp9 antibodies does become visible in the absence of anti-capsid antibodies as shown in the following experiment.

2. Prohead-absorbed anti-phage serum

The immunoelectrophoresis results using anti-phage serum suggested that all of the coat protein determinants on phage were also present on proheads. To test this, I absorbed anti-phage serum with proheads. I expected that this absorption would eliminate coating of both the phage and prohead shells but leave the phage tails specifically coated. The results of such an experiment are shown in Figures 36 and 37.

I was surprised to find that, in general, only phage particles were present on the grids even though I applied the identical mixture of structures as used in Figure 35. Occasionally, proheads and spirals were present, as in the rarer fields shown in Figure 37, but there were virtually no T4 phage. According to the rationale previously discussed, I have interpreted these observations to mean that all the antibodies reactive with proheads and spirals have been absorbed. As expected, on the other hand, prohead absorption apparently has left behind anti-gp9 antibodies which bind to the phage tail and aid its adherence to the grid.

As shown in Figures 36 and 37, the antibody-coated phage tails appear as rather indefinite but substantial extensions of the phage capsids (see arrows). Although phage tails which have not been incubated with serum may occasionally have a somewhat disordered character, in general, they

Figure 36

Absence of Coating Other than of Phage Tails
by Prohead-absorbed Anti-phage Serum

Electron micrograph of the antigen mixture after incubation with prohead-absorbed anti-phage serum. Note that the field contains almost exclusively phage particles. Arrows point to phage tails whose morphology have been visibly altered by antiserum incubation. The phage (top) and prohead (bottom) capsids at the extreme right of the figure show some evidence of coating, indicating that the serum may not be fully absorbed. Most of the capsids of the phage, however, appear antibody-free. Magnification about 110,000 x.

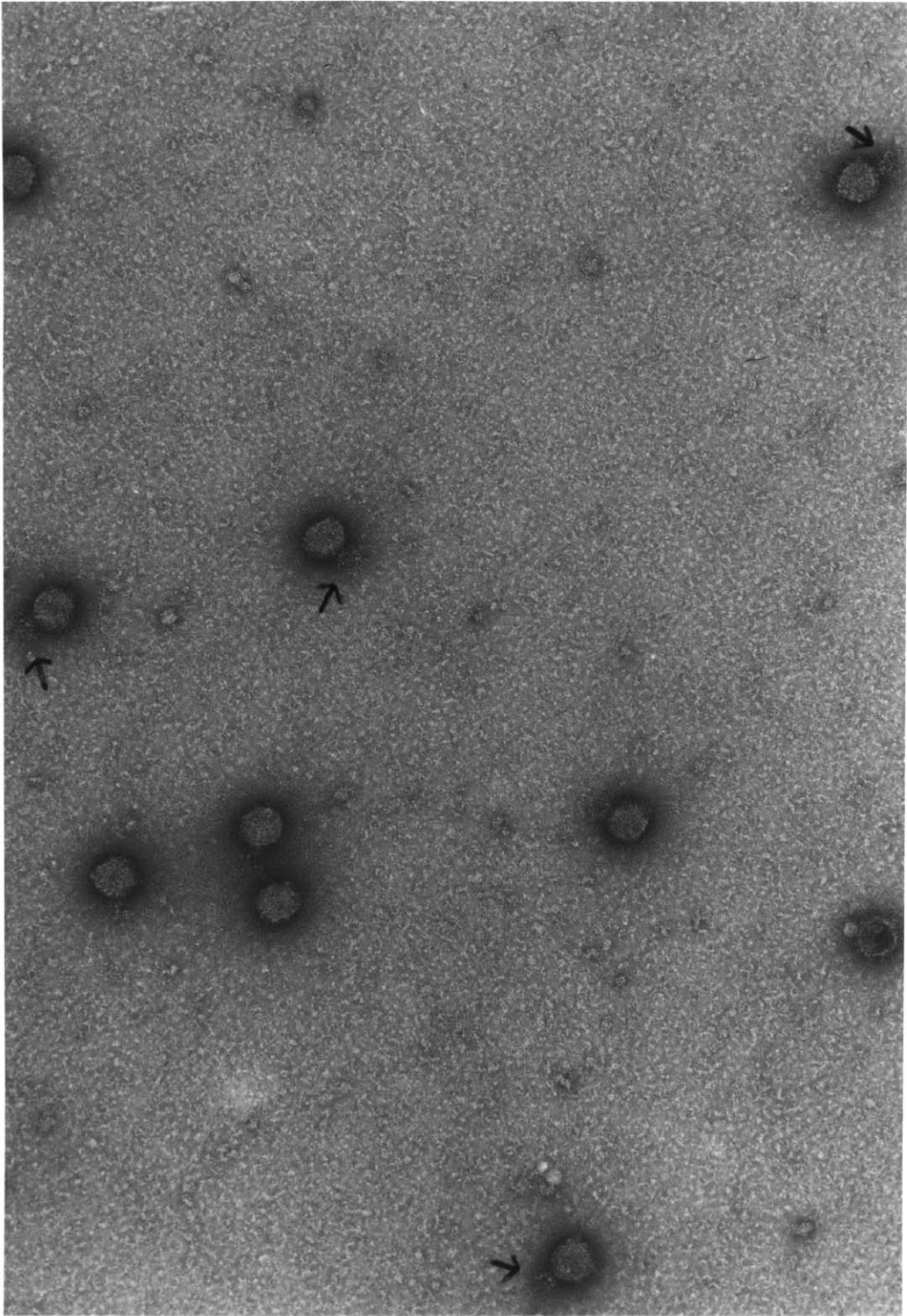
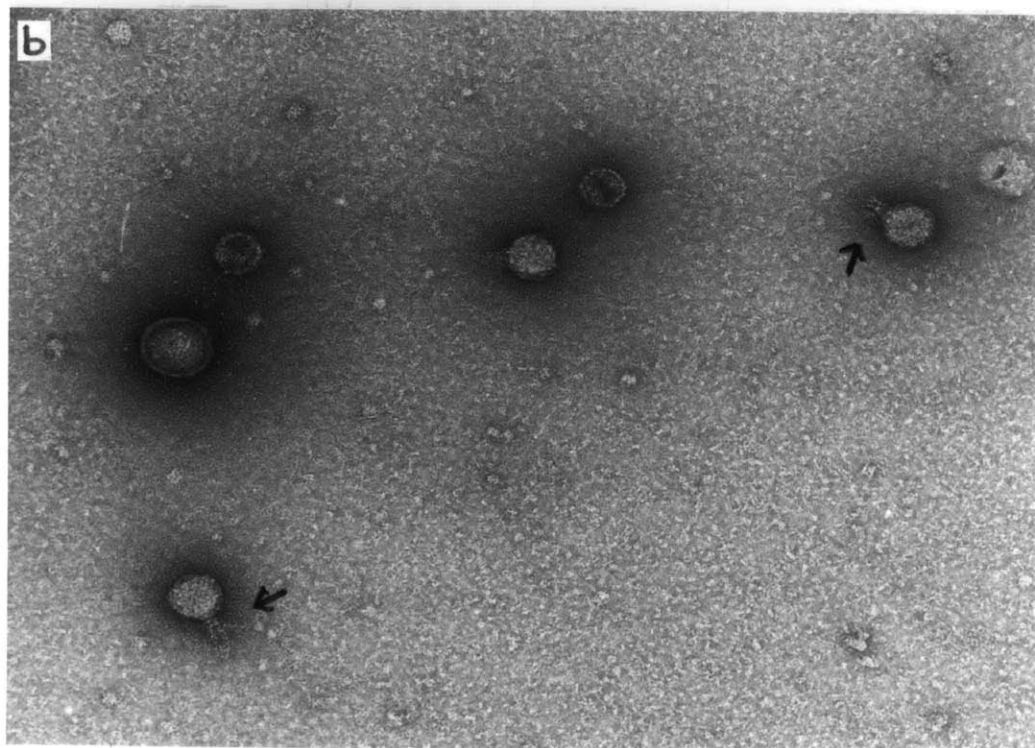
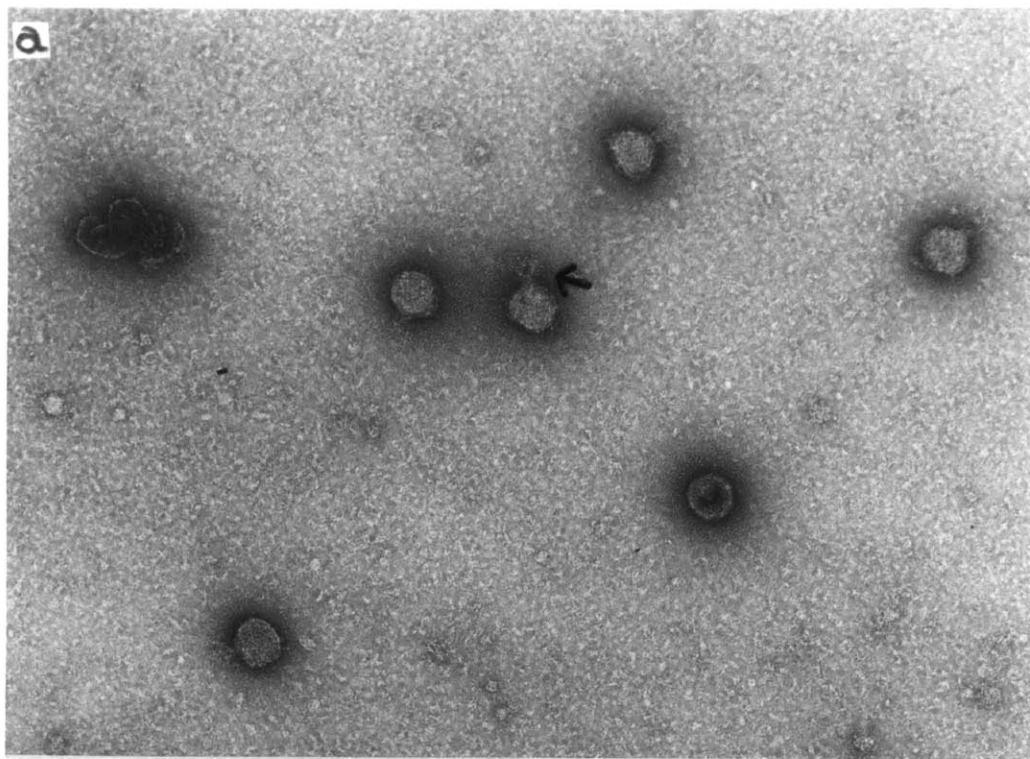


Figure 37

Absence of Coating of P22 Spirals and Proheads
by Prohead-absorbed Anti-phage Serum

(a) Electron micrograph of antigen mixture in the prohead-absorbed anti-phage serum showing absence of antibody coating of the P22 spiral. Arrow points to phage tail amplified by antibody coating. Magnification about 110,000 x.

(b) Electron micrograph of antigen mixture as in (a) showing the absence of antibody coating of the proheads by prohead-absorbed anti-phage serum, showing that the serum is, at least, substantially absorbed. Arrows point to representative examples of antibody-coated tails. Magnification about 110,000 x.



are almost always shorter, denser, and more resolved than tails treated with prohead-absorbed anti-phage serum. Note that antibody-coated tails are difficult to see even in the absence of anti-capsid antibodies; this explains, in Figure 35 for example, why antibody-coated tails were not more obvious in the reaction of phage with whole serum.

The most significant feature of these experimental results is the absence of coating on the shells of the phage particles. Thus, prohead absorption removes all anti-gp5 antibodies from the serum. This confirms the earlier result that all gp5 antigenic determinants present in the capsid of the phage are also present in the precursor prohead shell.

C. Coating of Particles by Anti-prohead Serum

1. Whole serum

Results from immunoelectrophoresis experiments showed that anti-prohead serum precipitated proheads and phage. Reaction of the particle mixture with anti-prohead serum as seen in the electron microscope is shown in Figure 38. The appearance of the particle is basically the same as particles which had been reacted with anti-phage serum (Figure 35). P22 proheads, phage and spirals are coated with antibody; T4 phage are not. The antibody-coated proheads in this experiment appear fully penetrated by stain.

Thus, antibodies made against proheads specifically coat P22 phage, proheads and spirals. The specificity of these reactions is investigated in the following experiments.

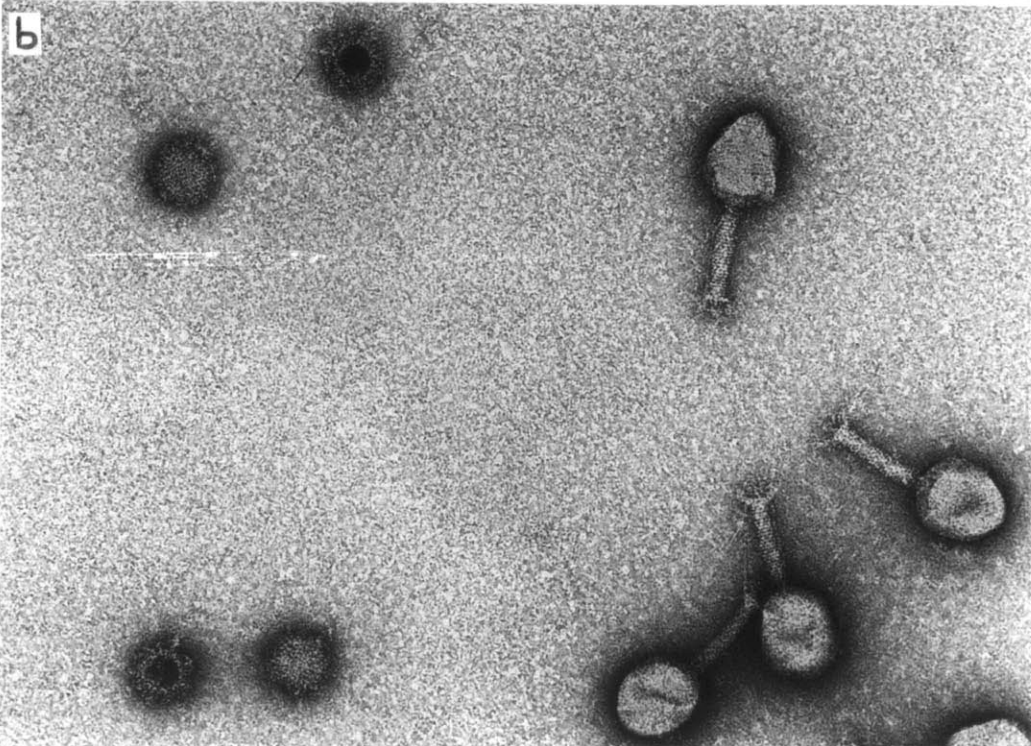
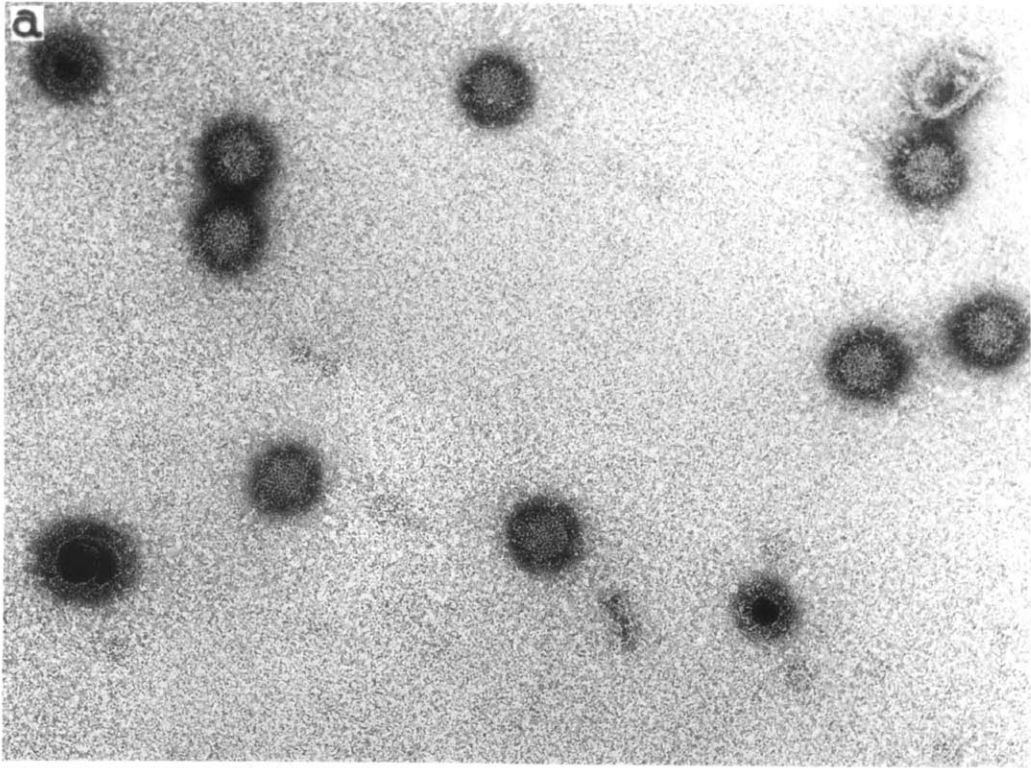
2. Phage-absorbed serum

Exhaustive absorption of anti-prohead serum by phage should remove most of the anti-coat protein antibodies from the serum. From the

Figure 38

Specific Coating of P22 Particles by Anti-P22 Prohead Serum

(a) Electron micrograph of the antigen mixture after reaction with anti-P22 prohead serum. Phage, proheads and the spirals are coated with antibodies. Magnification about 110,000 x. (b) Electron micrograph of antigen mixture as in (a) except that the absence of T4 phage coating by the antibody shows the P22 specificity of the serum.



immuno-electrophoretic results the remaining antibody should be primarily anti-scaffolding protein, and antibody directed against coat protein determinants only found on proheads. The standard mixture was treated with phage-absorbed anti-prohead serum, and the results are shown in Figure 39.

Again in this experiment, the number of particles present on the grids was substantially lower in the case of particle-absorbed serum than with whole serum. In this experiment, T4 phage could be found on the grids, though few in number. Wherever possible, these fields containing T4 phage were used for electron micrographs, which is why T4 phage appear in each micrograph in Figure 39. A few P22 phage were also present on the grids. Relative to T4 and P22 phage, spirals were present in significant numbers. Proheads formed the largest class of particles on the grids. This distribution of particles is consistent with the expected levels of residual antibody activity, given that the more that antibodies are present against a particular particle class, the more likely these particles are to stick to the grid.

As shown in Figure 39, the phage particles are not coated, as expected since the serum is fully phage-absorbed. Antibody coating of the proheads is substantially reduced, compared to the amount of coating produced by whole anti-prohead serum at the same dilution (see Figure 38). The reduced amount of coating is significant, however, when compared with the relatively antibody-free T4 and P22 control phage in the same field. The coating was increased specifically by incubation with more concentrated serum (see Figure 40, for example). Therefore,

Figure 39

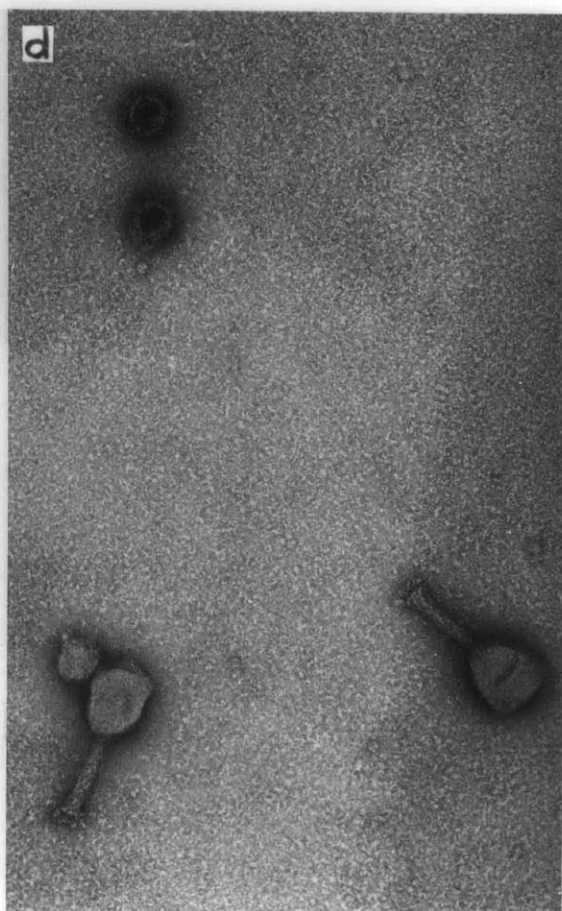
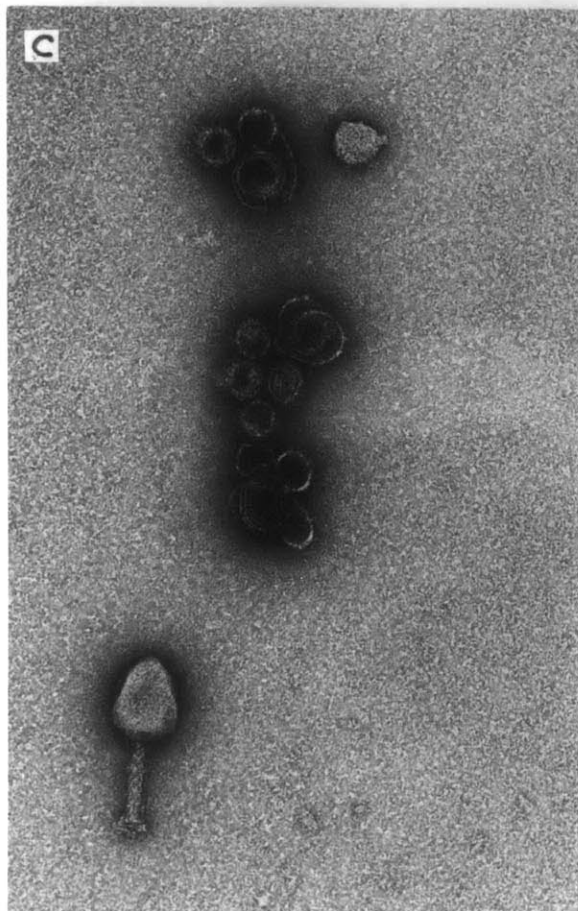
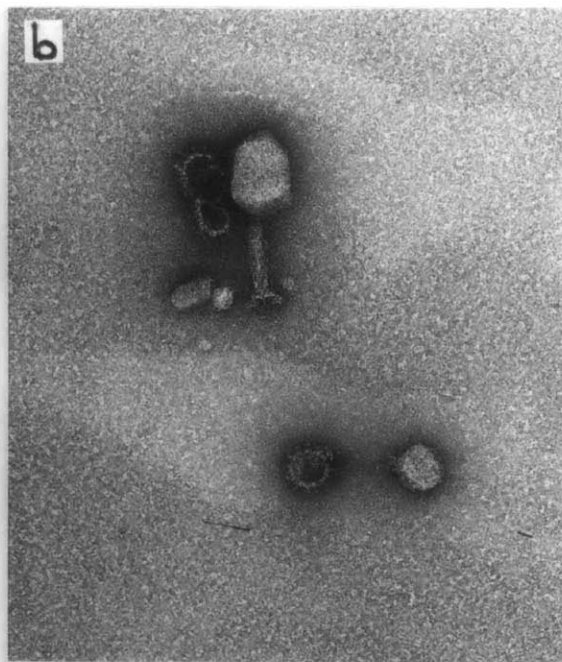
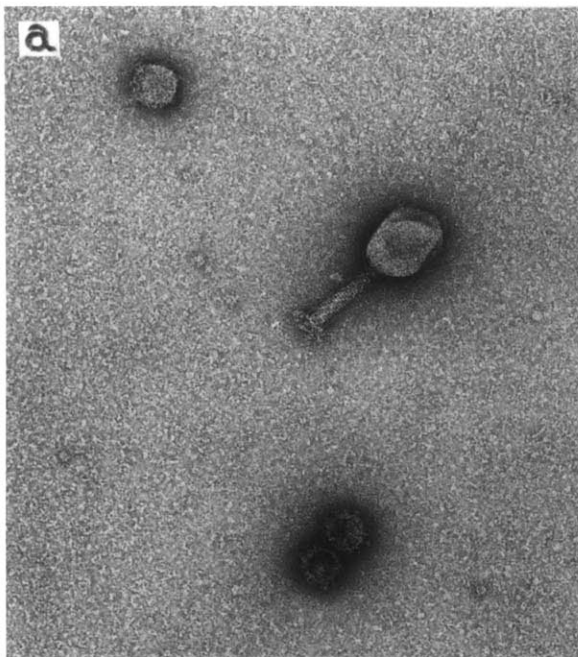
Coating of Proheads by Phage-absorbed Anti-Prohead Serum

(a) Electron micrograph of antigen mixture after reaction with phage-absorbed anti-prohead serum. Note that P22 phage is uncoated showing that the serum has been fully absorbed with phage. The proheads in this panel are clearly antibody-coated.

(b) Electron micrograph of antigen mixture as in (a) except for the presence of a spiral structure. This spiral appears to be coated with antibody on its upper edge. As such, it is representative of a minority class of the spirals which reacts with the residual antibodies of the phage-absorbed anti-prohead serum. The prohead in this panel clearly shows antibody binding.

(c) Electron micrographs as in (a) and (b). The spirals in this panel appear antibody-free and these are representative of the antibody-binding characteristics of the majority of the spirals. The proheads are not so clearly coated with antibody as in panel (a) and (b) but for some their edges do appear somewhat more indefinite than in unreacted proheads.

(d) Electron micrograph as in (a) - (c). The level of coating of these proheads in this panel is detectable but lower than in panels (a) and (b).



these results show that, as predicted, absorption of anti-prohead serum with phage removed a large fraction of the prohead-coating antibodies. A smaller residual antibody fraction continued to coat proheads after absorption and this presumably included anti-gp8 antibodies.

The coating of the spirals in this experiment is rather interesting. Most of the spirals examined did not show detectable antibody binding. However, there seemed to be a smaller population of spirals (roughly 15%) which were coated by a small but significant number of antibodies. The coating of the spiral in panel b is representative of the appearance of this fraction. Indications that there might be two populations of spirals were also present in previous immunoelectrophoresis experiments (see Figure 27a). One class of spirals appears to be antigenically identical to phage; a second, smaller class seems to be antigenically related to proheads in a way that phage are not. As the spirals in both the immunoelectrophoresis and the electron microscopy experiments were made from an 8⁻amH202 lysate, it's possible that a small number of spirals carried an antigenic gp8 fragment. Thus, such spirals would be precipitated by the prohead-specific antibodies in the anti-prohead serum. However, immunoelectrophoresis experiments suggested that anti-prohead serum contained a fraction of anti-gp5 antibodies that recognized capsid determinants unique to proheads (see Figure 18b). It may be, then, that gp5 in spirals is in one of two states: in one form, representing the major class, gp5 resembles the mature form found in the phage capsid; in the other, gp5 displays an additional set of sites such as those found on proheads. In this model,

it is these prohead-specific gp5 determinants which lead to coating of spirals by phage-absorbed anti-prohead serum.

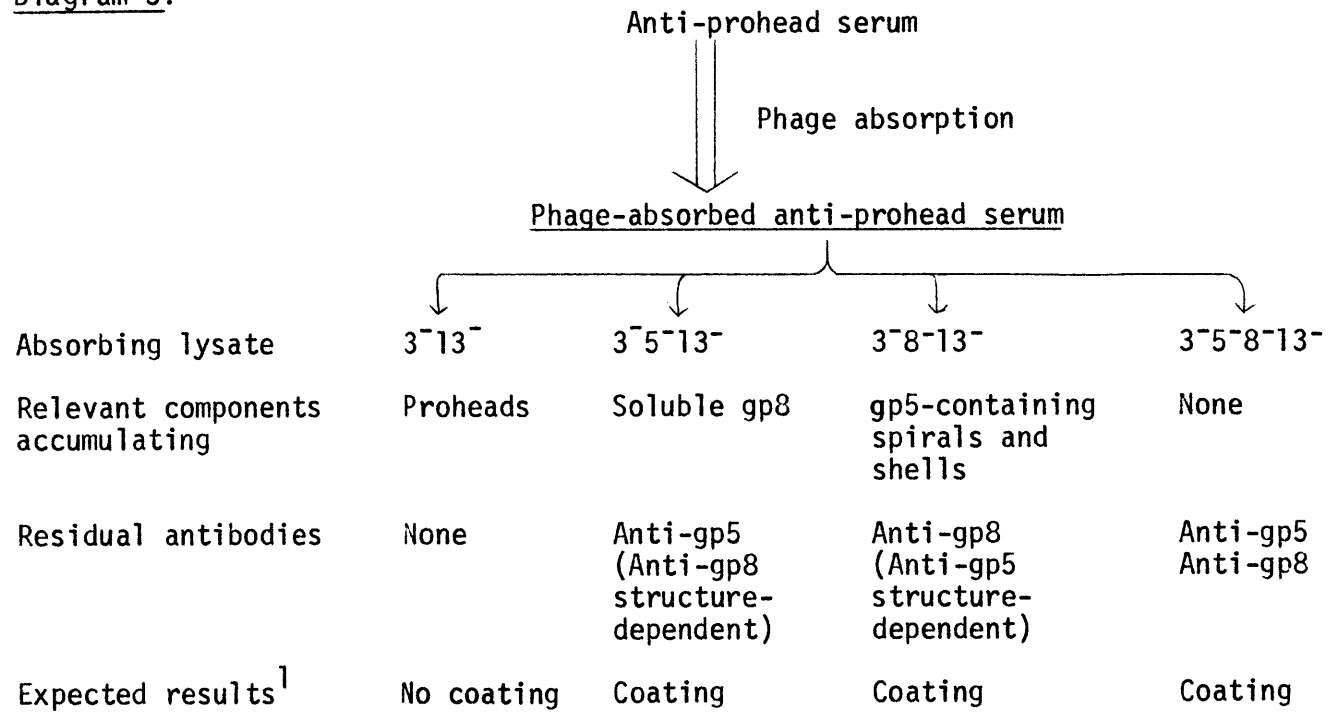
In summary, the antibodies in phage-absorbed anti-prohead serum which coat proheads are likely to be, in large part, directed against the scaffolding protein. However, it is not possible from this experiment alone to exclude the possibility that these antibody molecules are directed against gp5 capsid determinants which are found only in proheads. Coating of a fraction of the spirals by the phage-absorbed serum may also be explained by either model. To sort out these possibilities, I further absorbed the phage-absorbed anti-prohead serum with amber mutant lysates. This experiment is presented in detail below.

3. Lysate-absorbed serum

In these experiments, I attempted to genetically identify the antibody classes responsible for the coating of proheads by phage-absorbed serum. Results from previous immunoelectrophoresis experiments suggest that the prohead coating observed in the electron microscope is probably caused by the reaction of residual antibody fractions with accessible gp8 subunits (see Figures 28 and 30) and prohead-specific gp5 capsid determinants (see Figure 18b). To separate the anti-gp8 and prohead-specific anti-gp5 classes from one another, I further absorbed the phage-absorbed anti-prohead serum with phage amber mutant lysates. The protocol and rationale used for the serum absorption are outlined in Diagram 3.

First, I used several aliquots of purified phage to completely absorb a large pool of anti-prohead serum. This supplied the starting material, phage-absorbed anti-prohead serum. The phage-absorbed serum

Diagram 3:



¹ From previous immunoelectrophoresis experiments.

was divided into four aliquots to be absorbed with four different, concentrated lysate preparations: $3^{-}13^{-}$, $3^{-}5^{-}13^{-}$, $3^{-}8^{-}13^{-}$, and $3^{-}5^{-}8^{-}13^{-}$ lysates. (The 13^{-} mutation is not relevant to these discussions and I will no longer refer to it).

(a) Immuno-electrophoresis of absorbing lysates

The antigenic composition of these lysates was analyzed by immuno-electrophoresis and the results are shown in Figure 40. Panels a and d show, using whole anti-prohead serum, the immuno-electrophoretic patterns of the starting lysates, which were 200-fold concentrated serum. The 3^{-} lysate, in the central section of panel a, contains both soluble gp8, which results in the dense, outer precipitin arc, and pro-heads, which yield the inner, very dense precipitates (see Chapter II for the identification of precipitin arcs). When gp5 is effectively deleted from this lysate by mutation, as in the $3^{-}5^{-}$ lysate in the lower section of panel a, the structure-related precipitin arcs disappear while the soluble gp8 continues to be precipitated. Deletion of gp8 from a 3^{-} lysate by mutation removes the soluble gp8 band, but the dense arcs caused by the aberrant gp5 aggregates present in the lysate persist, as shown in the central section of panel d. No gp8 amber fragment band is detectable, as expected, because the lysate was made by an infecting phage carrying the $8^{-}\underline{am}N123$ allele.

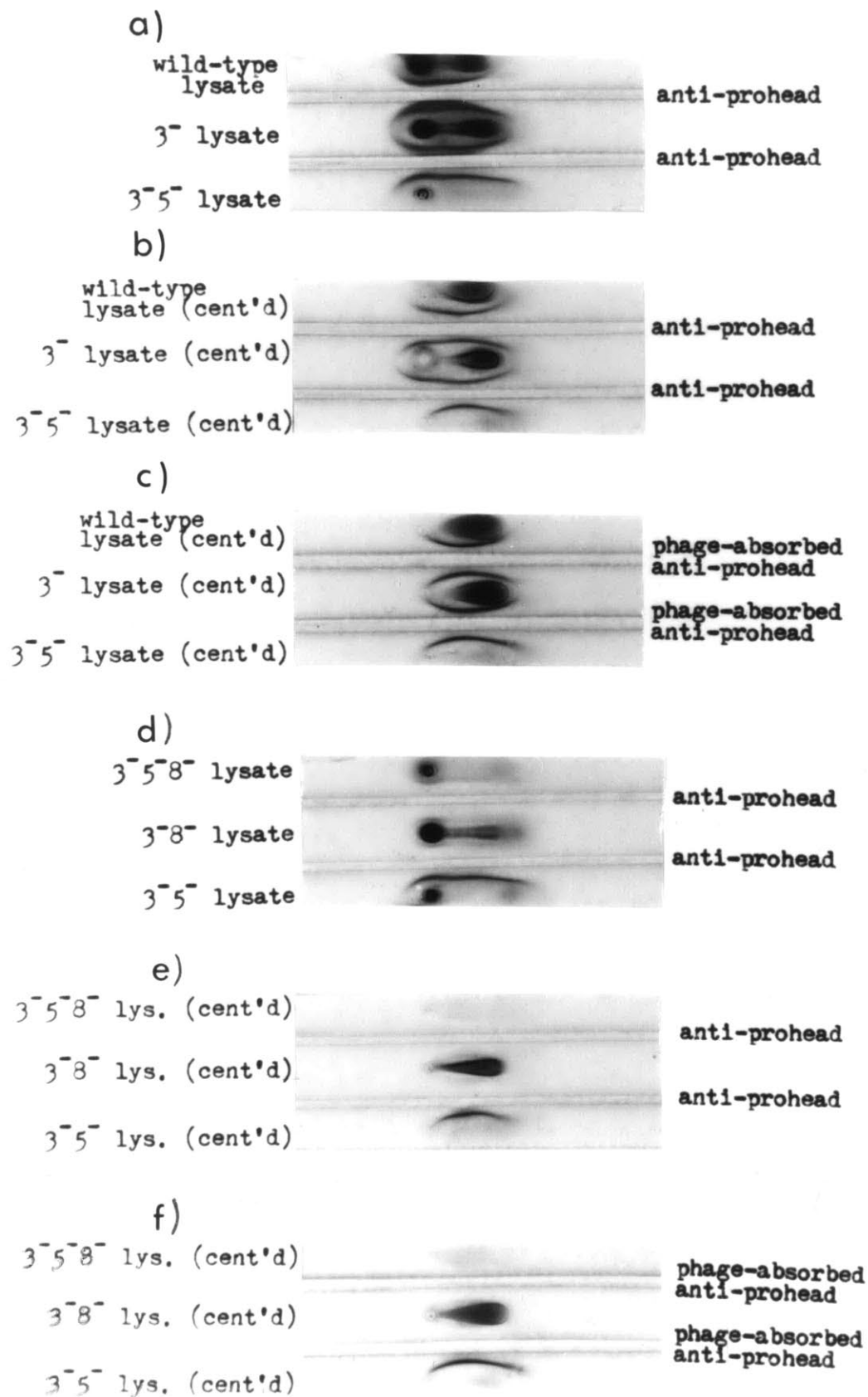
Prior to serum absorption, the lysates were centrifuged to remove rapidly sedimenting material which would contribute to background interference in the electron microscopic observation of the serum-containing samples. The effect of centrifugation on the antigenic components was examined in panels b and c. Centrifugation mainly removed gp5-dependent reactions from directly around the antigen wells. Presumably, either the

Figure 40

Immuno-electrophoresis of Lysates Used for
Absorption in Electron Microscopy Experiments

Antisera and lysates have been described in Materials and Methods, Section j, ii, 1, and iv, and Section j, iii, respectively. Immuno-electrophoresis was as described in the figure legend to Figure 17 and in Materials and Methods, Section i, iii.

(a) and (d) Immuno-electrophoresis using whole anti-prohead serum of the absorbing lysates and a wild-type control lysate before lysate centrifugation. (b) and (e) Immuno-electrophoresis using whole anti-prohead serum of the absorbing lysates and wild-type lysate after lysate centrifugation. Note that reactions immediately around the antigen well are removed by lysate centrifugation. (c) and (f) Immuno-electrophoresis of centrifuged, absorbing lysates and wild-type lysate using the phage-absorbed serum used in the electron microscopy experiments. Of particular interest is the fact that the aberrant aggregates of gp5 contained in the 3⁻⁸ lysate in the central section of panel f continue to be precipitated by the serum after phage-absorption.



gp5 itself was removed through association with rapidly sedimenting material, or the sedimentation of large lysate components released the gp5-containing structures from some complex which was electrophoretically retarded. The latter seems to be the case for the structures in the 3⁻8⁻ lysate in panel e where some of the density around the antigen well seems to have shifted to the typical structure position as a result of lysate centrifugation.

Finally, the lysates were immunoelectrophoresed against phage-absorbed serum to reconstruct the actual conditions which existed during lysate absorption of the serum for the electron microscopy experiments. As expected, the precipitation of gp8 is relatively unaffected by the absorption of the serum with phage, as shown in panel c and the bottom of panel f. The proheads in the 3⁻ lysate in panel c also continue to be precipitated; however, phage-absorption has obviously reduced the number of anti-capsid antibodies which are reactive because the prohead structures travel considerably farther before being precipitated. Perhaps the most important information from this set of experiments is shown in the central reaction of panel f. The aberrant aggregates of gp5 present in the 3⁻8⁻ lysate are precipitated by the phage-absorbed serum, although the number of antibodies participating in the reaction has been considerably reduced by the prior phage absorption. Thus, this absorption depletes the serum of at least a portion of the prohead-specific anti-gp5 antibodies. This experiment will be of importance in showing absorption of phage-absorbed serum with this 3⁻8⁻ lysate for the electron microscopy experiments reduced the concentration of the anti-capsid antibodies in the serum.

(b) Rationale of the lysate absorptions

Having characterized the antigenicity of the lysate components in reaction with phage-absorbed anti-prohead serum, we can predict the residual antibody activity which should remain after lysate-absorption, as illustrated in Diagram 3. One aliquot of the serum, absorbed with a 3^{13} lysate, served as the negative control. The prohead structures in this lysate which have been shown to react with the phage-absorbed serum (Figure 40c) should remove all of the antibodies directed against proheads. Thus, proheads reacted with this absorbed serum should not appear coated when examined in the electron microscope.

Another aliquot of phage-absorbed serum was incubated with a 3^{58} lysate to serve as the positive control. The lysates were centrifuged prior to their use as absorbing antigens, and SDS-gel electrophoresis experiments have shown that, typically, the gp5 amber fragment pellets quantitatively with the debris (data not shown). In addition, no gp8 amber fragment was detected in this lysate by immunoelectrophoresis (see Figure 40f). Therefore, absorption of phage-absorbed serum with a 3^{58} lysate should leave all anti-gp5 and anti-gp8 antibodies active; prohead coating by this serum should approximate that of the starting material, phage-absorbed serum.

The absorptions of prime interest involved the 3^{5} and 3^{8} lysates. As discussed for the 3^{58} lysate above, the 3^{5} lysate totally lacks gp5; however, it contains soluble antigenic gp8, as shown in Figure 40c and f. Therefore, incubation of the serum with a 3^{5} lysate should remove the anti-gp8 antibodies, but leave behind prohead-specific anti-capsid antibodies as shown in Diagram 3.

In the converse experiment, I absorbed the serum with a 3⁻⁸ lysate. As shown by immunoelectrophoresis, (see Figure 40 d-f) the lysate did not contain a detectable gp8 fragment. However, the gp5-containing structures in this lysate do react with the phage-absorbed serum. Thus, absorption of phage-absorbed anti-prohead serum with a 3⁻⁸ lysate should remove anti-capsid antibodies, but leave behind anti-gp8 antibodies.

I have described the absorption of phage-absorbed anti-prohead serum with a 3⁻⁸ lysate and a 3⁻⁵ lysate as a means of separating anti-gp8 antibodies from prohead-specific anti-gp5 antibodies. The discussion has been somewhat oversimplified, however. As always in using mutant lysate absorptions to generate mono-specific sera, there is the assumption that the form of the antigen in the lysate can remove all of the antibodies which were generated against the protein when it existed in the structure. To the degree to which this is not true, absorption of the serum with a lysate will leave behind structure-specific antibodies. These are indicated in parentheses in Diagram 3. For example, the absorption of anti-gp8 antibodies by the soluble gp8 in the 3⁻⁵ lysate may leave behind a fraction of anti-gp8 antibodies which can be absorbed only by gp8 as it exists in the prohead structure. Thus, in this instance, binding of the unabsorbed structure-dependent anti-gp8 antibodies would contribute to the coating of proheads.

(c) Technical difficulties

Substantial technical difficulties were encountered with the experiment just described. First, it required large amounts of absorbing antigen. For example, to generate fully phage-absorbed serum required about 7×10^{14} phage/ml serum. To generate enough serum to divide up

into separate aliquots for lysate absorptions required almost 2×10^{15} phage total. Second, in adding equal volumes of concentrated lysates to the phage-absorbed serum at the lysate absorption step, I was also adding a complex mixture of heterogeneous material which contributed significantly to the background material against which the binding of very small, fine antibodies had to be distinguished. Even though I clarified the sera of particles of about the size of ribosomes by high speed centrifugation, there remained substantial particulate matter in the backgrounds. Third, the levels of coating that I obtained in the positive control samples after lysate absorption were always lower than I expected given the results of pilot experiments in which I simply diluted the phage-absorbed serum with buffer. This was presumably caused by non-specific precipitation occurring under the highly concentrated conditions of the absorptions. I was not able to directly compensate totally for this reduced antibody recovery by concentration of the absorbed serum, since this concentrated the background material as well. In the experiment presented here, a satisfactory balance was reached by concentrating the absorbed serum 10-fold. However, in a second larger experiment not shown, working with greater quantities of material, a 10-fold concentration of the serum increased the background material to unsatisfactory levels.

(d) Coating of particles by lysate-absorbed serum

1. Control sera

A gallery of particles from the antigen mixture as they appear after incubation with the four classes of absorbed sera are shown in Figure 41. Phage are presented in the left-most column. As the starting serum is fully phage-absorbed, these phage images serve as a

Figure 41Coating of Proheads by Lysate-absorbed,
Phage-absorbed Anti-prohead Sera

Electron micrograph of prohead coating by phage-absorbed anti-prohead sera which have been further absorbed with lysates as described in the text. The first column contains phage as negative controls. Spirals, in the second column, are also not coated. Column 3-8 contain proheads which have, in rows a-c, been roughly arranged in decreasing order of antibody coating.

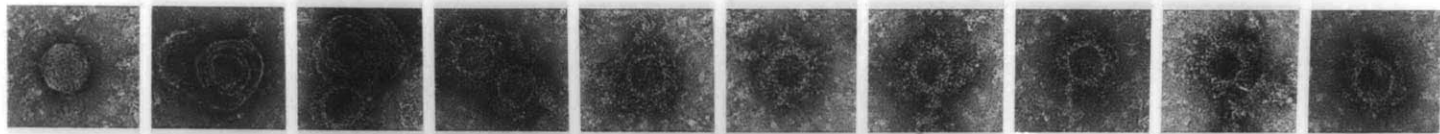
Row (a) Phage-absorbed serum containing anti-coat protein and anti-scaffolding protein coats proheads. The third panel contains both a spiral (top, uncoated) and a prohead (lower, coated).

Row (b) Coating of proheads by anti-scaffolding protein antibodies as discussed in the text.

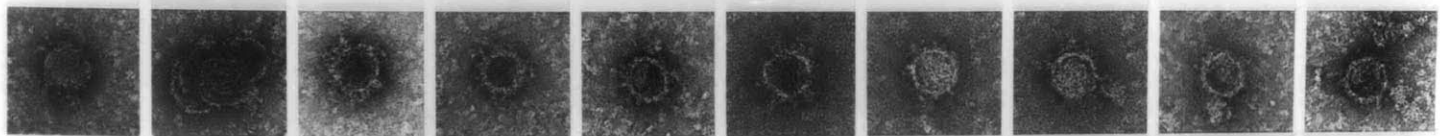
Row (c) Coating of proheads by prohead-specific anti-coat protein antibodies, as described in the text.

Row (d) Absence of prohead coating by phage-absorbed serum which has been absorbed with proheads.

a)



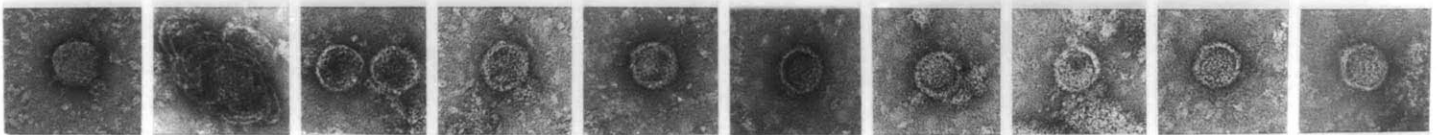
b)



c)



d)



negative control for coating. Spiral structures are shown in the second column. In general, these also were uncoated. This is to be expected as the sample population was small and previous electron microscopy experiments showed that about 15% of the spirals were coated by phage-absorbed serum. Finally, in columns 3-8, I show a progression of prohead structures arranged very roughly in order of my estimation of decreasing amounts of antibody coating.

The positive and negative controls for prohead coating, as discussed previously, are shown in the upper and lower rows, a and d. Although there is considerable background material, I think the difference in prohead coating between these two rows is clear and in the direction expected. The top row shows the coating of proheads which have been incubated with 3⁻5⁻8⁻ lysate-absorbed, phage-absorbed anti-prohead serum. Anti-gp5 and anti-gp8 antibodies should remain active after this absorption, as indicated in Diagram 3. As expected, then, the proheads from this antiserum incubation show a considerable amount of coating. The edges of the proheads show diffuse projections all about their surfaces. The coated proheads also display more internal stain indicating some rearrangement of the inner proteins.

In contrast to these proheads, the appearance of the proheads in the bottom row is much more nearly that typical of unreacted proheads. The proheads in the bottom row have been incubated with phage-absorbed serum that had been absorbed with a 3⁻ lysate. As this lysate accumulates proheads, all of the antibodies reactive against proheads have apparently been removed by absorption and thus, these proheads appear antibody-free. The edges of these particles are more clearly defined

and no rougher than those of untreated proheads. Only rarely are protrusions evident, and they are probably the result of the superposition of the particle edge over dense background material. Note also that these proheads resemble untreated proheads in that they are not penetrated by stain. Thus, despite the numerous technical difficulties described previously, antisera incubated with control lysates coated proheads in the expected manner.

2. 3⁻⁵ lysate absorbed serum

Now we ask: does phage-absorbed serum contain a prohead-specific class of anti-gp5 antibodies which will coat proheads? As illustrated in Diagram 3, the serum used as a probe in this experiment has been absorbed with a 3⁻⁵ lysate so that prohead-specific anti-capsid antibodies should be left behind. Structure-specific antibodies may be present as well. The residual coating activity of this serum against proheads is shown in row c. Although it is difficult to see small amounts of antibody coating against the rather granular background, after examining a number of proheads. I estimated that the level of prohead coating by this absorbed serum ranged from little to none at all. I have tried to arrange the proheads in a series which is representative of this range of coating, from a prohead on the left typical of the most coated particles in the preparation to ones on the right which appear antibody-free.

3. 3⁻⁸ lysate-absorbed serum

Immunoelectrophoresis experiments had suggested a most interesting result, that is, that scaffolding protein was accessible in proheads (see Figure 29). The experiment in row b shows the results of asking whether gp8 is ^{accessible} using electron micro-

scopy. As illustrated in Diagram 3, absorption of phage-absorbed anti-prohead serum with 3⁻⁸ lysate should leave behind anti-gp8 antibodies and possibly, structure-dependent anti-capsid antibodies as well. As shown in row b the proheads show a range of appearances from what I consider fairly well coated to sparsely coated. There were not any proheads which seemed to be totally antibody free and the general level of coating in this experiment was higher than that of the most coated proheads in the experiment of row c. The internal morphology of these particles was mixed, but the majority were fully penetrated by the stain.

4. Discussion

One question of primary importance which I wished to answer in this experiment was whether gp8 determinants were accessible in the prohead structure. This problem is best approached through a comparison of the results of the absorption of the serum by the 3⁻⁵ and 3⁻⁸ lysates. Absorption of the serum with a 3⁻⁵ lysate established the maximal level of coating which can be produced by the binding of prohead-specific anti-gp5 antibodies. Immunoelectrophoresis experiments showed that at least some of these anti-capsid antibodies could be removed by the gp5 aggregates in the 3⁻⁸ lysate. Therefore, since the level of prohead coating was greater using serum that had been absorbed with a 3⁻⁸ lysate as opposed to a 3⁻⁵ lysate, another set of antibodies must be involved. Given the genetic constitutions of the absorbing lysates, the observed prohead coating by 3⁻⁸ lysate-absorbed, phage-absorbed serum is most probably the result of anti-gp8: gp8 interactions. At the least, prohead coating by this serum is caused by a combination of anti-gp8 and structure-

dependent anti-capsid antibodies. Thus, this experiment leads to same conclusion as did several immunoelectrophoresis experiments; that is, gp8 as it exists in the prohead structure is accessible to reaction with anti-gp8 antibodies in the environment.

There are two interpretations of these data possible at the molecular level. The first and simpler hypothesis is that gp8 is normally exposed at the surface of the prohead. Clearly, there must be direct interaction of the gp8 molecule with the capsid subunits to direct the assembly of gp5 subunits into a shell of the proper dimensions. Perhaps the capsid and scaffolding proteins retain their association at the surface of the completed shell. Such extensions of the gp8 molecule into the outer capsid shell may facilitate its exit during DNA packaging.

Alternatively, in a more complicated scheme, binding of anti-capsid antibodies to the outer shell may cause a rearrangement of the capsid subunits. In analogy to the in vivo situation, these changes in gp5 may trigger the movement of gp8 out of the capsid shell where upon it becomes trapped at the surface. According to this hypothesis, then, gp8 exits through the coat proteins lattice during virus maturation, and we are observing an intermediate stage in this process. For this hypothesis to be true, absorption of the phage-absorbed serum with 3⁻⁸ lysate must leave behind a sufficient population of anti-capsid antibodies to induce this conformational change, which is possible. Also the model predicts that the internal material visible in proheads by electron microscopy, the scaffolding protein, will be disrupted by the antibody binding. Proheads which have been reacted with antiserum always appeared emptier

than control proheads. This re-arrangement seemed to require a certain minimal number of antibodies. For example, in Figure 38, reaction of the proheads with whole anti-prohead serum seems to result in very empty-looking proheads. After absorption of this serum with phage, proheads coated by the residual antibodies, present in lower concentration, appear somewhat fuller, as in Figure 39. However, ten-fold concentration of this phage-absorbed serum, which is effectively the case in the positive control series in Figure 41 (row a) seems to render the prohead again relatively empty-looking. The proheads in row b of Figure 41 also appear mostly empty, that is until the level of coating drops to that shown by 3^{-5} lysate-absorbed phage-absorbed anti-prohead serum. From this point on, the proheads maintain a somewhat full appearance. The question of the appearance of proheads reacted with the anti-capsid antibodies of anti-phage serum is interesting. Although it was possible that only prohead-specific anti-capsid antibodies would release gp8, in fact, a number of proheads which have been reacted with anti-phage serum also appear empty (see Figure 35).

Either interpretation leads to an interesting conclusion about prohead structure. Either the scaffolding protein is normally exposed on the prohead; or, reaction of the coat protein with antibody induces release of the scaffolding protein through the capsid lattice, presumably reflecting its passage out of the capsid shell in vivo.

The second general question addressed by these experiments was the existence and location of prohead-specific coat protein deter-

minants. These were detected by absorption of phage-absorbed anti-prohead serum with a 3⁻⁵ lysate. This serum absorption left behind a fraction of antibodies which coated the prohead surface indicating that prohead-specific gp5 determinants did indeed exist. Although the low resolution of the data precludes any statements about the precise location of the antibodies, they appeared to be distributed over the entire capsid shell.

Thus, a set of coat protein determinants appears to be exposed uniformly at the surface of the proheads but unavailable on the phage. In the simplest interpretation of these results, one can assume that the capsid subunits change their conformation during the prohead-to-phage transition in such a way that the prohead-specific gp5 determinants become buried. X-ray diffraction studies of proheads and phage have showed that the prohead precursor shell expands during phage maturation, but without radical alteration of coat protein subunit clustering (Earnshaw, et al., 1976). Nevertheless, these studies using highly specific antibodies have succeeded in detecting what is probably a very slight configurational rearrangement of the coat protein molecules during capsid expansion.

GENERAL DISCUSSION

The analysis of the neutralizing activity of serum directed against P22 phage showed clearly that the primary target for direct inactivation of phage was the tail protein. The kinetics of inactivation indicated that one antibody molecule is sufficient to inactivate the phage. Further experiments are required to determine whether the inactivated phages are incapable of absorbing to Salmonella cells, or whether the antibody blocks a later step in the infection process.

Serum generated against precursor proheads was about as effective in precipitating mature phage as was the anti-phage serum. The serum also contained neutralizing anti-tail antibodies at about 20% of the level in anti-phage serum. This activity was not blocked by proheads themselves and must have been induced by contaminants in the prohead preparation. The contaminating ghosts were present at about the 1% level (Figure 3), and contaminating soluble gp9 was less than could be detected by SDS-gel electrophoresis. This result is of interest in regard to the general question of the immunogenicity of proteins. First, P22 tail protein must represent a highly immunogenic protein. Tail protein could only have accounted for a very small fraction of the total protein in the prohead immunogen preparation, yet it induced a significant antibody response. Although the factors contributing to its high immunogenicity were not investigated, the observed

dominance of the tail protein in antigenic competition has practical ramifications. Its behavior illustrates how minor impurities in vaccine preparation may induce disproportionate antibody responses. Secondly, the results suggest that had the prohead preparation been highly pure, the precursor to the mature virus would probably not have induced a direct neutralizing antibody species. Though not necessarily of a general nature, these results may be relevant to the question of whether precursor particles may be of prophylactic value in immunization against the mature virion. In terms of the actual immune defense against viruses, it has not been established whether only the direct neutralizing antibody species function in the protection of the organism, or whether non-neutralizing antibodies are also important. In a study of foot-and-mouth disease virus, immunization with the purified target of the virus neutralizing antibodies provided protection against the disease in field tests (Bachrach et al., 1975). The question of protection by non-neutralizing antibodies was not addressed.

Naively, one might have expected that extensive coating of the phage capsid, as was seen in the electron microscopy experiments, would have led to phage inactivation. The results of the serum blocking experiments suggested that this was not the case. Although a portion of the neutralizing antibodies were probably anti-coat protein antibodies, they did not constitute a major fraction of the neutralizing antibodies, nor were they highly effective in neutralizing the phage, showing as they did, multi-hit kinetics. These results suggest that,

sults suggest that, once the DNA is stably packaged, the capsid shell may relinquish its role as a dynamic organelle and become a relatively passive protective shell. In this interpretation, the effective transfer of the DNA from the virus to the host would be mediated almost exclusively by the tail apparatus. Addition of the tail to the capsid may even result in a final change in the capsid conformation to achieve maximum stability. Binding of antibodies to the tail parts seems to be the general mechanism by which antisera neutralize phage. This is true for phage λ in which the phage-neutralizing antibodies are directed against the adsorption organelle, the gene J tail fiber (Buchwald and Siminovitch, 1969). Similarly, the neutralizing antibodies against T4 phage are directed against the T4 tail fibers (Edgar and Lielausis, 1965) and baseplate spikes (Berget and King, unpublished experiments). As the experiments in Chapter I of this thesis and earlier experiments show (Israel *et al.*, 1967), the virus neutralizing antibodies against phage P22 are also directed against the tail structure.

The presence in anti-prohead serum of one antibody class, which inhibited phage neutralization by another, generated serum blocking curves quite different from those produced in situations where neutralizing antibody classes act independently. In addition, the existence of inhibiting antibodies implied that the multi-hit inactivation of the phage was the result of direct neutralization. If the loss in phage titer were simply the result of particle agglutination, then an inhibiting class of antibodies could not exist because all antibodies precipitate their antigen.

Two of the amber fragments of scaffolding protein gave positive precipitin reactions in immunoelectrophoresis with anti-

bodies generated against the whole protein. The identification of antibodies in the serum directed against the scaffolding protein was considerably facilitated by the characteristic immunoelectrophoretic behavior of these amber fragments. This was expressed in both their altered electrophoretic mobilities and diffusion behavior, as well as in reactions of partial identity with the complete polypeptide chain. This type of analysis may provide a general method for the identification of antigens whose amber fragments retain antigenicity.

Originally, I hoped to use antibodies to locate several of the minor proteins on the phage structures. In fact, injection of phage and phage precursor structures into rabbits generated antibodies against only two minor proteins, the tail and scaffolding proteins. In the process of characterizing the anti-prohead serum, I unexpectedly discovered that, in the presence of antibodies, scaffolding protein is accessible in proheads. This constitutes the major finding in this thesis and is supported by several lines of evidence.

First, the very fact that injection of prohead structures into a rabbit induced antibodies against the scaffolding protein is consistent with its being accessible to the environment. Although arguments have been made that protein denaturation occurs during emulsification of the antigen in adjuvant (Sela, 1972), recent studies have shown that hemoglobin and myoglobin remain undenatured after mixture with adjuvant (Berkofsky, *et al.*, 1976; Smith, *et al.*, 1977). Third, even proheads which have experienced only mild conditions

bind anti-scaffolding protein antibodies: In immunoelectrophoresis experiments, proheads were able to absorb anti-scaffolding protein antibodies from the serum. Direct observation in the electron microscope of antibody-coated proheads showed that anti-scaffolding protein antibodies bound over the entire prohead surface.

The binding of anti-gp8 all over the prohead shows that the scaffolding molecules either are normally accessible or become available (through antibody incubation) over the entire surface of the shell. This suggests that the exit of the scaffolding protein might take place through the lattice of the coat protein. In fact, the prohead shell expands about 10% in the overall transition (Earnshaw et al., 1976) making this a plausible hypothesis. The fact that there are coat protein antigens present on the prohead, but absent from the mature shell indicates that in this transition there is sufficient movement of the subunits so that an antigenic site can be buried or rendered unavailable. In fact, it is clear from micrographs of negatively stained P22 proheads that the precursor shell is serrated or much rougher than the mature shell. The easiest way to picture this is to assume an open lattice for the prohead with perhaps the scaffolding protein penetrating through. In the expansion of the coat lattice and exit of the scaffolding protein molecules, the coat subunits may reorient or change conformation so as to close up the lattice holes.

It is also possible that antibodies to the capsid protein trigger

a change in the conformation of the capsid shell so that gp8 becomes available for reaction with the anti-scaffolding antibodies in the environment. From the electron micrographs of antibody-coated proheads, it is clear that the binding reaction results in a rearrangement of the prohead structure, at least with respect to the scaffolding molecules. The occupation of the center of the particle by the stain suggests that the gp8 molecules have moved out to the shell. It is possible that the antibody-coated proheads represent proheads in transition, intermediate structures trapped in the process of releasing their scaffolding protein. Proheads coated with anti-phage serum, which lack antibodies against gp8, had the same appearance. This suggests that this transition may be triggered by anti-capsid protein. All of these observations can be accounted for by the following model:

The majority of the mass of the scaffolding protein is situated within the prohead as suggested by electron microscopic studies (Casjens and King, 1974; Lenk et al., 1975) and X-ray diffraction studies (Earnshaw et al., 1976). However, a part of the chain protrudes through the capsid lattice and is exposed. Thus, on injection into a rabbit, anti-scaffolding protein and anti-capsid protein are produced. When these antibodies are reacted with proheads, they bind to the exposed determinants. The binding of anti-coat antibodies to the prohead triggers the rearrangement of the coat from the prohead to the mature shell, or to an intermediate stage in the transition. In this process, gp8 moves through the coat protein lattice to the surface leaving the inside of the particle empty. Antibodies directed against gp8 bind to the exposed scaffolding protein, probably before and after the transition. In a certain sense the antibody reaction may mimic the SDS treatment of

proheads which results in the expansion of the shell and the release of the scaffolding protein. Earnshaw (personal communication) has recently found that 8^- shells which lack the scaffolding protein, will expand to the mature size when treated with SDS. Thus, the expansion is a property of the coat protein alone, and does not require gp8. In the absence of the coat protein, the scaffolding protein accumulates as soluble subunits (Casjens and King, 1974), and does not self-associate. People have generally thought that gp8 was specifically aggregated into an inner shell with the capsid. However, it may be that though gp8 molecules are close together inside the capsid, they are not tightly bound to each other, but rather are bound to the capsid lattice. When this lattice rearranges they are released. In this model, I envision the scaffolding protein as copolymerizing with the coat protein providing the extra information to give the coat lattice its proper curvature. Once the prohead is completed, a further reaction, presumably involving DNA binding, triggers the rearrangement of coat protein, which then releases gp8, through the expanded coat protein lattice.

REFERENCES

- Adams, M.H. (1959) Bacteriophages. Interscience Publishers, N.Y.
- Appleyard, G. (1961) Nature London 190: 465-66.
- Arnon, R. (1972) In Immunity in Viral and Rickettsial Diseases, Advances in Experimental Medicine and Biology, Vol. 31, p. 209. (A. Kohn and M. Klingberg, eds.) Plenum Press, N.Y.
- Bachrach, H.L., D.M. Moore, P. McKercher, and J. Polotnick (1975) J. Immunol. 115: 1636.
- Berkofsky, J.A., A. Schechter, and H. Kon (1976) J. Immunol. 115: 270.
- Bijlenga, R.K.L., D. Scraba, and E. Kellenberger (1973) Virology 56: 256-267.
- Bijlenga, R.K.L., R. v.d. Broek, and E. Kellenberger (1974) J. Supramolec. Struct. 2: 45-59.
- Borek, F. (1972) Immunogenicity, North-Holland Research Monographs, Frontiers of Biology, Vol. 25. North-Holland Pub. Co., London.
- Botstein, D., R. Chan, and C. Waddell (1972) Virology 49: 268-82.
- Botstein, D., and M. Levine (1968) J. Mol. Biol. 34:621-41.
- Botstein, D., C. Waddell, and J. King (1973) J. Mol. Biol. 80: 669-95.
- Buchwald, M. and L. Siminovitch (1969) Virology 38: 1-7.
- Cann, J.R. (1968) In Methods in Immunology and Immunochemistry, Vol. 2, Ch. 6. (C. Williams and M. Chase, eds.) Acad. Press, N.Y.
- Casjens, S.R. and R.W. Hendrix (1974) J. Mol. Biol. 88:535-45.
- Casjens, S.R., T. Hohn, and A.D. Kaiser (1972) J. Mol. Biol. 64:551.
- Casjens, S. and J. King (1975) Ann. Rev. Biochem. 44:555.
- Caspar, D.L.D. and A. Klug (1962) Cold Spring Harbor Symp. Quant. Biol. 27:1-24.

- Chan, R., and D. Botstein (1972) Virology 49: 257.
- Clausen, J. (1971) In Immunochemical Techniques for the Identification and Estimation of Macromolecules (T.S. Work and E. Work, eds.) American Elsevier Publishing Co., Incorp. N.Y.
- Crick, F.H.C. and J.D. Watson (1956) Nature 177: 473-5.
- Davenport, F.M., A.V. Hennessy, F.M. Brandon, R.G. Webster
C.D. Barret, Jr., and G.O. Lease (1964) J. Lab. Clin. Med.
63: 5-13.
- Earnshaw, W.C., S. Casjens, and S.C. Harrison (1976) J. Mol. Biol.
104: 387-410
- Edgar, R.S., and I. Lielausis (1965) Genetics 52: 1187-1200.
- Eisen, H.N. (1974) Immunology: An Introduction to Molecular and Cellular Principles of the Immune Responses. Harper and Row, N.Y.
- Epstein, R.H., A. Bolle, C.M. Steinberg, E. Kellenberger,
E. Boy de la Tour, R. Chevalley, R.S. Edgar, M. Sussman,
G.H. Denhardt, and I. Lielausis (1963)
Cold Spring Harbor Symp. Quant. Biol. 28: 375.
- Fenner, F. (1972) In Immunity in Viral and Rickettsial Diseases, Advances in Experimental Medicine and Biology, Vol. 31, Ch. 1. (A. Kohn and M. Klingberg, eds.) Plenum Press, N.Y.
- Fraenkel-Conrat, H. and R.C. Williams (1955) Proc. Nat. Acad. Sci. (USA)
41: 690-8.
- Grabar, P. (1964) In Immuno-electrophoretic Analysis: Applications to Human Biological Fluids (P. Grabar and P. Burtin, eds.) American Elsevier Publishing Co., Incorp. N.Y.
- Hendrix, R.W. and S. Casjens (1975) J. Mol. Biol. 91: 187-99.
- Hoffman, B. and M. Levine (1975) J. Virol. 16: 1547-59.
- Hohn, B. and T. Hohn (1974) Proc. Nat. Acad. Sci. (USA) 71: 2372-6.
- Hohn, B., M. Wurtz, B. Klein, A. Lustig, and T. Hohn (1974)
J. Supramolec. Struct. 2: 302.
- Hohn, T., H. Flick, and B. Hohn (1975) J. Mol. Biol. 98: 107-120.

- Hohn, T. and B. Hohn (1973) J. Mol. Biol. 79: 649.
- Horne, R.W. and P. Wildy (1961) Virology 15: 348-73.
- Israel, V., T. Anderson, and M. Levine (1967) Proc. Nat. Acad. Sci. (USA) 57: 284-95.
- Israel, V., H. Rosen, and M. Levine (1972) J. Virol. 10: 1152.
- Iwashita, S. and S. Kanegasaki (1975) Virology 68: 27-34.
- Iwashita, S. and S. Kanegasaki (1976) Eur. J. Biochem. 65: 87-94.
- Kaiser, A.D. and T. Masuda (1973) Proc. Nat. Acad. Sci. (USA) 70: 260.
- Kaiser, A.D., M. Syvanen, and T. Masuda (1975) J. Mol. Biol. 91: 175-86.
- Kanegasaki, S. and A. Wright (1973) Virology 52: 160.
- Kasel, J.A., M. Huber, F. Loda, P.A. Banks, and V. Knight (1964) Proc. Soc. Exp. Biol. Med. 117: 186-90.
- Kellenberger, E., F. Eiserling, and E. Boy de la Tour (1968) J. Ultrastruct. Res. 21: 335-60.
- Kerr, C. and P.D. Sadowski (1974) Proc. Nat. Acad. Sci. (USA) 71: 3545-49.
- Kikuchi, Y. and J. King (1975) J. Mol. Biol. 99: 645-72.
- King, J., D. Botstein, S. Casjens, W. Earnshaw, S.C. Harrison, and E.V. Lenk (1976) Phil. Trans. R. Soc. Lond. B 276: 37-49.
- King, J. and S. Casjens (1974) Nature 254: 112-19.
- King, J., E.V. Lenk, and D. Botstein (1973) J. Mol. Biol. 80: 697-731.
- Langer, W.L. (1976) Sci. Amer. 234: 112-17.
- Laemmli, U.K. (1970) Nature 227: 680-5.
- Laemmli, U.K. (1975) Proc. Nat. Acad. Sci. (USA) 72: 4288-92.
- Laemmli, U.K., and M. Favre (1973) J. Mol. Biol. 80: 575-99.
- Laemmli, U.K., E. Molbert, M. Showe, and E. Kellenberger (1970) J. Mol. Biol. 49: 99-113.
- Laemmli, U.K., J.R. Paulson, and V. Hitchins (1974) J. Supramolec. Struct. 2: 276-301.

- Lenk, E.V., S. Casjens, J. Weeks, and J. King (1975) Virology 68: 182-99.
- Levine, M. (1972) Current Topics in Microbiol. and Immunol. 58: 135-56.
- Lew, K. (1974) Thesis, Ph.D., Massachusetts Institute of Technology.
- Luftig, R.B., W.B. Wood, and R. Okinawa (1971) J. Mol. Biol. 57: 555-73.
- McConnell, M. (1976) Thesis, Ph.D. Tufts Medical School.
- Murialdo, H. and L. Siminovitch (1972) Virology 48: 785-823.
- Neurath, R.A. and B.A. Rubin (1971) Viral Structural Components as Immunogens of Prophylactic Value, Monographs in Virology, Vol. 4. (J.L. Melnick, ed.) S. Karger, Pub., Houston.
- Pereira, H.G. (1972) In Immunity in Viral and Rickettsial Diseases, Advances in Experimental Medicine and Biology, Vol. 31, Ch. 9. (A. Kohn and M. Klingberg, eds.) Plenum Press, N.Y.
- Poteete, A.R. and J. King (1977) Virology 76: 725-39.
- Raj, A.S., A.Y. Raj, and H. Scmieger (1975) Molec. Gen. Genet. 135: 175-84.
- Ray, P. and H. Murialdo (1975) Virology 64: 247-63.
- Rhoades, M., L.A. MacHattie, and C.A. Thomas (1968) J. Mol. Biol. 37: 21-40.
- Roeder, G.S., and P. Sadowski (1977) Virology 76: 263.
- Rott, L. (1965) In Haas und Vivell, p. 25. Cited in Neurath and Rubin (1971).
- Sela, M. (1972) In Immunity in Viral and Rickettsial Diseases, Advances in Experimental Medicine and Biology, Vol. 31, p. 258. (A. Kohn and M. Klingberg, eds.) Plenum Press, N.Y.
- Showe, M. and L. Black (1973) Nature New Biol. 242: 70-75.
- Simon, L. (1972) Proc. Nat. Acad. Sci. (USA) 69: 907-11.
- Smith, J., J. Hurrell, and S. Leach (1977) J. Immunol. 118: 227.

- Streisinger, G., R.S. Edgar, and G.H. Denhardt (1964) Proc. Nat. Acad. Sci.(USA) 51: 775-79.
- Streisinger, G., J. Emrich, and M.M. Stahl (1967) Proc. Nat. Acad. Sci. (USA) 57: 292-5.
- Susskind, M., D. Botstein, and A. Wright (1974) Virology 62: 350-66.
- Takeda, K., H. Uetake, and S. Toyama (1975) Int. Virol. Abstr. 3: 213.
- Tosi, M. and D.L. Anderson (1973) J. Virol. 12: 1548-59.
- Tye, B., J. Huberman, and D. Botstein (1974) J. Mol. Biol. 85: 501-32.
- Uriel, J. (1958) J. Clin. Chim. Acta 3: 234-384.
- Uriel, J. (1964) In Immunoelectrophoretic Analysis: Applications to Human Biological Fluids, p. 58. (P. Grabar and P. Burtin, eds.) American Elsevier Publishing Co., Incorp. N.Y.
- Van Holde, K. (1971) Physical Biochemistry, Prentice-Hall, Inc., N.J.
- Wilcox, W.C. and H.S. Ginsberg (1963) J. Exp. Med. 118: 295-306.
- Winkler, F.K., C.E. Schutt, S.C. Harrison, and G. Bricogne (1977) Nature 265: 509-73.
- Wright, A. and S. Kanegasaki (1971) Physiol. Rev. 51: 748.
- Yamamoto, N. and T.F. Anderson (1961) Virology 14: 430-39.
- Yanagida, M. (1972) J. Mol. Biol. 65: 501-17.
- Yanagida, M. and C. Ahmad-Zadeh (1970) J. Mol. Biol. 51: 411-21.
- Zachary, A., L.D. Simon, and S. Litwin (1976) Virology 72: 429-44.
- Zinder, N.D. and J. Lederberg (1952) J. Bacteriol. 64: 679-99.